Generation of Ground Motions for Mid-America Cities

Y. K. Wen and C. L. Wu
University of Illinois at Urbana-Champaign

Introduction

Mid-America is a region of moderate seismicity. Infrequent moderate to large events had occurred in the past and can occur again and cause large losses. The performance of the building stock and other structures under future earthquakes is a serious concern. The major threats of future seismic events come from the New Madrid Seismic Zone (NMSZ) and several other areas of moderate seismicity. As ground motion records of engineering interest in this area have been scarce, to evaluate the performance of buildings and structures and estimate loss/cost, simulation of future events based on current data and knowledge is necessary. A method of simulation is developed for this purpose. The method is based on the latest information of seismicity in this region, the most recent ground motion models and simulation methods appropriate for engineering applications in this region. A strong emphasis is placed on uncertainty modeling and efficiency in application to performance evaluation and fragility analysis. The procedure may be improved as more knowledge on earthquakes in this region and more accurate and efficient methods of ground motion modeling become available. A brief description of the method of simulation and results obtained for three Mid-America cities is given in the following.

Selection of Locations and Soil Profiles

Site locations of special interest in this study are Memphis TN (35.117°N, 90.083°W), Carbondale IL (37.729°N, 89.246°W), and St. Louis MO (38.667°N, 90.190°W). These cities are selected for study because they present a cross-section of the mid-America cities at risk. Since ground motions are strongly dependent on local soil condition and yet the soil profile variation within a city has not been mapped in detail, in this study the soil condition of a city will be assumed to have small variation and can be approximately modeled by a generic profile. Ground motions at the bedrock, however, will also be generated for these cities that if detailed information of local soil variation is available, one can use appropriate soil amplification computer software to obtain the surface ground motions.

Method of Simulation

The ground motion simulation method basically follows the procedure proposed by Herrmann and Akinci (1999) that is largely based on Boore's point-source simulation method SMSIM (1996). To catch some of the important near-source effects due to large events, however, the finite fault model by Beresnev and Atkinson (1997, 1998) is also used for magnitude-8 events. The soil amplification is modeled by the quarter-wavelength method by Boore and Joyner (1991, 1997). The tectonic and seismological data are mainly taken from USGS Open-File Report 96-532 (Frankel et al. 1996). A large number of possible future events and ground motions are generated from which uniform hazard response spectra

(UHRS) are obtained for each city for exceedance probabilities of 10%, 5%, and 2% in 50 years. Finally, to facilitate fragility analysis, suites of 10 ground motions are selected from the large pool of simulated ground motions such that the medians of the response spectra of the suites match those of UHRS in a least square sense at two probability levels, 10 % and 2% in 50 years. UHRS can be used directly for probabilistic performance (fragility) evaluation of linear structures and suites of ground motions can be used for the same purpose of nonlinear structures. Details of the simulation method are given in the following.

Reference Area and Occurrence Model

All probable earthquake sources in the Central and Eastern United States (CEUS) are considered; for a given city, however, only those that fall within the reference area (effective zone) of the city thus have significant contributions to the seismic risk are used in the simulation. Different cities may share some of the seismic sources and hence the same simulated seismic events. Considering the relatively low attenuation in the CEUS, the effective zone is defined as a circular area with a radius of 500 km centered at a specific site location, a value used by most researchers (e.g. USGS OFR-96-532). Only earthquakes with body wave magnitude greater than 5 are considered. The statistics of occurrence and magnitude from the USGS OFR-96-532 are used in the simulations. Fig. 1 shows the annual occurrence rate per 0.1×0.1degree square for earthquakes of magnitude 5 or larger for the zone of interest. The occurrence in time is generated according to a Poisson process. The magnitude given the occurrence is then generated according to the magnitude distribution for events of magnitude less than 8 following 1996 USGS Open File Report. The magnitude-8 events are generated separately using Poisson process with a mean recurrence time of 1000 years (Frankel et al. 1996) and with an epicenter uniformly distributed within the New Madrid fault zone shown in Fig. 2. A total of 9000 simulations of 10-year period are carried out. As a result, 9260 ground motions are generated in Memphis TN, 9269 in Carbondale IL and 8290 in St. Louis MO. Fig. 3 shows the epicenters and magnitudes of earthquakes corresponding to 600 simulations of 10 years record in the region of interest in CEUS. The four cities under study are also shown to show the proximity of the events to each city. It corresponds, therefore, to about 6000 years of records. Most of the events are in the NMSZ and the East Tennessee Seismic Zone. According to the simulation results, the occurrence rates of earthquakes of magnitude 5 and above in the reference areas for Memphis, Carbondale, and St. Louis are 0.0989, 0.0980 and 0.0882 per year, respectively. These values are very close to the actual occurrence statistics.

Source and Path Models

The majority of the seismic sources are modeled as point sources due to lack of knowledge on the fault structure in the CEUS. However, the finite fault model is used for earthquakes of moment magnitude 8 in the New Madrid Seismic Zone since the seismotectonic information of such events is better known. The earthquake occurrence is assumed Poissonian for all events including the magnitude-8 earthquakes. For point sources, the two-corner-frequency model (Atkinson and Boore 1995) for generic S-wave type ground motions on hard rock is used since this model has been shown to give better ground motion prediction in the CEUS (Atkinson and Boore 1998). To account for near-field effects of large earthquakes, the fault plane of a magnitude-8 event in New Madrid Seismic Zone is divided into a number of sub-faults, each treated as a point source. The resulting ground

motion is a combination of waveforms from different sub-faults accounting for difference in arrival times and path attenuation. This so-called finite fault model by Beresnev and Atkinson (1997, 1998) emphasizes the effects of fault dimension, rupture propagation, directivity, and source-receiver geometry. The one-corner-frequency point-source model (Brune 1970, Frankel et al. 1996) was used for each sub-fault. The examples of application in Beresnev and Atkinson (1997,1998) showed that the model produces ground motions that match well earthquake records on rock sites in the 1985 Michoacan, Mexico, the 1985 Valpara×so, Chile, the 1988 Saguenay, Qu■bec, and the 1994 Northridge earthquakes. For soil sites, however, their model tends to overestimate the ground motions because of soil nonlinearity which is not considered. More detailed descriptions of the models are given in the following.

Point-Source Model

The mathematical form for the Fourier amplitude spectrum of the point-source model is:

$$A(M_0, R, f) = E(M_0, f) \cdot D(R, f) \cdot P(f) \cdot I(f) \tag{1}$$

in which, f is frequency (Hz), R is focal distance, and M_0 is the moment magnitude. The various functions are:

$$E(M_0, f) = C \cdot (2pf)^2 \cdot M_0 \cdot \left\{ \frac{1-e}{1+\left(\frac{f}{f_A}\right)^2} + \frac{e}{1+\left(\frac{f}{f_B}\right)^2} \right\}, \text{ source spectraum} \tag{2}$$

in which, $C = \dfrac{R_p \cdot F \cdot V}{4p \cdot r \cdot b^3}$

R_p = 0.55, radiation pattern

F = 2 , free-surface amplification

V = 0.7071, partition factor

ρ = 2.8 gm/cm^3, crustal density

β = 3.6 km/sec, shear wave velocity

ε = weighting parameter

f_A, f_B (Hz) = corner frequencies

$\log e = 2.52 - 0.637 \cdot M_W$

$\log f_A = 2.41 - 0.533 \cdot M_W$

$\log f_B = 1.43 - 0.188 \cdot M_W$

$M_0 = 10^{1.5 \cdot M_W + 16.05}$ (dyne-cm)

$D(R, f) = D_g(R) \cdot D_m(R, f)$, diminution factor (3)

$$D_g(R) = \begin{cases} 1/R & if \quad R \le 70\,km \\ 1/70 & if \quad 70 \le R \le 130\,km \\ (1/70)(130/R)^{0.5} & if \quad 130\,km \le R \end{cases}$$, geometric attenuation

$D_m(R, f) = e^{\frac{p \cdot f \cdot R}{b \cdot Q(f)}}$ and $Q(f) = 680 \cdot f^{0.36}$, anelastic material attenuation

$$P(f) = e^{-pkf} \cdot \frac{1}{\sqrt{1 + \left(\frac{f}{f_{\max}}\right)^8}}$$, high-cut filter (4)

where f_{max} = 50 Hz is used and κ depends on the local soil condition.

$I(f) = \frac{1}{(2pf)^p}$; p = 0 for acceleration, 1 for velocity, and 2 for displacement. (5)

The total duration T consists of source and path durations. The latter takes a tri-linear form of source-site distance (Atkinson and Boore, 1995):

$$T = T_0 + T_p \quad (6)$$

in which, R is hypocentral distance (km) and

Source duration $T_0 = \frac{1}{2 \cdot f_A}$ (sec)

Path duration $T_p = \begin{cases} 0 & if \quad R \le 10\,km \\ 0.16 \cdot (R - 10) & if \quad 10 \le R \le 70\,km \\ 9.6 - 0.03 \cdot (R - 70) & if \quad 70 \le R \le 130\,km \\ 7.8 + 0.04 \cdot (R - 130) & if \quad 130 \le R \le 1000\,km \end{cases}$

The focal depth is modeled as a random variable following a specified distribution given in Table 1, based on historical data (EPRI Report, 1993, Wheeler and Johnston, 1992,1993).

Finite Fault Model

For the finite fault model, a rupture plane of 140 km (along strike) by 33 km (along dip) (Johnston 1996) with a vertical strike-slip faulting and 34.69° azimuth is assumed, which is an approximate estimate based on USGS OFR-96-532. A total of 64 (16x4) sub-faults are used. The anelastic attenuation $Q(f) = 670 * f^{0.33}$ is used following Beresnev and Atkinson (1998). The epicenter is assumed to occur equally likely within the NMSZ zone shown in Fig.2. The orientation of the fault is assumed to be along that of the NMSZ. Once rupture occurs, it propagates toward both ends of the rupture surface. The slip distribution (asperity) within the rupture surface is modeled by a correlated random field according to Saikia and Sommerville (1997), Sommerville et al (1999) with the following wave number spectrum.

$$A(k_x, k_y) = \frac{1}{\sqrt{1+[(k_x / C_x)^2 + (k_y / C_y)^2]^n}} \quad (7)$$

in which k_x and k_y are the wave numbers and C_x and C_y are correlation length constants depending on magnitude. This random field model is then modified to ensure larger slip in the middle than at the edge of the rupture surface, a feature observed in recent earthquakes.

A stress drop of 200 bars is used for the finite fault model. A drop 150 bars is also tested for finite fault model. As expected, it causes lower spectral values in low frequency range in the 2% in 50 years hazard level. Local soil profiles are also used in conjunction with this model.

Local Site Effect/Soil Amplification

Soil amplification due to local site soil profile is considered. The quarter wavelength method (QWM) (Joyner et. al., 1981, Boore and Joyner, 1991, Boore and Joyner, 1997, Boore and Brown, 1998) is used to model the soil amplification. Soil profiles are based on boring log data in Memphis, Carbondale and St. Louis (Hashash, Herrmann,1999). The amplification is approximated by

$$A = \sqrt{r_0 b_0 / r_s b_s} \quad (8)$$

in which r and β are the density and shear wave velocity at the source(subscript 0) and site(subscript s). At the site, the frequency-dependent effective velocity β_s is defined as the average velocity from the surface to a depth of a quarter wavelength for a given frequency. At high frequency, the soil attenuation is accounted for by

$$P(f) = exp(-p\,kf) \quad (9)$$

in which κ is a term that accounts for shear velocity and damping over the soil column.

According to Herrmann and Akinci (1999), κ = 0.063 sec, 0.043 sec and 0.0076 sec for Memphis, Carbondale and St. Louis, respectively. The "representative" profiles for the three cities used in this study are shown in Tables 2 to 4. The resultant soil amplification as function of frequency for the three cities are shown in thick lines in Figs. 4 to 6. It is seen that while amplification at St. Louis is restricted to the high frequency range (> 3 Hz) due to the very shallow soil layer on hard rock, the much deeper soil layers in Memphis and Carbondale produce much larger amplification in the longer period range. For comparison, the soil amplification at these three cities based on the well-known computer software SHAKE is also shown for bedrock ground motions of 10 % and 2 % probability of exceedance in 50 years. The soil amplification factor used in 1997 NEHRP for soil classification of B/C boundary is also shown since this is the soil condition used for USGS national earthquake hazard maps. Note that the quarter-wavelength model will give good estimate of the averaged amplification and will miss the peaks and valleys. Also, it has a tendency of overestimating the amplification in the high frequency range for ground motion

of very high intensity when effects of soil nonlinearity may be significant. In spite of these limitations, the agreements, however, are generally good. In passing, it is pointed out that soil amplification considering nonlinear effects is an extremely complex problem. SHAKE is the most widely used program but is based on an equivalent linear wave propagation method. It is expected to yield good results when the excitation intensity is not very high and the soil layer is not very deep. It is therefore expected to work better for the St. Louis soil profile than those of Memphis and Carbondale. There are other truly nonlinear programs available for this purpose. However, they have not been commonly accepted by engineers, therefore are not used for comparison in this study.

Uncertainty in Attenuation

Path attenuation due to geometric radiation and material damping in the earth crust is accounted for by semi-empirical formulae shown above. The uncertainty in the attenuation is modeled by a lognormal distribution with the median value given by the above Diminution Factor as function of distance and frequency. A coefficient of variation of 75% is assumed for the attenuation in the simulation. To prevent unrealistic large variation, cut-off limits of mean plus and minus three standard deviations are used.

Generation of Ground Motions, Uniform Hazard Response Spectra, and Selection of Suites of Ground Motions for Performance Evaluation

The procedure of simulation is shown in Fig 7. In each simulation, the magnitude, epicenter location, and focal depth are first generated according to the distribution for each parameter (see also Fig. 3). For each event of given epicenter, focal depth, magnitude and fault size (for magnitude-8 events), a ground motion is generated using the procedure outlined in the foregoing at the three cities. For the point-source events, the Fourier amplitude spectrum (Eq.(1)) as a function of the distance from the source to the city and the magnitude and distance dependent duration function are used to generate ground motion time histories. For this purpose, the computer software SMSIM (Boore 1996) is modified to include path attenuation uncertainty and soil amplification. The path attenuation factor is generated from a lognormal distribution. For the magnitude-8 events, the finite fault model is used in which the slip distribution is simulated according to the spatially correlated random field model. Ground motions are then generated from each sub-fault and superimposed. Ground acceleration time histories are generated for both ground surface considering the soil profile and for bedrock (or rock outcrop) for the three cities for each event. The process is then repeated for a large number of events equivalent to 90,000 years of records.

This large number of ground motion time histories allows one to obtain the uniform hazard response spectra (UHRS). At a given city, the response acceleration spectrum for each time history is first calculated. The annual and 50-year probability distribution of spectral acceleration for a given period is then obtained from which one can construct the UHRS for a given exceedance probability. The UHRS can be used to evaluate the performance of linear systems using method of modal superposition. That is, by modal analysis, one can obtain the maximum structural response for a given probability level for structural performance evaluation. For nonlinear systems, time history response analysis is generally required since modal superposition principle no longer applies. For this purpose,

suites of ground motions for each probability level are selected. The selection criterion is that the deviation of the median response spectra of the suite from the UHRS is minimized. The median value is used for it is less sensitive to sample fluctuation and it allows simple estimation of the underlying lognormal distribution parameter. To accomplish this, response spectral acceleration S_a at 10 key structural periods of the simulated ground motions are compared with those of the target UHRS for a given probability of exeedance. The ten ground motions with the smallest mean square logarithmic (log S_a) difference are selected. The resultant suite will have a median spectral acceleration that best matches the target UHRS. The matching of the spectral acceleration has been shown by Shome and Cornell (1999) to be the most effective means of selecting ground motions for probabilistic nonlinear structural demand analysis. For performance and fragility analysis of nonlinear structures, one can calculate the structural response by time history analysis of the structure under the suites of ground motions. The median response will have approximately the probability of exceedance equal to that of the ground motion suite. A more detailed performance and fragility analysis can be also performed using the time history response and an appropriate regression analysis (Wang and Wen 1999, Shome and Cornell 1999).

It is mentioned that the popular method of "de-aggregation" is not used is this study in selecting the events for ground motion generation for the following reasons:

(1) De-aggregation works best when there is a dominant event of certain magnitude (M) and distance (R) and not so well when the M-R "landscape" is flat. The favorable condition does not necessarily prevail in all sites.

(2) De-aggregation is dependent on structural response and probability level, i.e. events of spectral accelerations of different periods and different probabilities of exceedance have different M-R "landscape" and hence could result in different de-aggregations and suites of ground motions. It is suitable for purpose of performance evaluation of a particular structure but not the general building stock of wide range of natural frequencies.

(3) Magnitude and distance are much less important, compared to spectral acceleration, in terms of impact on the structural linear and nonlinear responses (Shome and Cornell 1999).

Limitations

As mentioned in the foregoing, and the source and path models and the quarter-wavelength method do not explicitly consider effects of surface waves (e.g., Dorman and Smalley 1994) and soil nonlinearity. Therefore, the change in frequency content with time and the nonlinear soil amplification of the ground motions are not modeled in this simulation. However, it is pointed out that comparisons of results by Boore and Joyner (1991,1996,1997) with observations and analytical results generally show the robustness of their methods. Also there have not been any efficient methods of modeling surface waves and nonlinear soil effects that can be adapted in a large-scale simulation as required in this study. Finally, as will be shown later that the uniform hazard response spectra based on the simulated ground motions compare favorably with those of 1997 USGS national earthquake hazard maps and the FEMA 273 recommendations. The response spectra are the most important measure of ground motion potential of causing severe structural response and damage. The UHRS and suites of simulated ground motions generated by the proposed method, therefore, represent

reasonably well the seismic hazards to buildings and other structures in these three cities. As efficient methods for modeling soil nonlinearity and surface waves become available, they will be incorporated into the simulation method.

Results

Comparison Results of Point-Source Model with Broadband Model

The accuracy and the validity of the point-source model can be found in the literature (Boore,1996). There have been no records of moderate to large events near any of the three cities that can be used for comparison with the simulated ground motions. The closest is the simulation results based on the broadband approach for St. Louis due to events of magnitude 6.5 to 7.5 in the NMSZ by Saikia and Somerville (1997). The broadband approach considers the details of the geometry of the fault, rupture surface, and wave propagation for low frequency motion and uses records for high frequency motion. For large-scale simulations, it requires detailed information of each fault which is generally unknown and it is also computationally too expensive. The results of these two methods for a rock site at St. Louis are compared. An event based on the point-source model is chosen whose source and path parameters are comparable to those of the magnitude-7 event studied by Saikia and Somerville. The response spectra of hard rock motions based on these two models are compared in Fig.8. It is seen that agreements are good in the period range from 0.2 sec to 3 sec.

Directivity Effects of Magnitude-8 Events

The near-source effects using the finite fault model are demonstrated by a comparison of the ground motions at Memphis due to two simulated events, both of magnitude 8. The location, size, and orientation of the faults are the same with a closest distance of 61.8 km from the fault surface to the site. The epicenters, however, are located such that one is far (186 km) from the site with the rupture propagating toward the site and the other closer (79 km) to the site with the rupture propagating generally away from the site (Figs.9 and 10). Sample rupture surface (33 km×140 km) slip distributions based on the correlated random field model and the corresponding discretizations for the finite fault model for the two events are shown in the figures. The time histories of the ground motion for a soil site at Memphis are shown in Fig.11 for both events. The directivity effects can be clearly seen that the former produces a shorter but more intense ground motion due to the "Doppler effect" even the epicenter is much farther away.

Uniform Hazard Response Spectra (UHRS) and comparison with USGS Hazard Maps and FEMA 273 Recommendations

The uniform hazard response spectra (UHRS) is an efficient means of representing seismic hazards for probabilistic performance (fragility) evaluation of linear structures and nonlinear structures (e.g., Collins et al 1996). The UHRS for Memphis, Carbondale, and St. Louis are obtained from the simulated ground motions. For a validation of the results, the UHRS at Memphis obtained in this study are first compared with those of 1997 USGS national earthquake hazard maps for B/C boundary soil classification (i.e. firm rock with an

average shear velocity of 760 m/sec in the top 30 m). This generic site condition facilitates the comparison with previous studies by USGS and other researchers. Fig.12 shows the UHRS for three probability levels for Memphis calculated from the simulated ground motions. The spectral accelerations at three periods (0.2sec, 0.3sec, and 1.0 sec) according to 1997 USGS national earthquake hazard maps for Memphis are also shown in the figure. The agreements are generally very good. Since the input seismicity data to these two models are essentially the same, the differences can be attributed to:

(1) The USGS study used a point-source model with the closest distance from the fault to the site for magnitude-8 events whereas a finite fault model with random location of the epicenter within the fault is used in this study.

(2) For point sources, the one-corner-frequency source model was used in the USGS study whereas the two-corner-frequency source model is used in this study (Eq.2) which has been shown to give better fit to records in CEUS (Atkinson and Boore 1998)

The UHRS for the three cities with the "representative" soil profiles shown in Tables 2 to 4 are obtained and compared with FEMA 273 recommendations for design. FEMA 273 spectra are for design check and are based on the 1997 USGS national earthquake hazard maps. There are five generic soil classifications according to the upper 30m of soil and the amplification factor is largely based on empirical results of Loma Prieta and Northridge earthquakes (e.g., Borcherdt, 1994). The UHRS for Memphis representative soil profile are shown in Fig.13. It is seen that compared with those for the B/C boundary, the UHRS are amplified almost by a factor of two for period greater than 1.0 sec. and reduced for T<0.3 sec due to the deep soil layer. The agreements are generally good for T>0.7 sec. The differences for T< 0.5 sec. are partly due to the differences in the source models as mentioned in the foregoing and partly due to the differences in soil amplification factors. The UHRS for the Carbondale representative soil profile are shown in Fig.14. The agreements are generally good. The UHRS for St. Louis representative soil profile are shown in Fig.15. There are some major differences. Compared with the FEMA Class C spectra, the UHRS are much lower for T> 0.2sec. and higher for T <0.2 sec because of the comparatively thin (16m) layer of soil on rock. The current results are more in agreement with the findings of Saikia and Somerville (1997) indicating a much lower seismic hazards for St. Louis. It is pointed out that the actual soil profile in the St. Louis area may have a wide variation and could differ significantly from the "representative profile" used in this study, especially at locations close to the Mississippi River. Deeper soil layer causing larger soil amplification at longer period is certainly possible at these locations. Ground motions at the surface can be generated from the bedrock ground motions using a proper soil amplification model when detailed information of soil profile is available.

Suites of Ground Motions for Memphis, Tennessee

For each of the two hazard levels, 10% and 2% in 50 years, ten ground motions are selected from the large number of simulated motions such that the median spectral accelerations best fit the target UHRS. The selection is done for both ground surface and the bedrock (or rock outcrop). The suite of ground motion time histories for a 10% in 50 years hazard are shown in Fig.16. The source (magnitude, epicentral distance, and focal depth) and path (attenuation uncertainty) parameters associated with each ground motion are also shown in the figure. It is seen that at this probability level, seven ground motions come from

magnitude-6 events at some distance, two from magnitude-5 events and one from magnitude-8 event. The response spectra of the ten ground motions are shown in Fig.17 with the target UHRS. The median constructed from the 10 sample ground motions and the16-to-84 percentile band are shown. The uncertainty in the median response spectra in terms of the 16-to-84 percentile band is about one third ($1/\sqrt{10}$) of that shown in the figure. What it entails is that the median value of structural responses under this suite of ground motions will have very small uncertainty due to record-to-record variation and will correspond to a probability of exceedance of 10% in 50 years. One can use it in the structural performance evaluation with some confidence. The suite of ground motion time histories for a 2% in 50 years hazard and the response spectra comparison are shown in Figs.18 to 19. It is seen that at such high intensity and low probability level, all ground motions come from magnitude-8 events. The scatters in the response spectra are larger but the maximum 16-to-84 percentile uncertainty band for the median value is still around 10 % or less. The sample ground motion time histories at rock outcrop (or bedrock) and the response spectra are shown in Figs.20 to 23. Without the soil amplification, the frequency content is seen to shift toward shorter periods and the spectral accelerations are generally much lower. These ground motions may be used as inputs to soil amplification software to obtain surface ground motions when detailed information of the site soil profile is available.

Suites of Ground Motions for St. Louis, Missouri

The time histories and response spectra of the suites of ground motions at St. Louis are shown in Figs. 24 to 27. The major feature of the surface ground motion is the lack of amplification for period greater than 0.5 sec because of the thin soil layer. At the 10 % in 50 years level, nine ground motions come from events of magnitude 6 to 7. At 2% in 50 years level, six come from magnitude-8 events with long duration. Smaller (magnitude 5 to 7) and closer events with shorter duration make up the rest. There is comparatively a much larger scatter at peak of the response spectra (period from 0.1 to 0.2 sec). The maximum 16-to-84 percentile band for the median, however, is still around 10 %. The ground motions and response spectra for rock outcrop (or bedrock) are shown in Figs. 28 to31. The compositions of the suites are similar. The ground motion levels are lower.

Suites of Ground Motions for Carbondale, Illinois

The time histories and response spectra of ground motions suites for Carbondale, Illinois soil sites are shown in Figs.32 to 35. There is a significant amplification of motion in the long period range because of the deep and soft soil profile. At the 10 % in 50 years level, all contributions come from events of magnitude 5.8 to 7.1. At the 2% in 50 years level, all come from magnitude-8 events. The 16-to-84 percentile bands are reasonably narrow. The suite of ground motions and response spectra for rock site are shown in Figs. 36 to 39. The trend is the same that compositions of the suites are similar to those for the soil site but the intensities are much lower.

Acknowledgments

Helpful comments and suggestions received in MAE center research coordination meetings and from R. B. Herrmann, Y. Hashash and J. P. Singh are appreciated. This work was supported by the Mid-America Earthquake Center under the Earthquake Engineering Research Centers Program of the National Science Foundation under Award Number EEC-9701785.

Reference

Atkinson, G.M., "Source Spectra for Earthquakes in Eastern North America," BSSA, Vol. 83, pp.1778-1798, 1993.

Atkinson, G.M., "Notes on Ground Motion Parameters for Eastern North America: Duration and H/V Ratio," BSSA, Vol. 83, pp.587-596, 1993.

Atkinson, G.M. and D.M. Boore, "Ground-Motion Relations for Eastern North America," BSSA, Vol. 85, No. 1, pp.17-30, Feb. 1995.

Atkinson, G.M. and D.M. Boore, "Evaluation of Models for Earthquake Source Spectra in Eastern North America," BSSA, Vol. 88, No. 4, pp.917-934, Aug. 1998.

Beresnev, I.A. and G.M. Atkinson, "Modeling Finite-Fault Radiation from the ω^2 Spectrum," BSSA, Vol.87, No. 1, pp.67-84, Feb. 1997.

Beresnev, I.A. and G.M. Atkinson, "FINSIM – a FORTRAN Program for Simulating Stochastic Acceleration Time Histories from Finite Faults," SRL, Vol. 69, No. 1, pp. 27-32, Jan/Feb 1998.

Beresnev, I.A. and G.M. Atkinson, "Stochastic Finite-Fault Modeling of Ground Motions from the 1994 Northridge, California, Earthquakes. I. Validation on Rock Sites," BSSA, Vol.88, No. 6, pp.1392-1401, Dec. 1998.

Beresnev, I.A. and G.M. Atkinson, "Stochastic Finite-Fault Modeling of Ground Motions from the 1994 Northridge, California, Earthquakes. II. Widespread Nonlinear Response at Soil Sites," BSSA, Vol.88, No. 6, pp.1402-1410, Dec. 1998.

Boore, D.M. and L.T. Brown, "Comparing Shear-Wave Velocity Profiles From Inversion of Surface-Wave Phase Velocities with Downhole Measurements: Systematic Differences Between the CXW Method and Downhole Measurements at Six USC Strong-Motion Sites," SRL, Vol. 79, No. 3, pp.222-229, May/June 1998.

Boore, D.M. and W.B. Joyner, "Estimation of Ground Motion at Deep-Soil Sites in Eastern North America", BSSA, Vol. 81, No. 6, pp.2167-2185, 1991.

Boore, D.M. and W.B. Joyner, "Site Amplifications for Generic Rock Sites," BSSA, Vol. 87, No. 2, pp.327-341, April 1997.

Boore, D.M., "SMSIM – Fortran Programs for Simulating Ground Motions from Earthquakes: Version 1.0," US Geological Survey, Open File Report 96-80-A, 1996

Borcherdt, R.D. 'New Developments in Estimating Site Effects on Ground Motion', Proceedings of Seminar on New Developments in Earthquake Ground Motion Estimation and Implications for Engineering Design Practice, Applied Technology Council, ATC 35-1, 1994.

Brune, J.N., "Tectonic Stress and the Spectra of Seismic Shear Waves from Earthquakes," J. Geophysical Research, Vol. 75, No. 26, pp.4997-5009, Sept. 1970.

Brune, J.N., “Correction,” J. Geophysical Research, Vol. 76, No. 20, p.5002, July 1971

Collins, K. R., Wen, Y. K., and Foutch, D. A. “Dual-Level Design: A Reliability-Based Methodology”, Earthquake Engineering and Structural Dynamics, Vol. 25, No. 12, pp. 1433-1467, 1996.

Dorman, J. and R. Smalley, “Low-Frequency Seismic Surface Wave in the New Madrid Zone,” SRL, Vol. 65, pp.137-148, 1994.

EPRI, “Guidelines for Determining Design Basis Ground Motions”, EPRI TR-102293, Project 3302, Final Report, Nov 1993.

Frankel, A., C. Mueller, T. Barnhard, D. Perkins, E.V. Leyendecker, N. Dickman, S. Hanson and M. Hopper, “National Seismic-Hazard Maps: Documentation”, USGS Open-File Report 96-532, June 1996.

Hashash, Y., “Typical Soil Profiles for Mid-America,” Personal Communication, Department of Civil and Environmental Engineering, University of Illinois at Urbana-Champaign, May 3 1999.

Harmsen, S., D. Perkins and A. Frankel, “Deaggregation of Probabilistic Ground Motions in the Central and Eastern United States,” BSSA, Vol. 89, No.1, pp.1-13, Feb. 1999.

Herrmann, R. B. “Generic Soil Profiles for St. Louis”, July, 1999, Personal Communication.

Herrmann, R. B. and A. Akinci, “Mid-America Ground Motion Models,” URL http://www.eas.slu.edu/People/RBHerrmann/MAEC/maecgnd.html, March 1999.

Johnston, A.C., “Seismic Moment Assessment of Earthquakes in Stable Continental Regions – I. Instrumental Seismicity,” Geophysical Journal International, Vol. 124, pp.381-414, 1996.

Johnston, A.C., “Seismic Moment Assessment of Earthquakes in Stable Continental Regions – III. New Madrid 1811-1812, Charleston 1886 and Lisbon 1755,” Geophysical Journal International, Vol. 126, pp.314-344, 1996.

Joyner, W.B., R.E. Warrick and T.E. Fumal, “The Effect of Quaternary Alluvium on Strong Ground Motion in the Coyote Lake, California, Earthquake of 1979,” BSSA,Vol. 71, No. 4, pp.1333-1349, August 1981.

Press, W.H., S.A. Teukolsky, W.T. Vetterling and B.P. Flannery, “Numerical Recipes in Fortran: The Art of Scientific Computing ,” 2nd Ed., Cambridage University Press, 1992.

Saikia, C.K. & P.G. Somerville, "Simulated Hard-Rock Motions in Saint Louis, Missouri, from Large New Madrid Earthquakes (Mw>=6.5)," BSSA, Vol. 87, No. 1, pp.123-139, Feb 1997.

Shome, N. and Cornell, C. A. “ Probabilistic Seismic Demand Analysis of Nonlinear Structures”, Rept. No. RMS-35, Department of Civil Engineering, Stanford University, March, 1999.

Somerville, P.G., K. Irikura, R. Graves, S. Sawada, D. Wald, N. Abrahamson, Y. Iwasaki, T. Kagawa, N. Smith and A. Kowada, “Characterizing Crustal Earthquake Slip Models for the Prediction of Strong Ground Motion,” SRL, Vol. 70, No. 1, pp.59-80, Jan/Feb 1999.

Wald, D.J., T.H. Heaton and K.W. Hudnut, "The Slip History of the 1994 Northridge, California, Teleseismic, GPS, and Leveling Data," BSSA, Vol. 86, No. 1B, pp.S49-S70, Feb. 1996.

Wang, C.- H. and Wen, Y. K. “Reliability and Redundancy of Pre-Northridge Low-rise Steel Buildings under Seismic Excitation”, Structural Research Series No. 624. Department of Civil and Environmental Engieering, Nov. 1988.

Wheeler, R.L. and A.C. Johnston, “Geological Implications of Earthquake Source Parameters in Central and Eastern North America,” SRL, Vol. 63, pp.491-514, 1992.

--,“Special Issue: The New Madrid Seismic Zone”, Seismological Research Letters, Vol 63, No. 3, July-Sept. 1992.

Table 1. Weights for the Depth Distribution Model (Wheeler and Johnston, 1992)

Depth (km)	Weight
0~ 5	0.250
5~10	0.500
10~15	0.050
15~20	0.050
20~25	0.015
25~30	0.135

Table 2. Representative Soil Profile of Memphis, TN

Layer	Soil column	Thickness (m)	Vs (m/sec)	Density (g/cm^3)
1	Alluvium	7.2	360	1.92
2	Alluvium	4.8	360	2.00
3	Alluvium	14.9	360	2.08
4	Loess	9.0	360	2.16
5	Fluvial Deposits	7.9	360	1.98
6	Jackson Formation	47.3	520	2.08
7	Memphis Sand	245.6	667	2.30
8	Wilex Group	83.3	733	2.40
9	Midway Group	580	820	2.50
10	Bed Rock	Half-Space	3600	2.80

Table 3. Representative Soil Profile of Carbondale, IL

Layer	Soil column	Thickness (m)	Vs (m/sec)	Density (g/cm^3)
1	Cahokis Alluvium	10.4	140	2.0
2	Henry Formation	10.0	250	2.1
3	Henry Formation	25.6	270	2.1
4	Mississipi Embayment	119.0	280	2.3
5	Pennsylvanian Limestone	835.0	2900	2.6
6	Bed Rock	Half-Space	3600	2.8

Table 4. Representative Soil Profile of St. Louis, MO

Layer	Soil column	Thickness (m)	Vs (m/sec)	Density (g/cm^3)
1	Modified Loess	5.7	185	1.9
2	Glacio-Fluvial	10.0	310	2.1
3	Mississipian Limestone	984.3	2900	2.6
4	Bed Rock	Half-Space	3600	2.8

Seismicity surrounding Memphis TN, Carbondale IL, and St. Louis MO

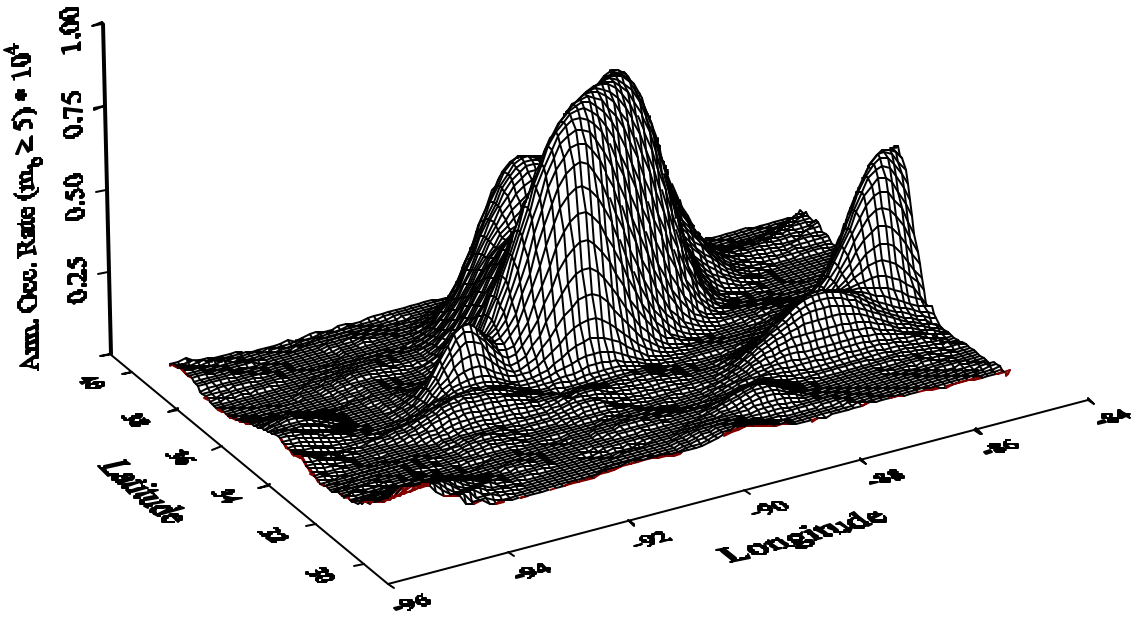

Figure 1. Annual occurrence rate per 0.1×0.1 degree square of earthquakes of M_b 5 or larger.

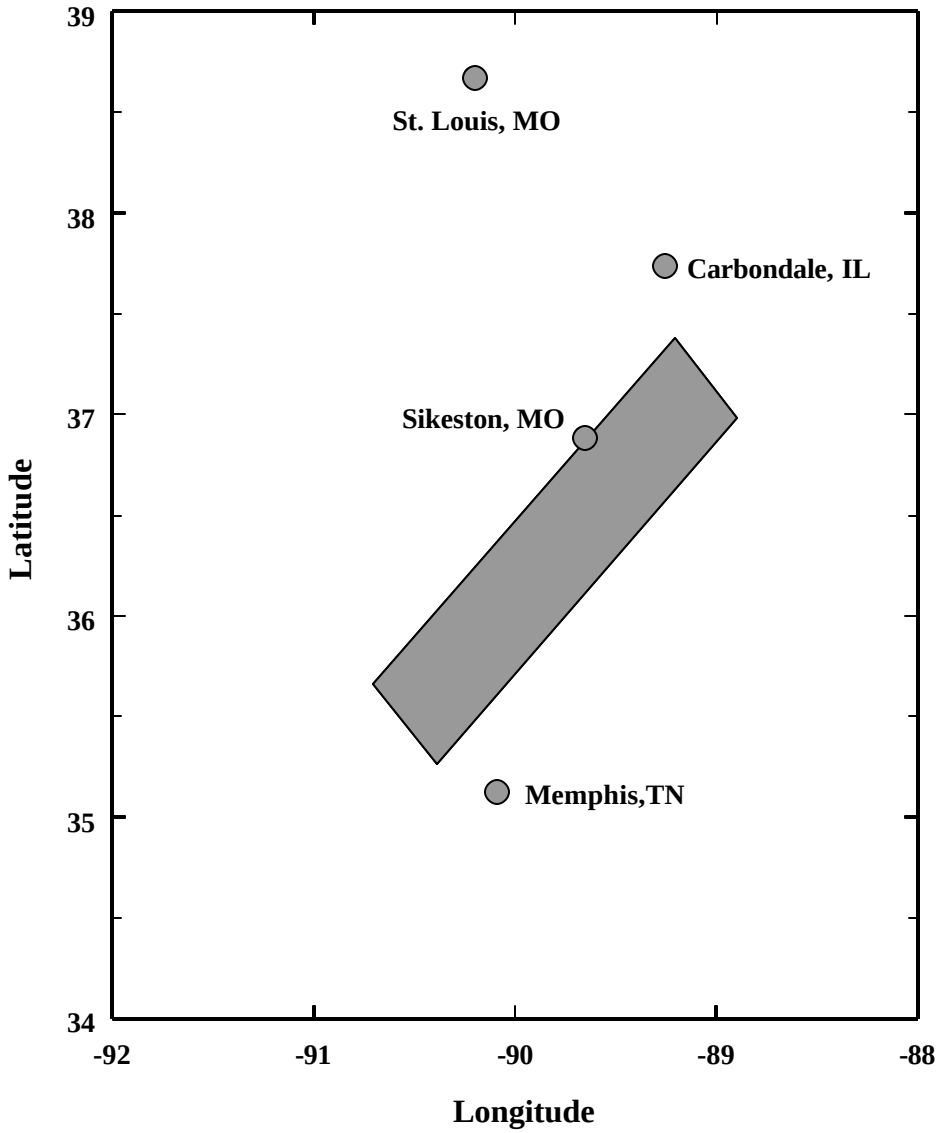

Figure 2. Seismic zone of M_w-8 earthquakes.

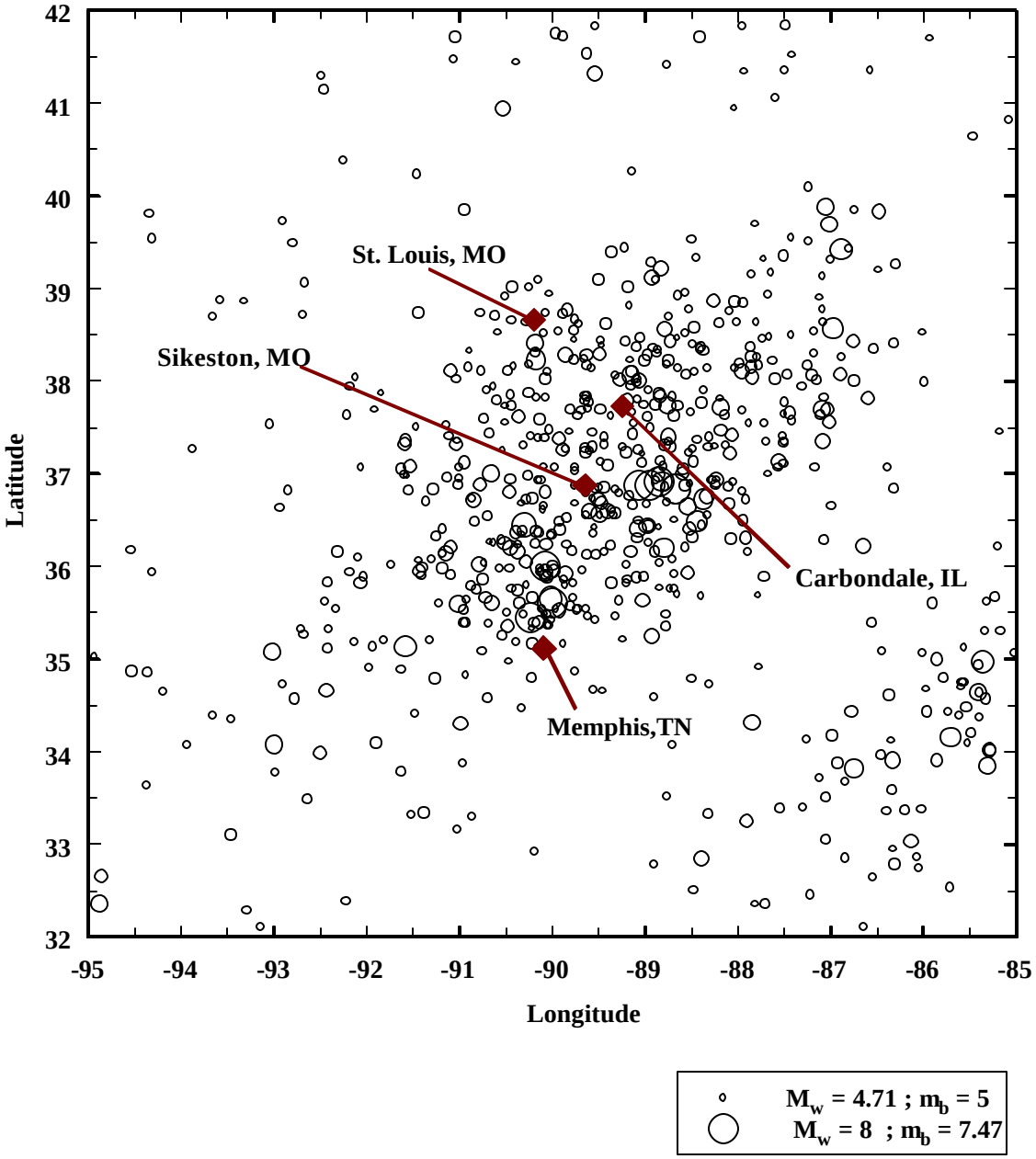

Figure 3. Epicenters and magnitudes of earthquakes of simulated 6000-year record.

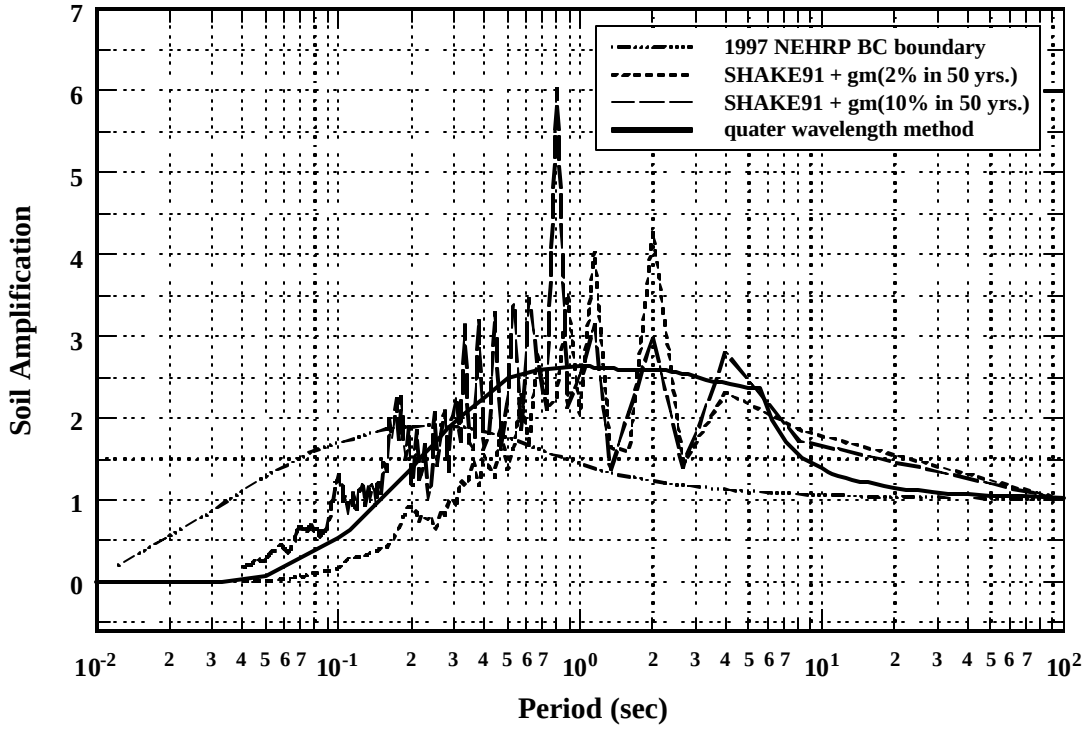

Figure 4. Soil Amplification Factor for Representative Soil Profile, Memphis, TN.

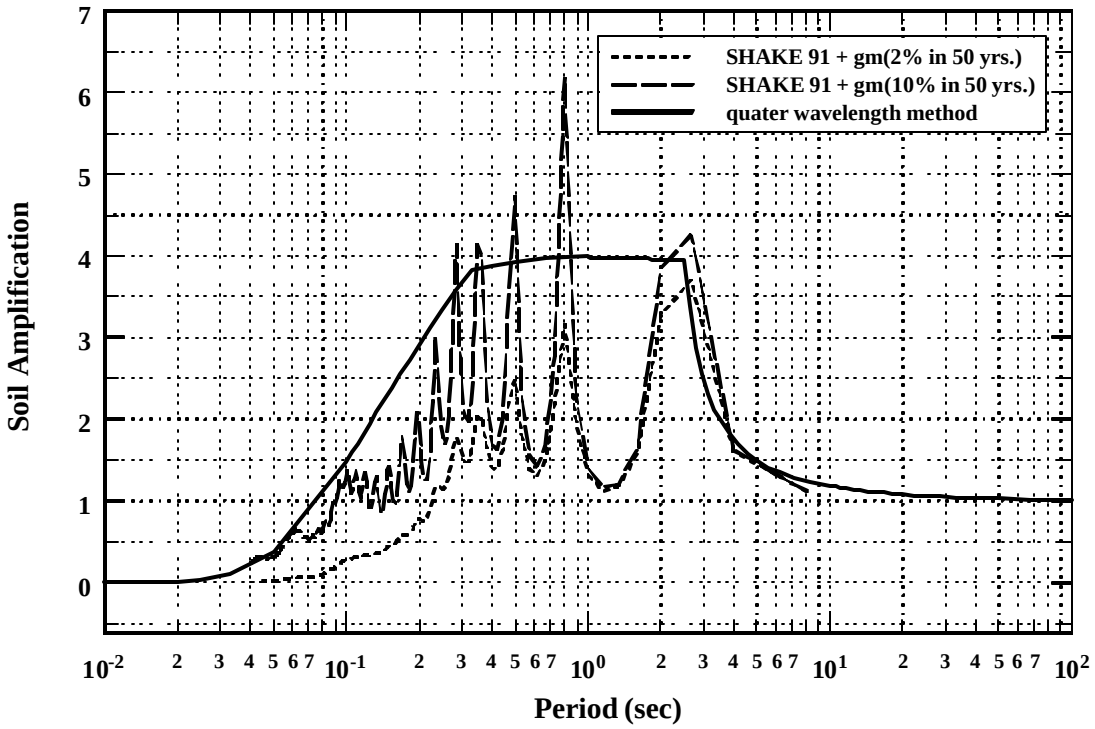

Figure 5. Soil Amplification Factor for Representative Soil Profile, Carbondale, IL

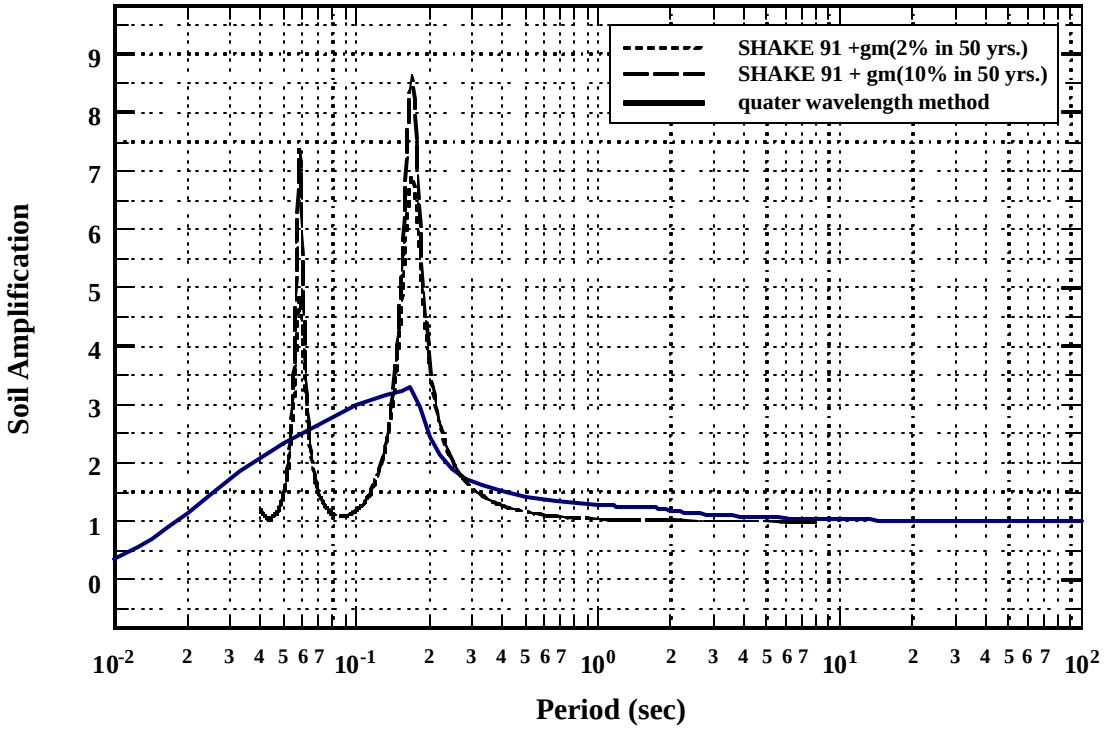

Figure 6. Soil Amplification Factor for Representative Soil Profile, St. Louis, MO.

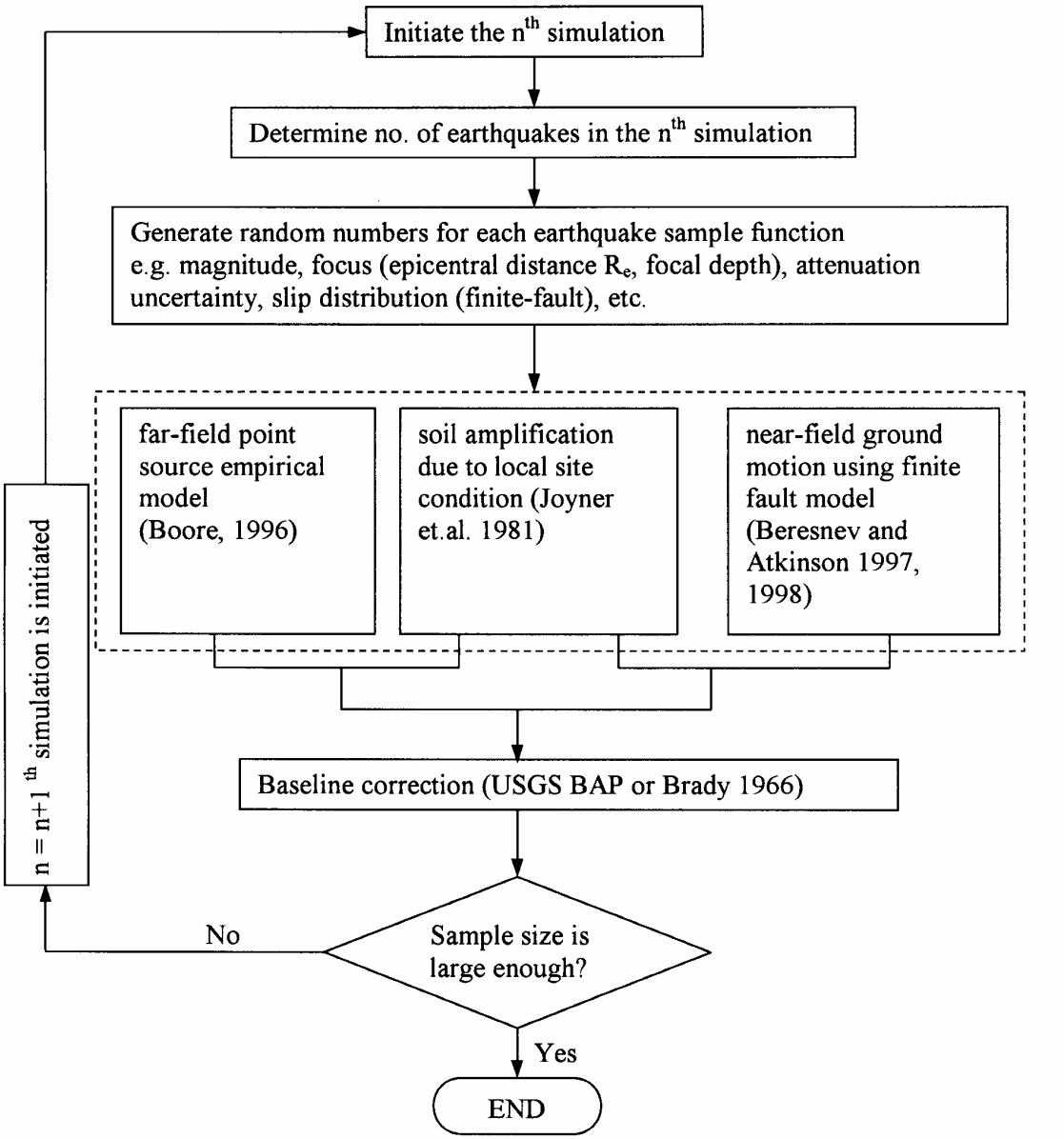

Figure 7. Ground Motion Simulation flowchart.

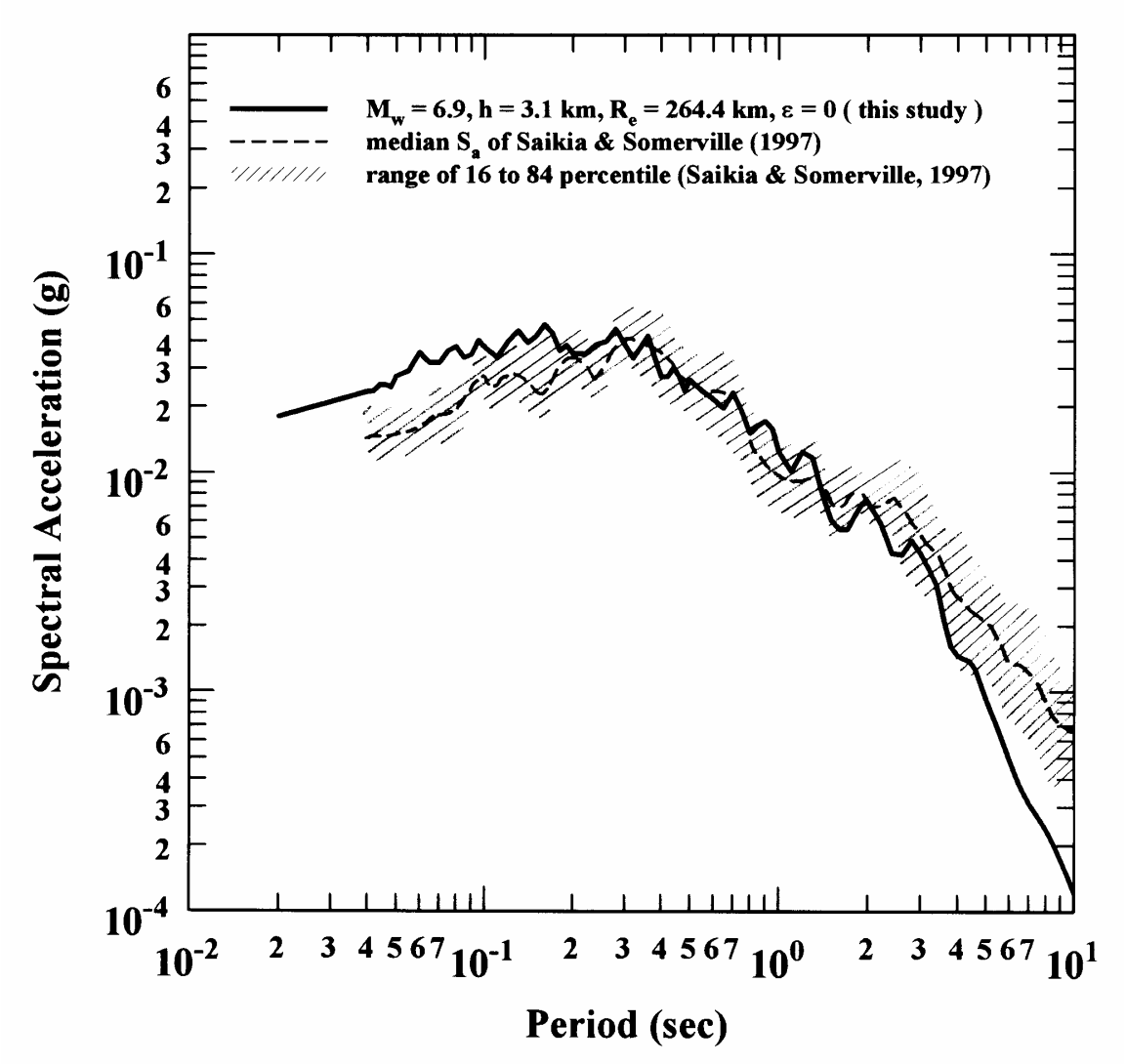

Figure 8. Comparison of Response Spectra Based on Point-Source Model with Saikia and Somerville's Broadband Model (1997).

M_w = 8, h = 25.6 km, R_e = 79.3 km, R_{jb} = 61.7 km, e = -0.69

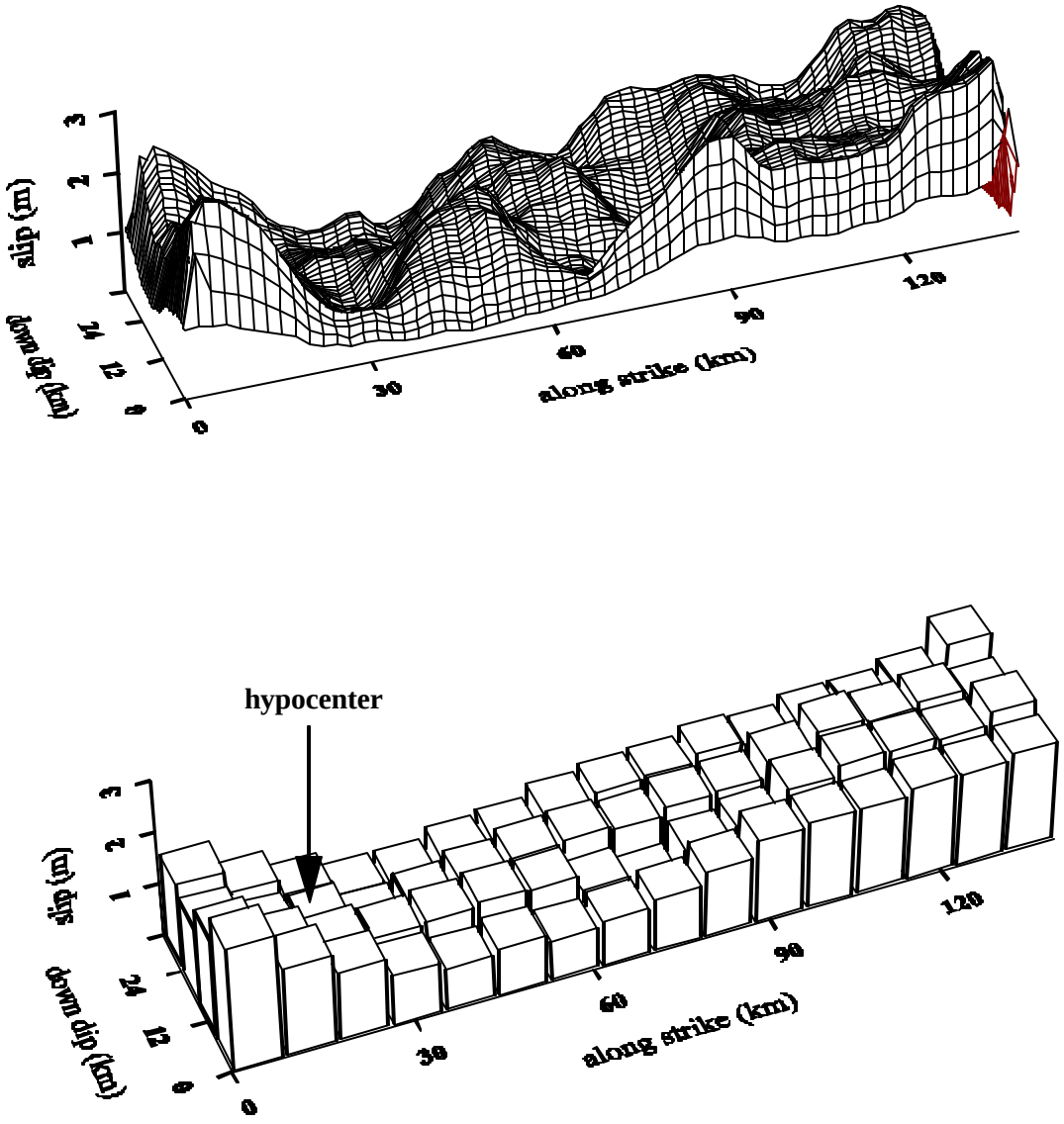

Figure 9. Sample of Random Slip Distribution Based on Correlated Random Field Model and Dicretization for Finite Fault Model.

M_w = 8, h = 33.9 km, R_e = 186.1 km, R_{jb} = 61.8 km, e = 0.09

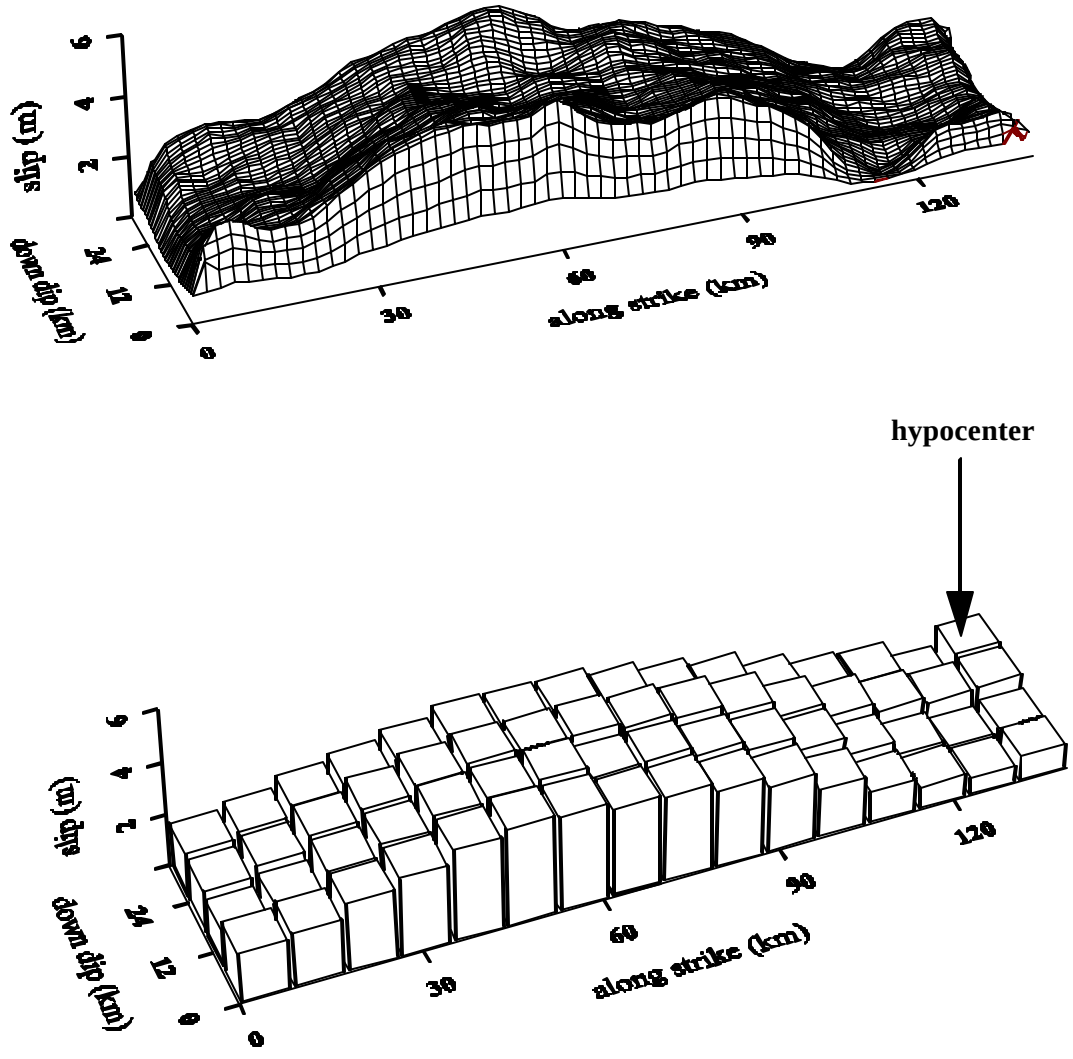

Figure 10. Sample of Simulated Slip Distribution Based on Correlated Random Field Model and Dicretization for Finite Fault Model.

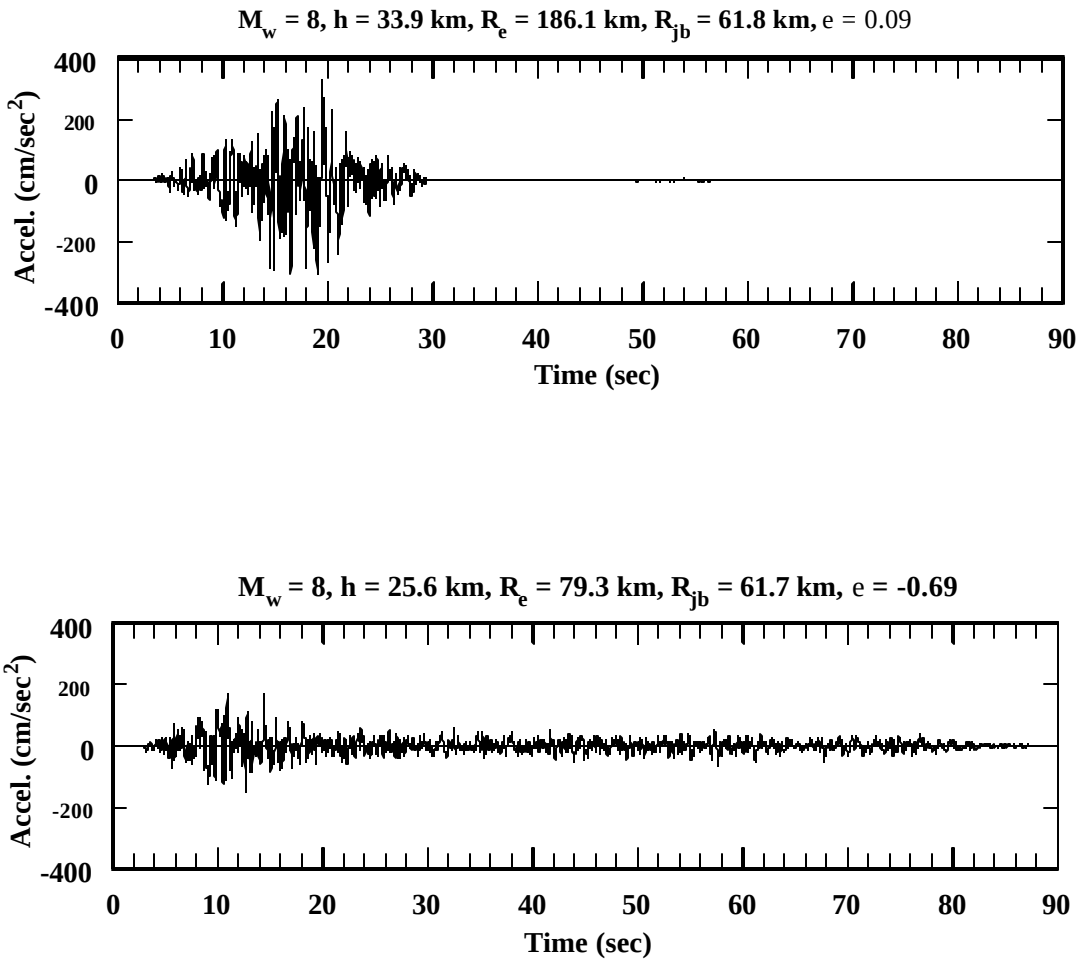

Figure 11. Near-Source "Doppler" Effects of Simulated Acceleration Time Histories at Memphis, TN, by the Finite Fault Model.

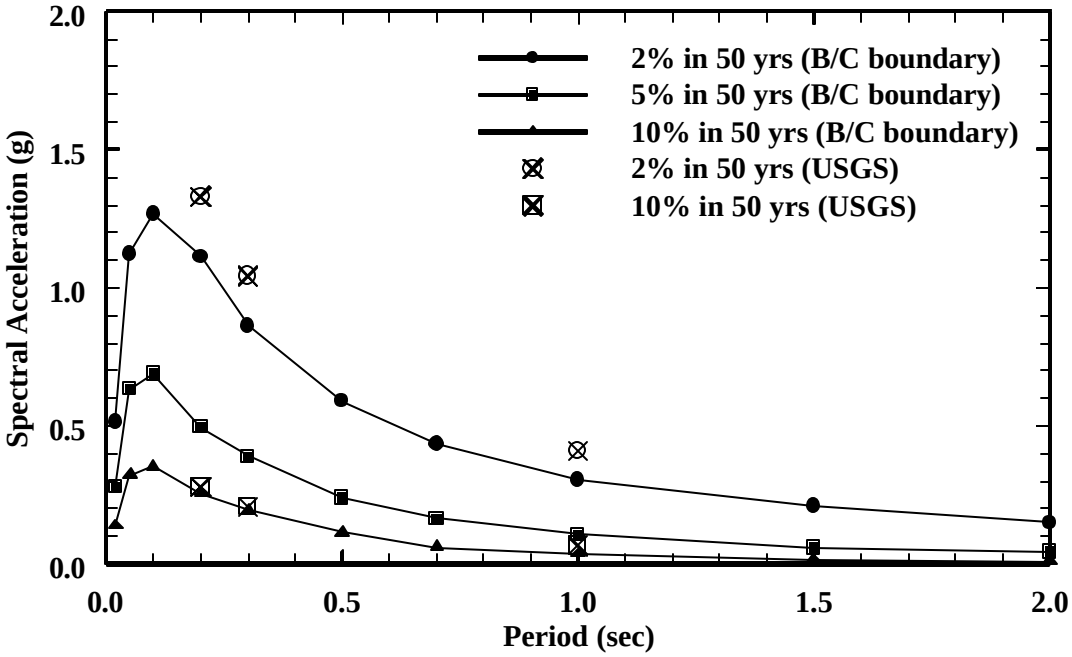

Figure 12. Uniform Hazard Response Spectra for B/C Boundary at Memphis and Comparison with USGS National Hazard Maps Results.

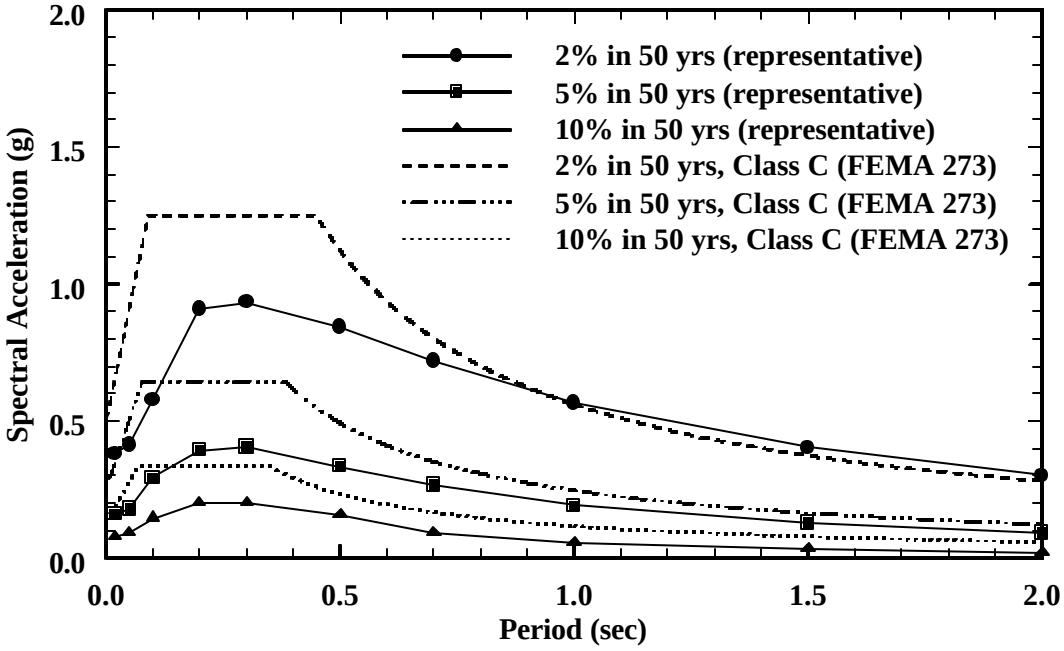

Figure 13. Uniform Hazard Response Spectra for Representative Soil Profile at Memphis, TN and Comparison with FEMA 273 Response Spectra.

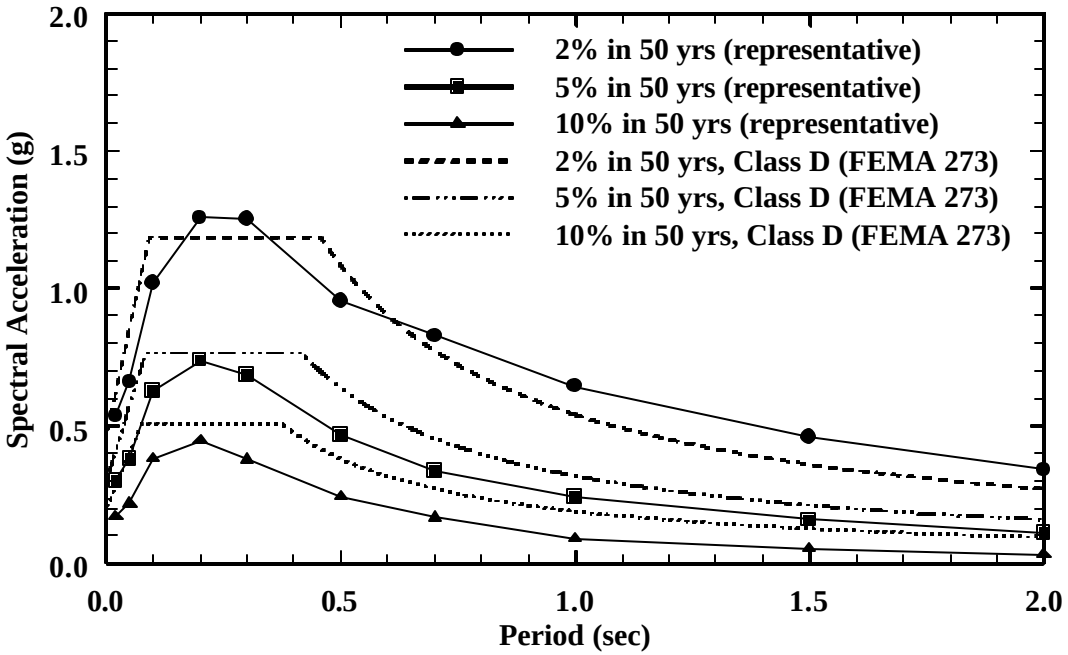

Figure 14. Uniform Hazard Response Spectra for Representative Soil Profile at Carbondale, IL and Comparison with FEMA 273 Response Spectra.

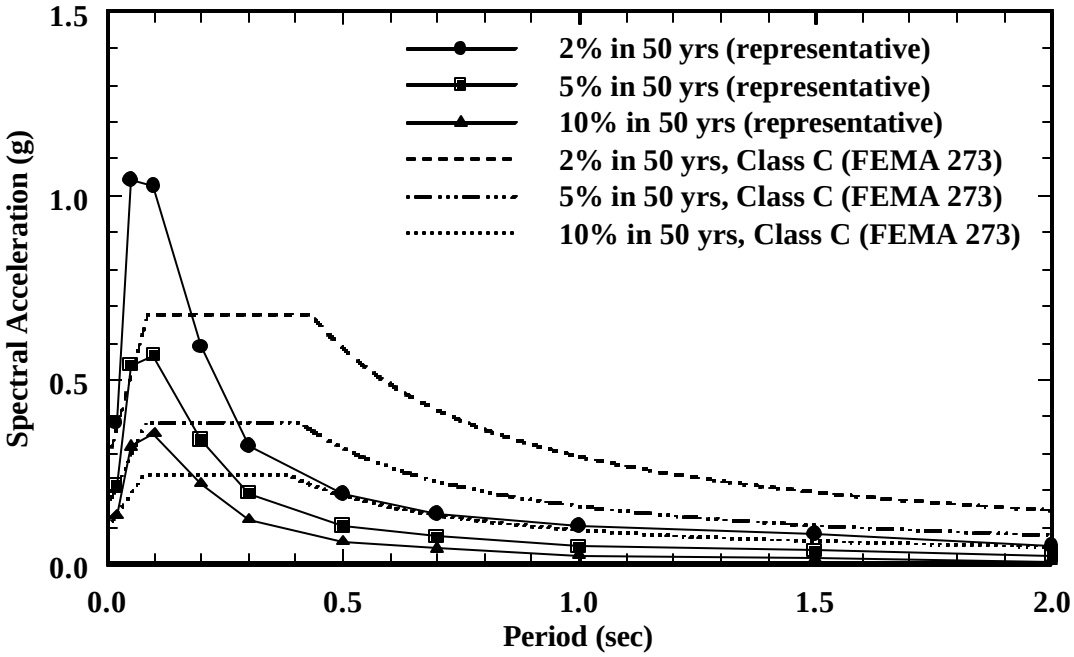

Figure 15. Uniform Hazard Response Spectra for Representative Soil Profile at St. Louis, MO and Comparison with FEMA 273 Response Spectra.

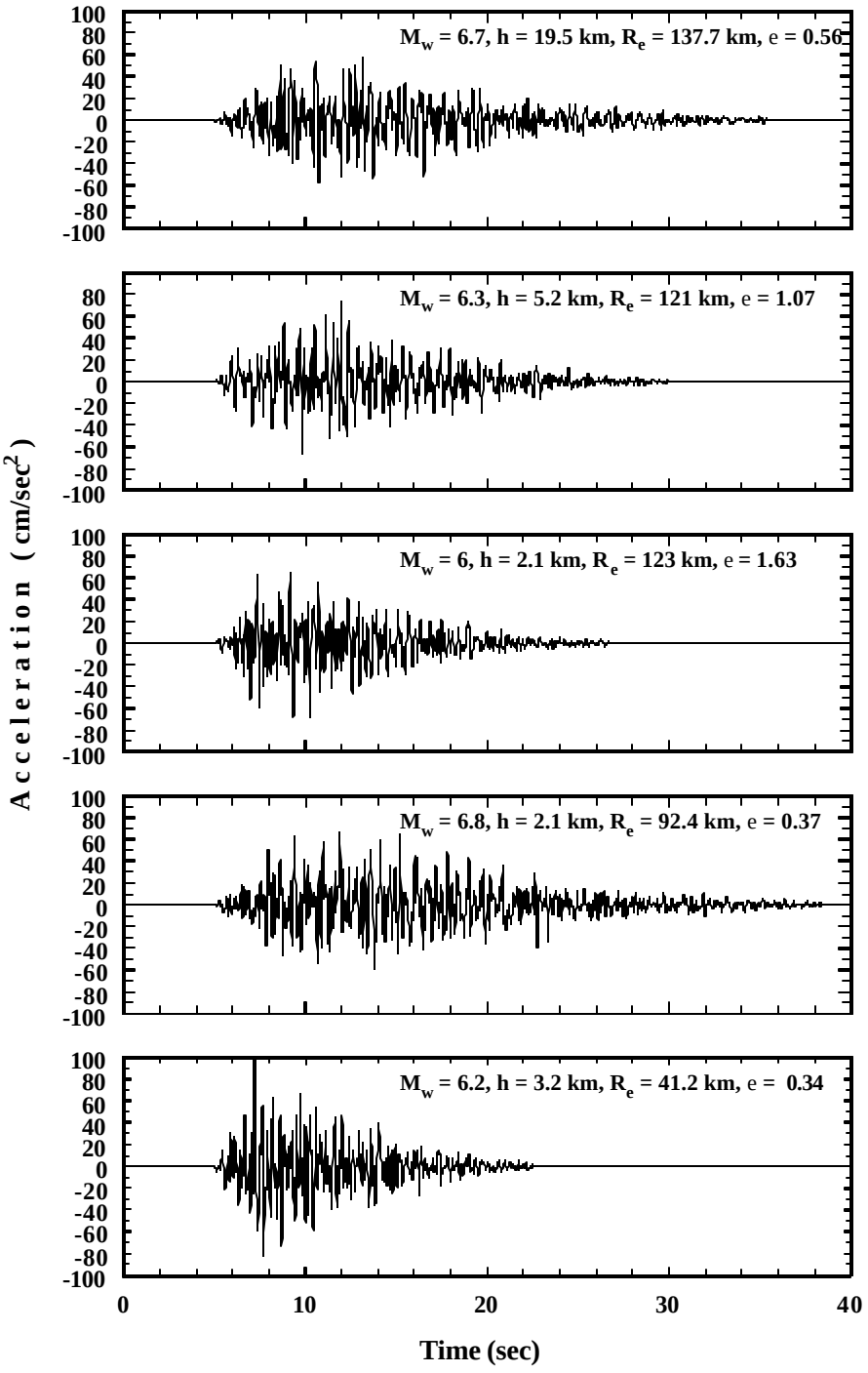

Figure 16. Suite of 10% in 50 years Ground Motions for Representative Soil Profile, Memphis, TN.

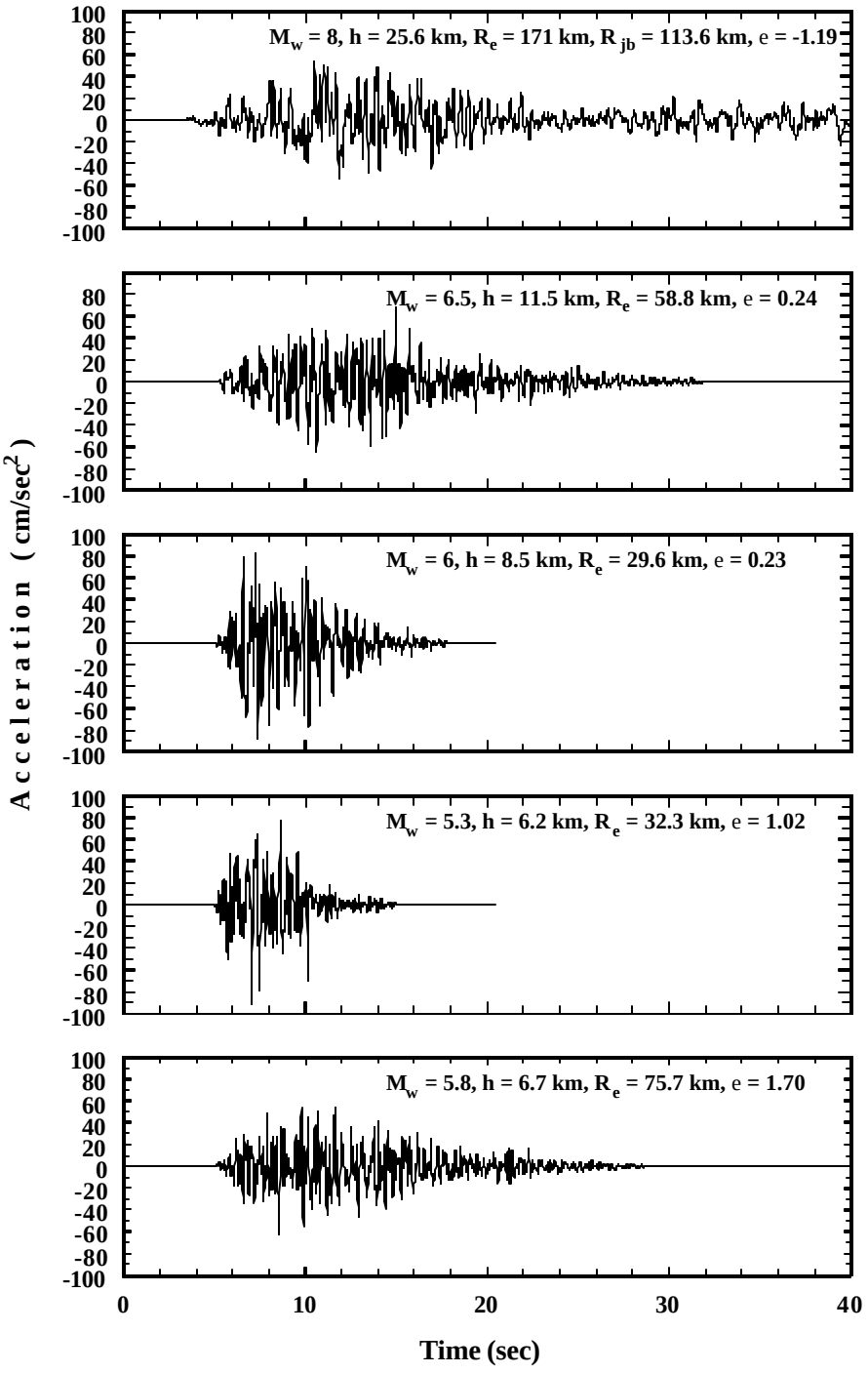

Figure 16. (continued)

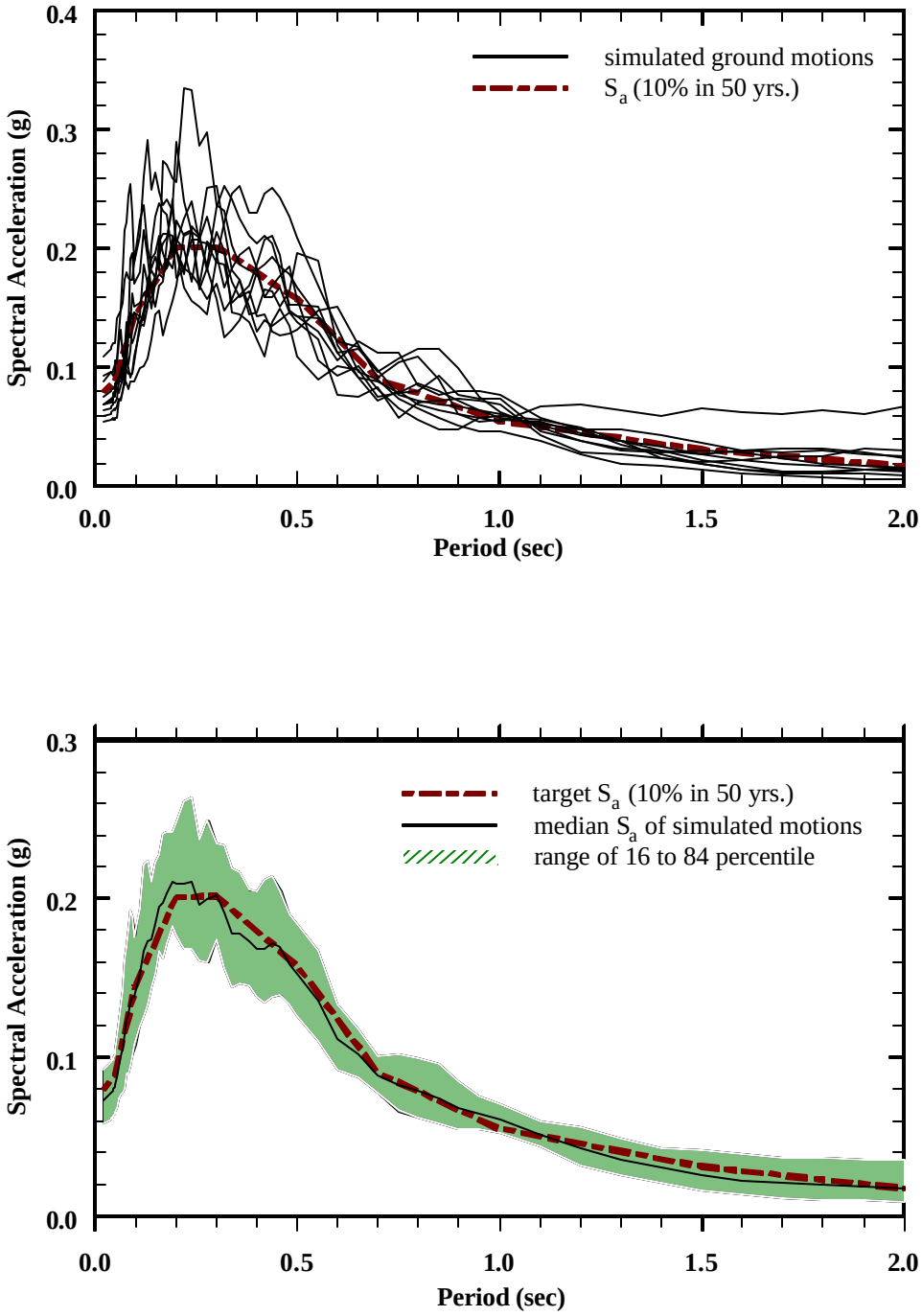

Figure 17. Response Spectra of 10% in 50 years Ground Motion Suite for Representative Soil Profile and Comparison with Target UHRS, Memphis, TN.

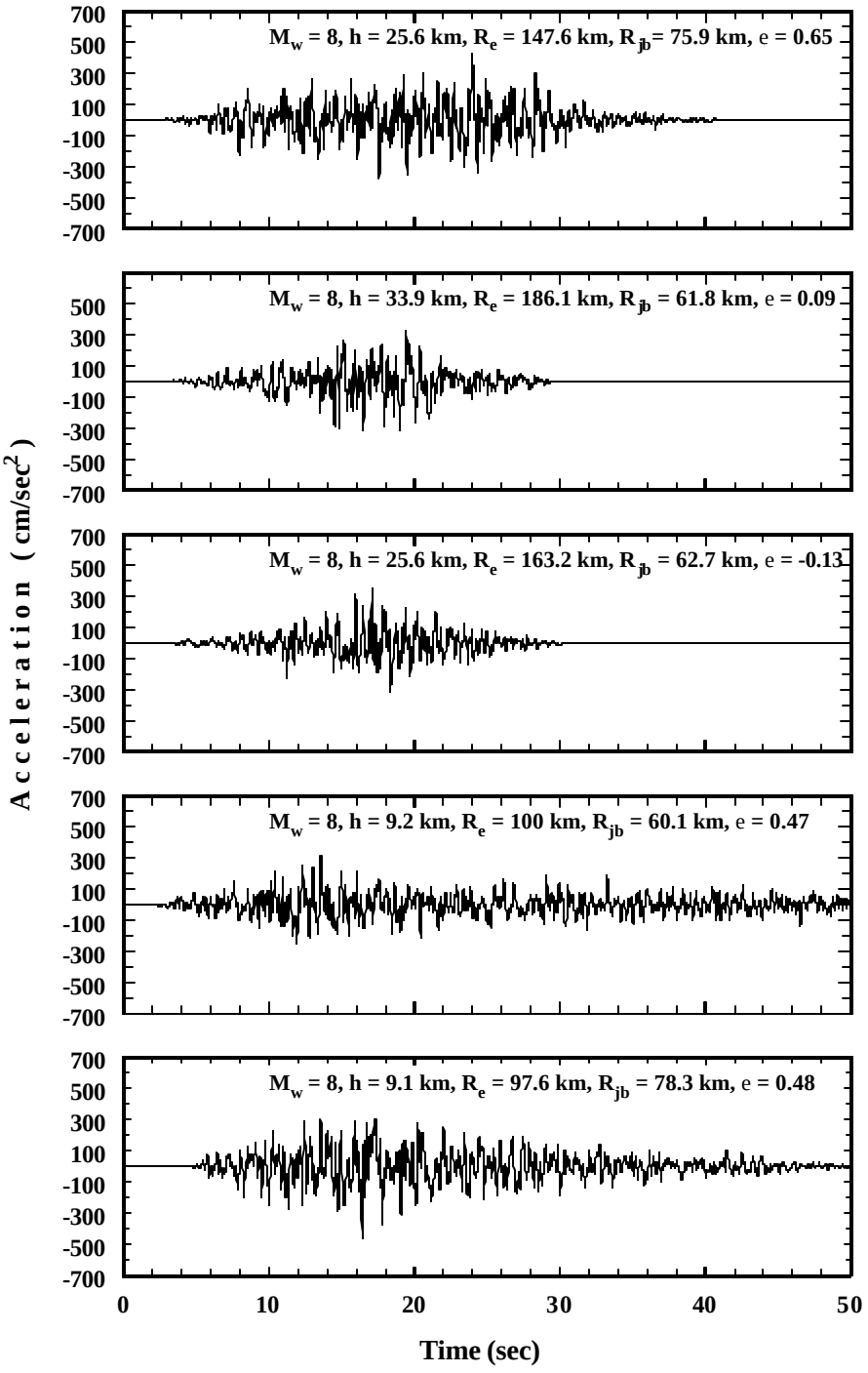

Figure 18. Suite of 2% in 50 years Ground Motions for Representative Soil Profile, Memphis, TN.

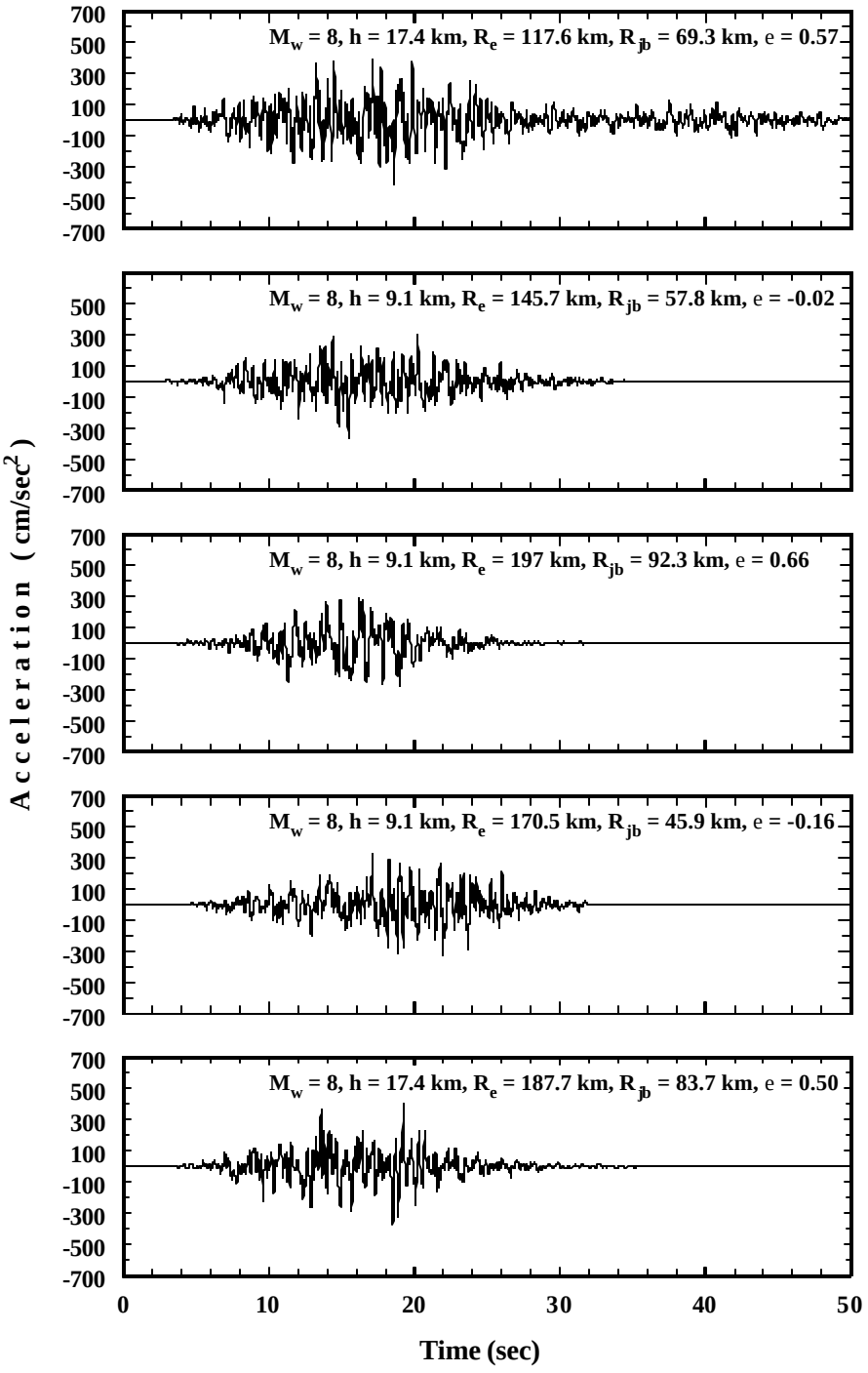

Figure 18 (continued).

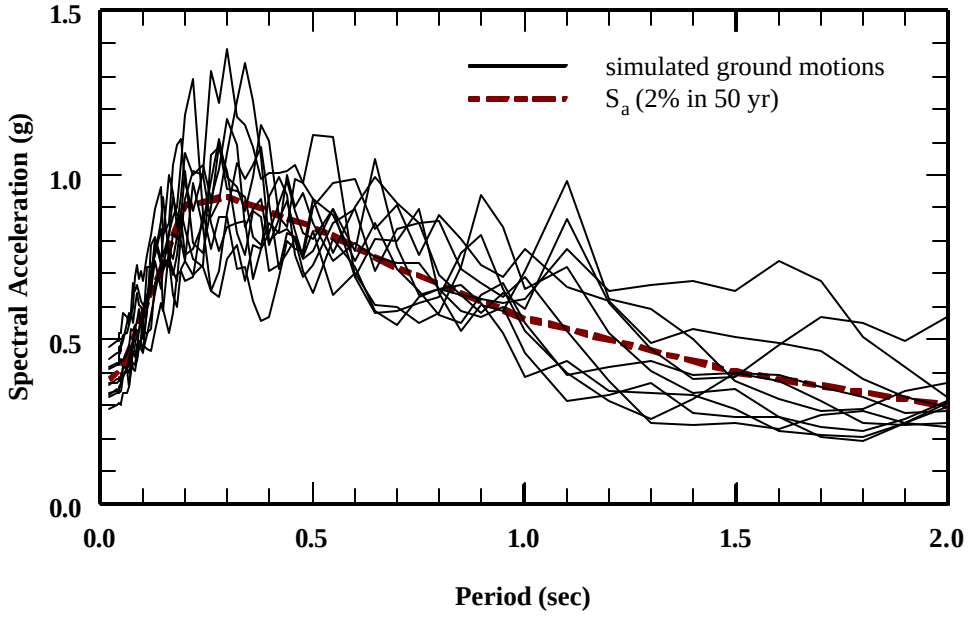

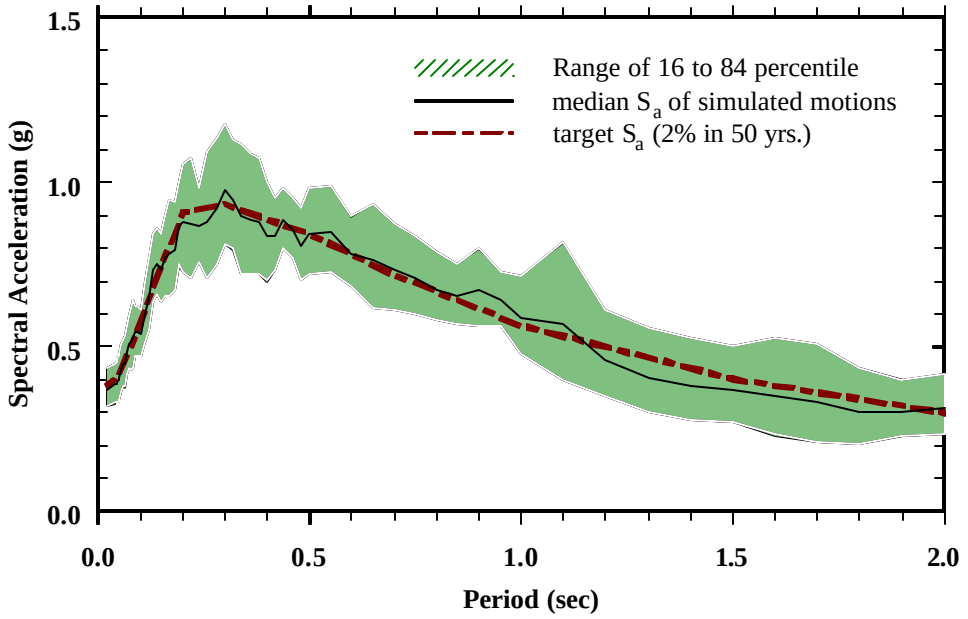

Figure 19. Response Spectra of 2% in 50 years Ground Motion Suite for Representative Soil Profile and Comparison with Target UHRS, Memphis, TN.

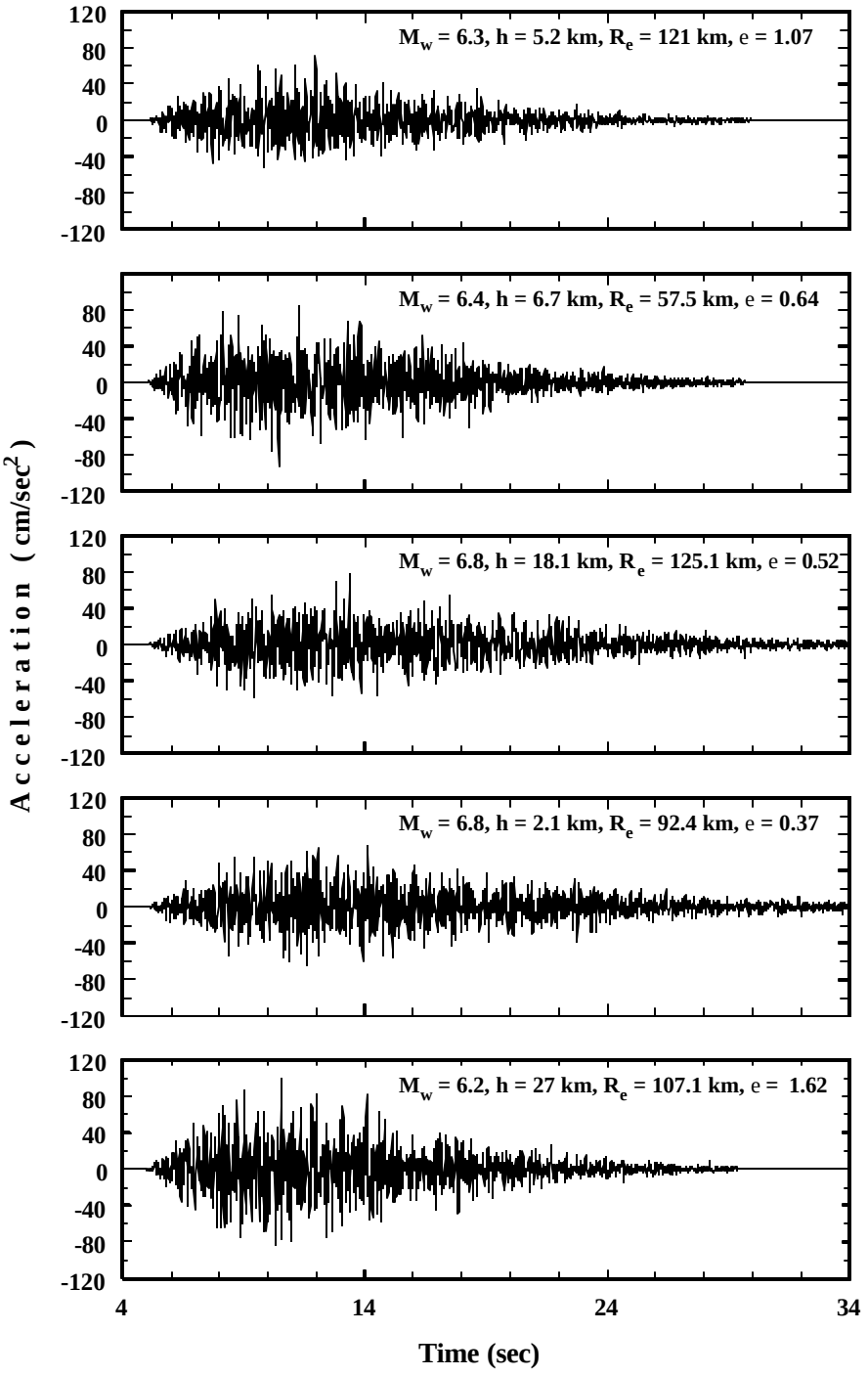

Figure 20. Suite of 10% in 50 yrs Ground Motions for Bedrock (Hard Rock) Memphis, TN.

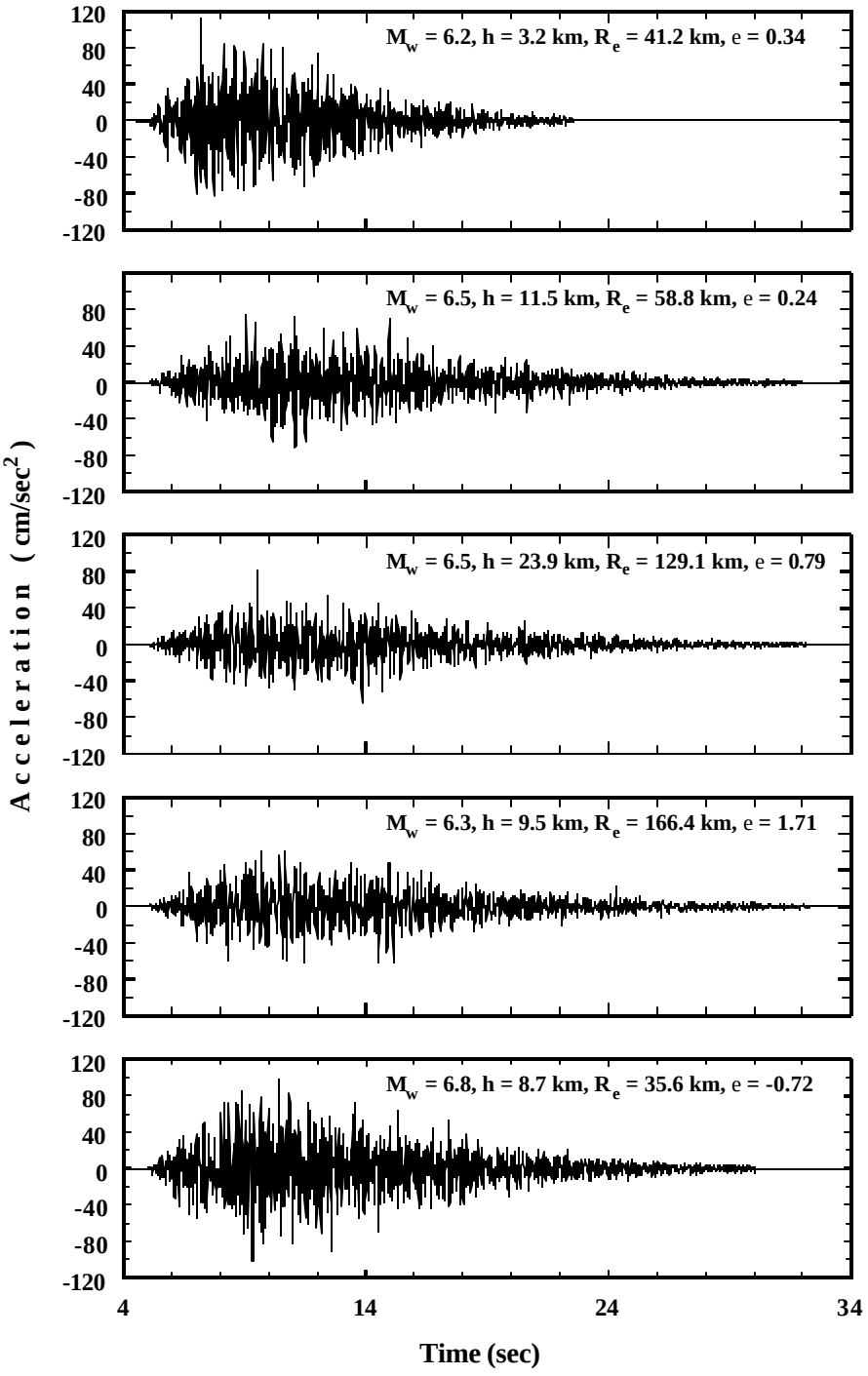

Figure 20 (continued).

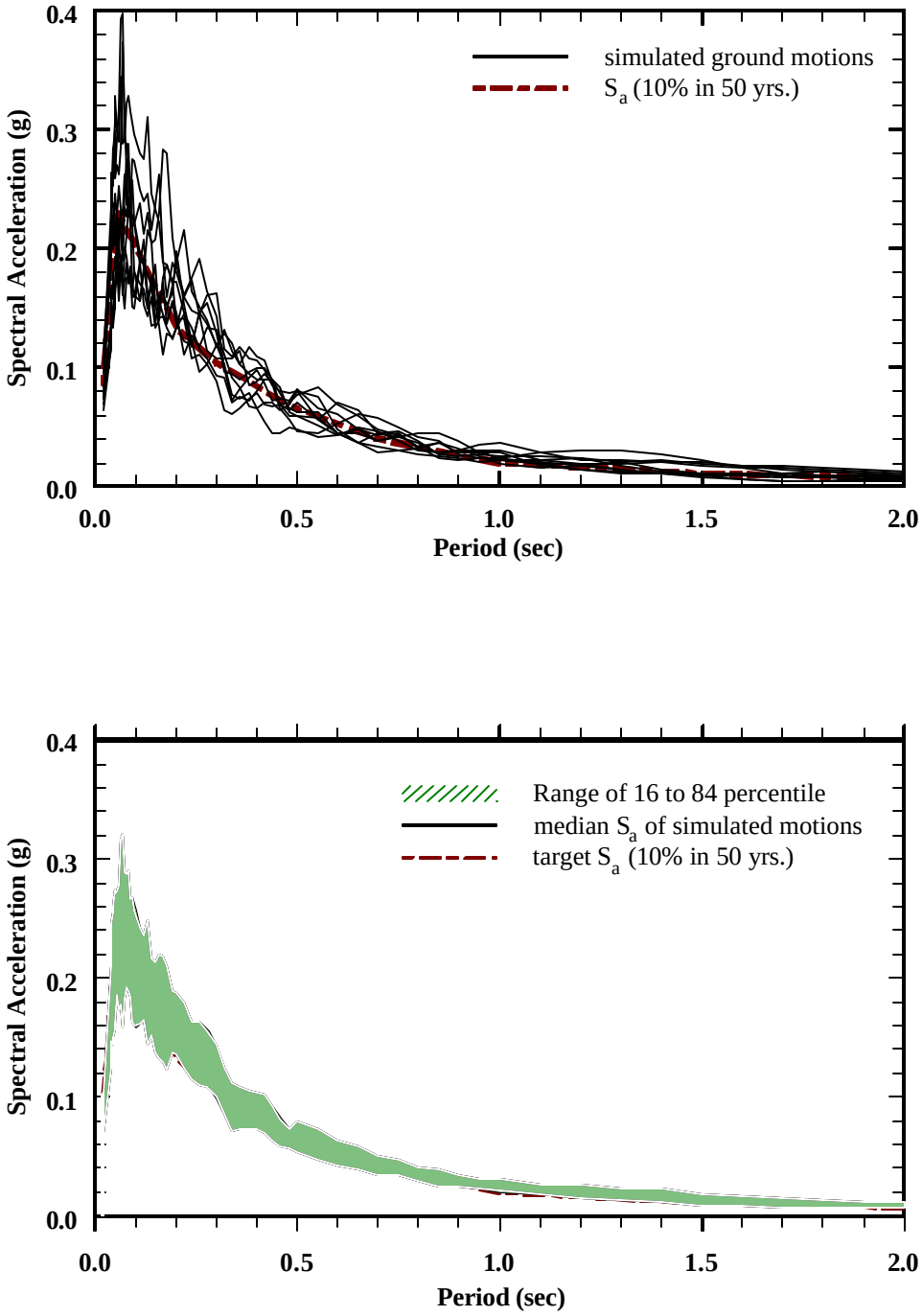

Figure 21. Response Spectra of 10% in 50 years Ground Motion Suite for Bedrock (Hard Rock) and Comparison with Target UHRS, Memphis, TN.

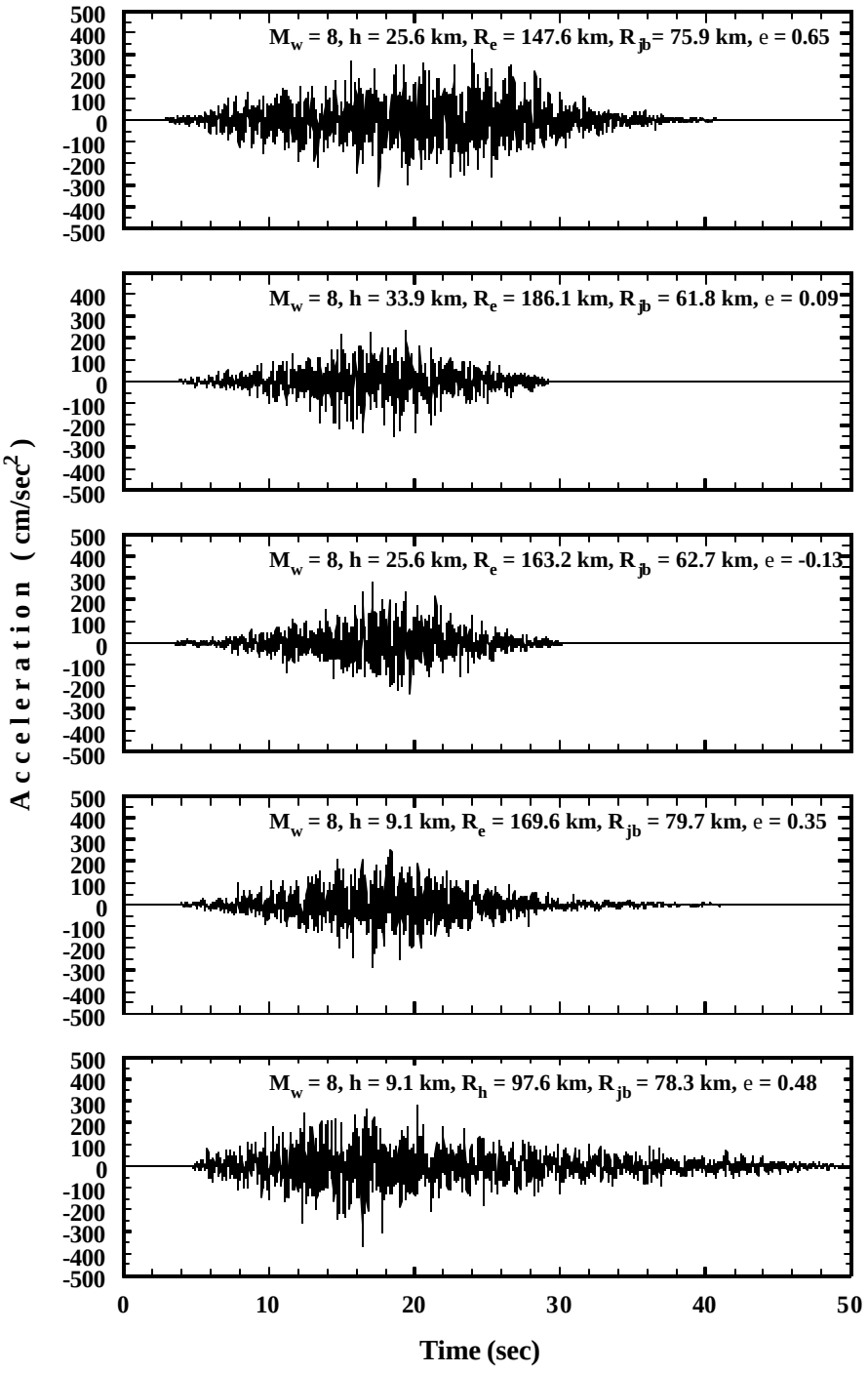

Figure 22. Suite of 2% in 50 years Ground Motions for Bedrock (Hard Rock), Memphis, TN.

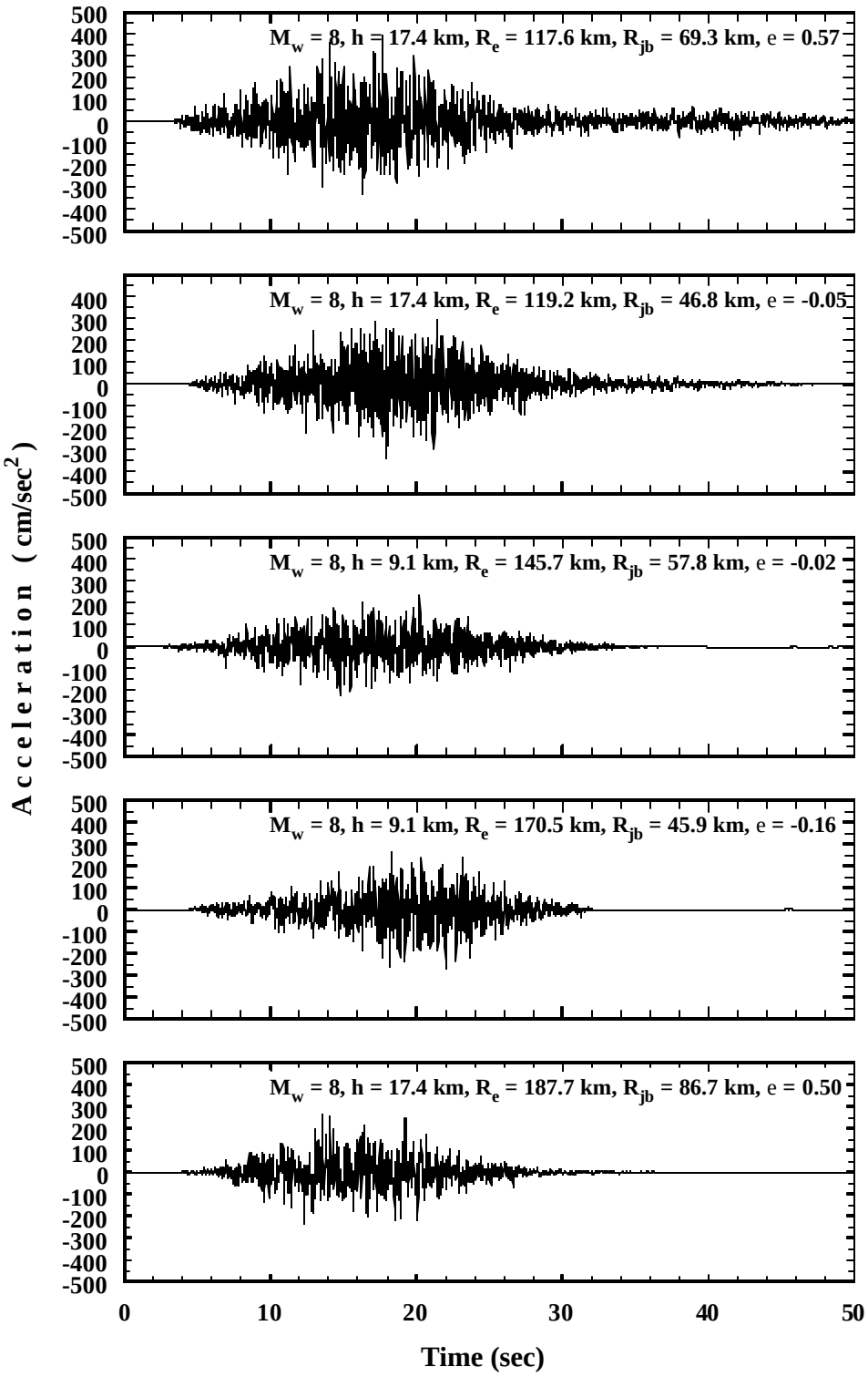

Figure 22 (continued).

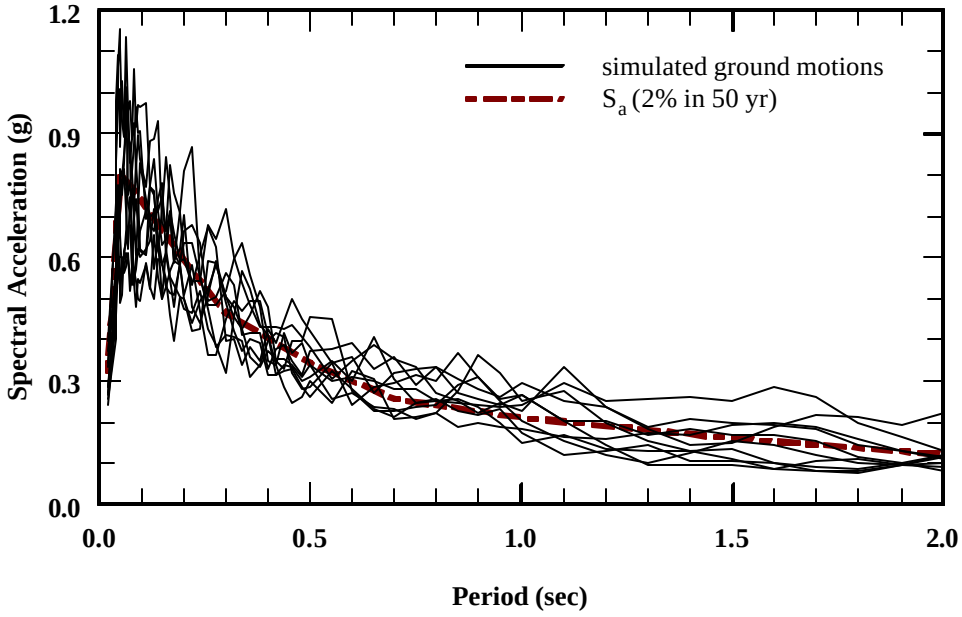

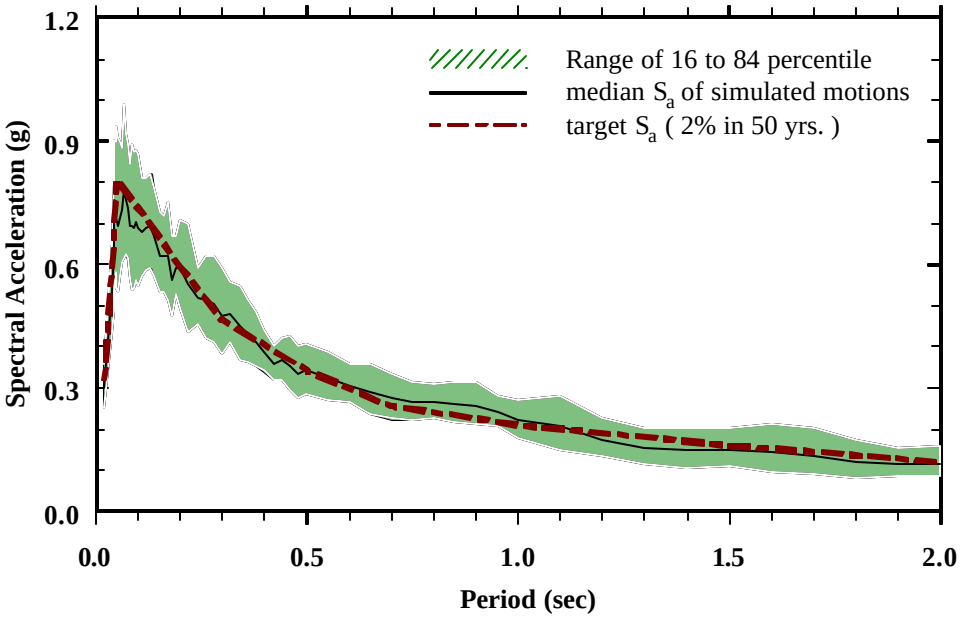

Figure 23. Response Spectra of 2% in 50 years Ground Motion Suite for Bedrock (Hard Rock) and Comparison with Target UHRS, Memphis, TN.

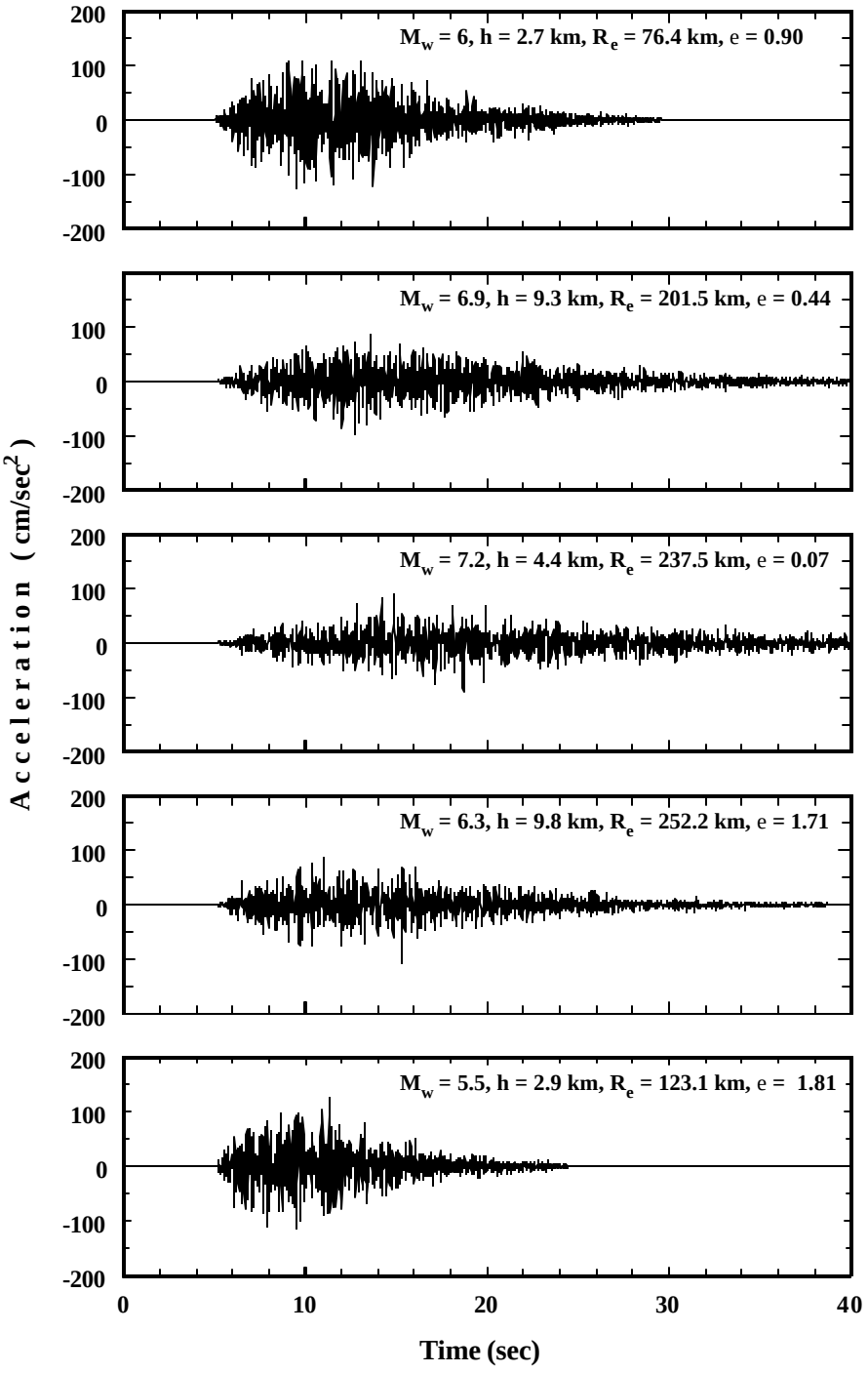

Figure 24. Suite of 10% in 50 years Ground Motions for Representative Soil Profile, St. Louis, MO.

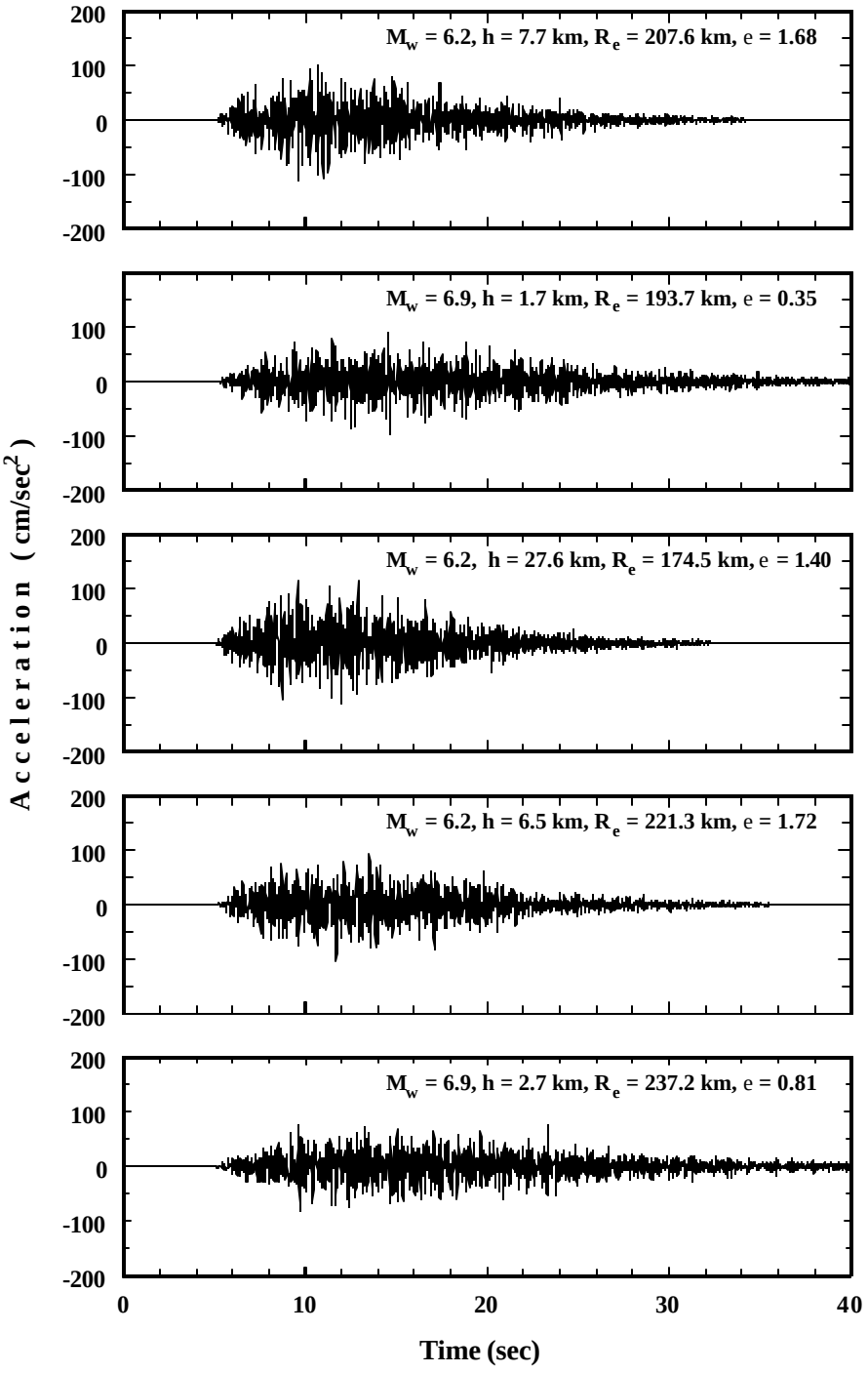

Figure 24 (continued).

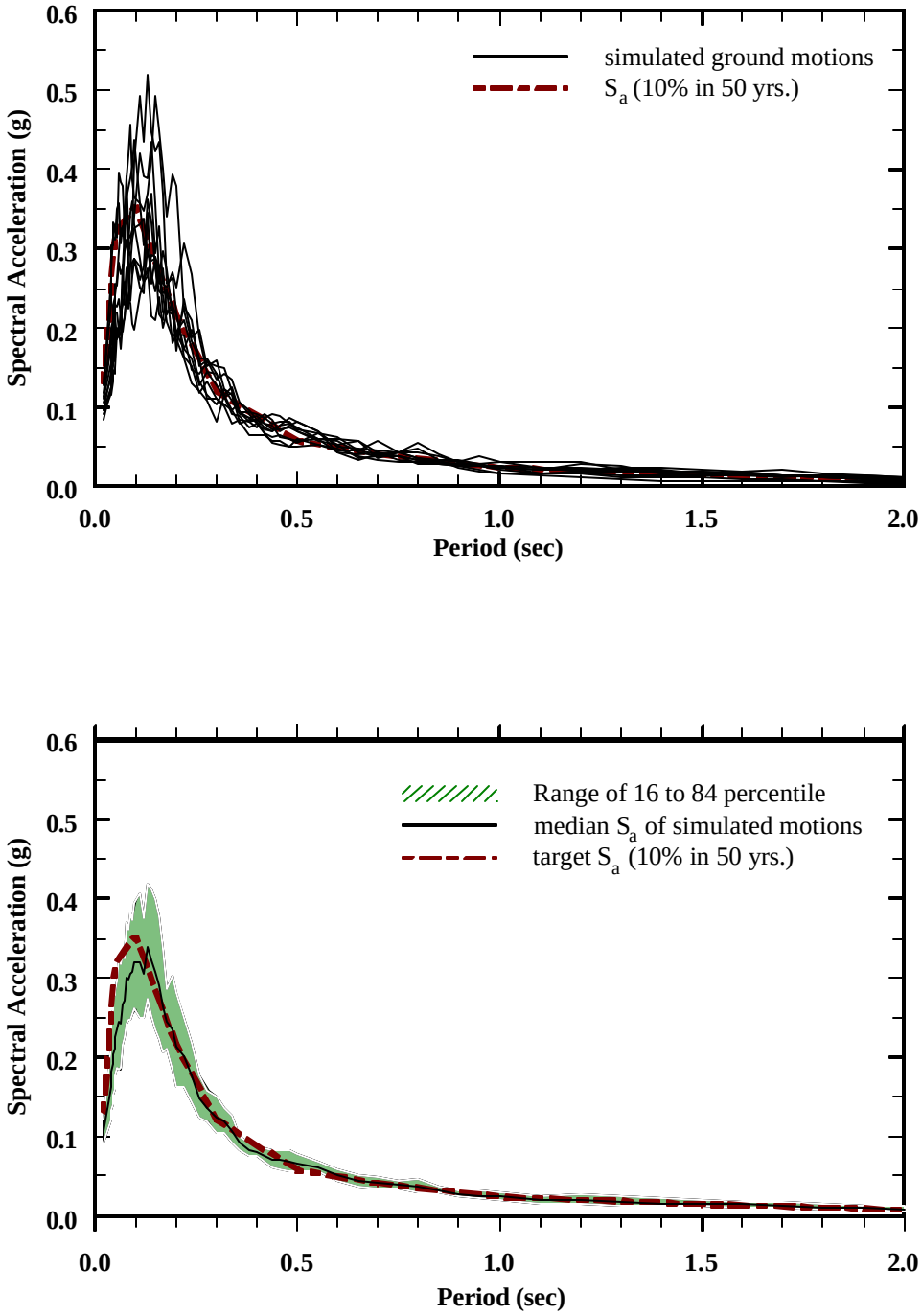

Figure 25. Response Spectra of 10% in 50 years Ground Motion Suite for Representative Soil Profile and Comparison with Target UHRS, St. Louis, MO.

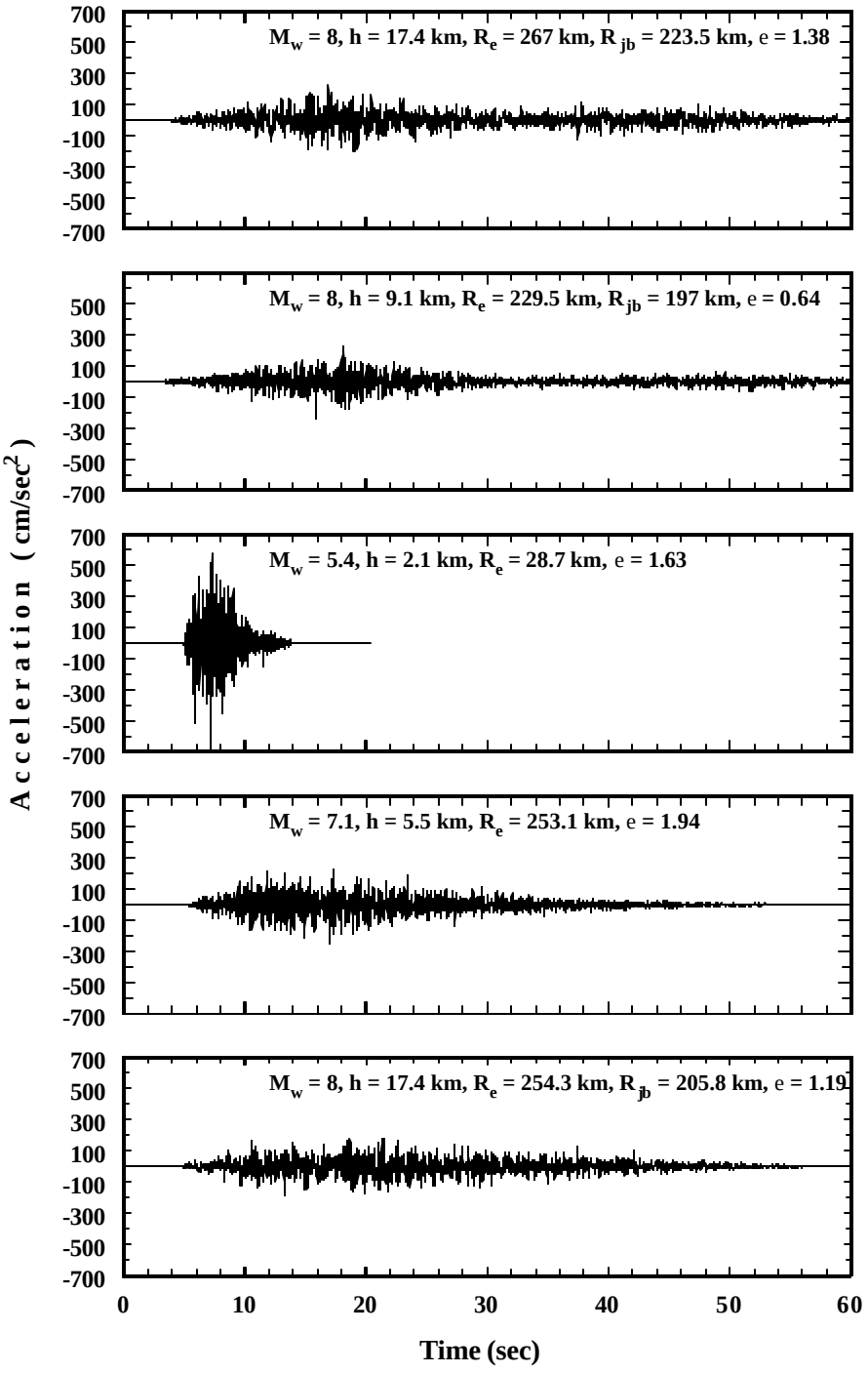

Figure 26. Suite of 2% in 50 years Ground Motions for Representative Soil Profile, St. Louis, MO.

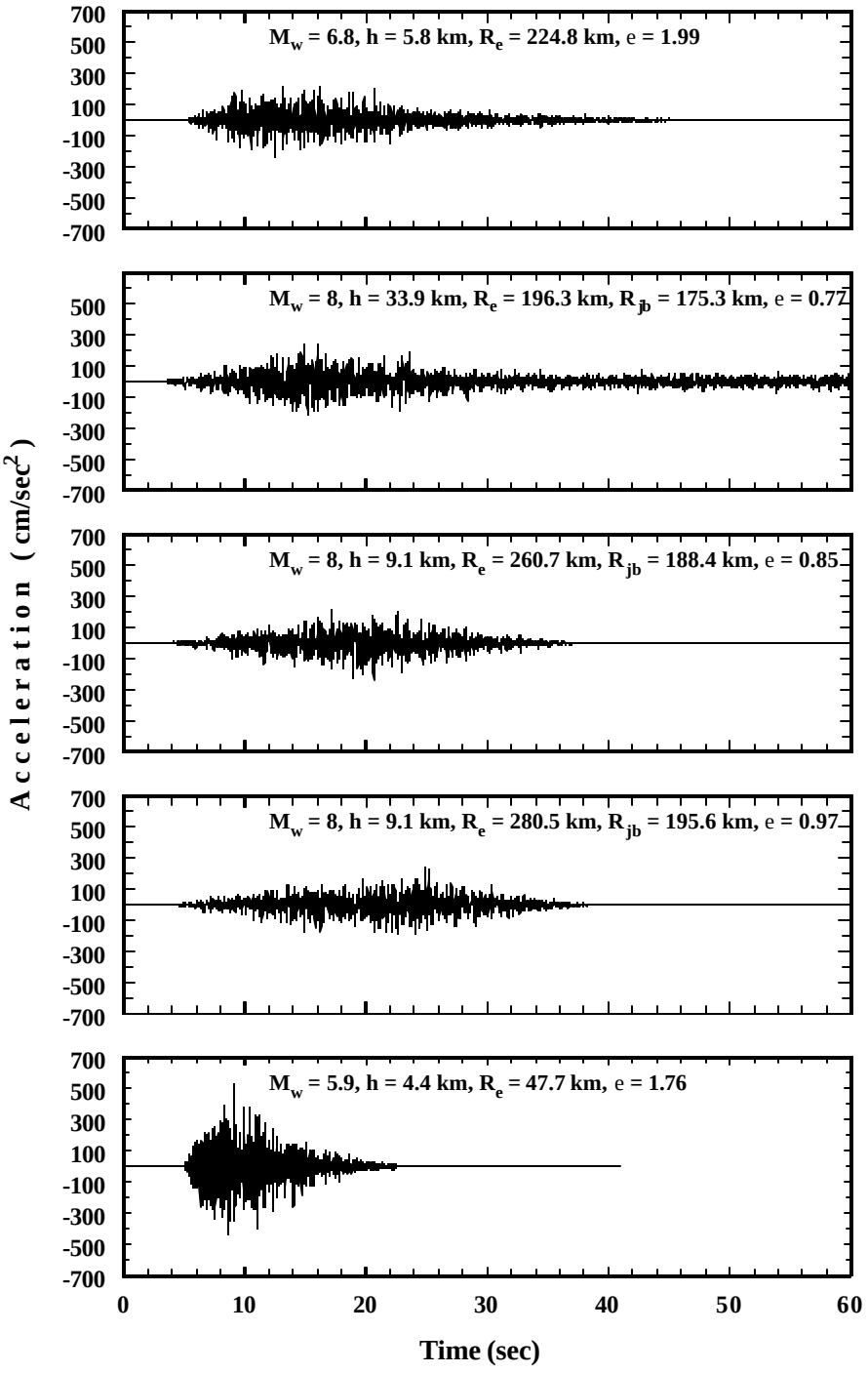

Figure 26 (continued).

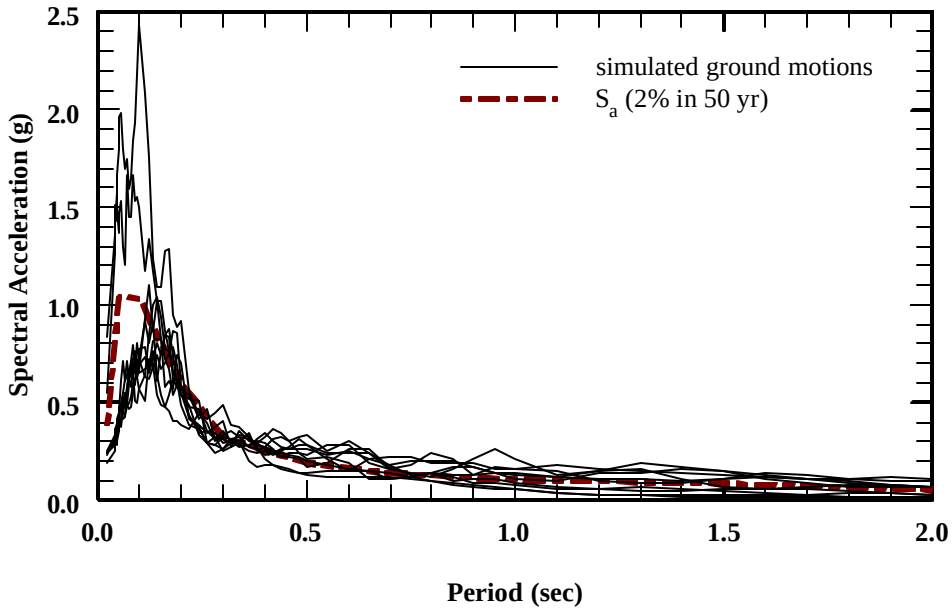

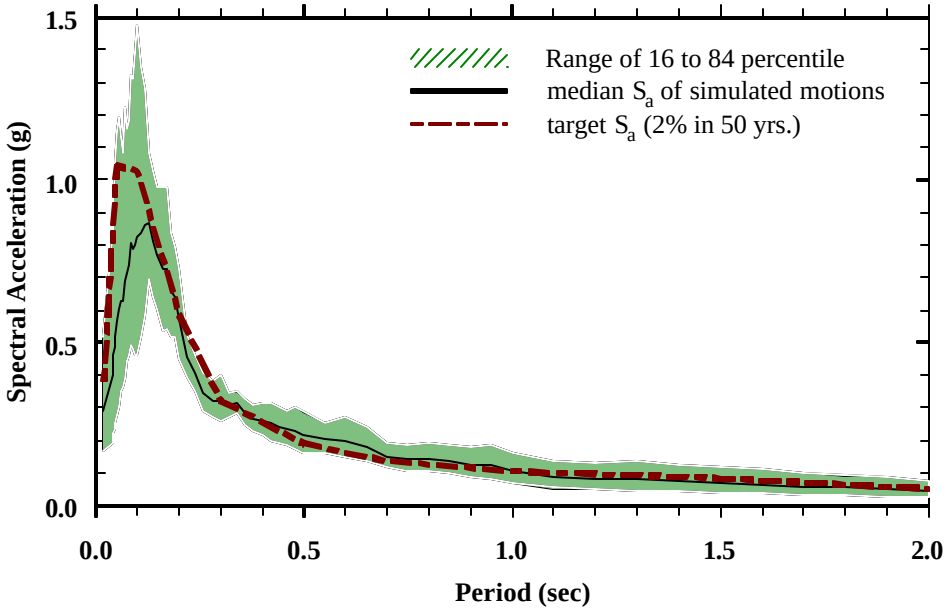

Figure 27. Response Spectra of 2% in 50 years Ground Motion Suite for Representative Soil Profile and Comparison with Target UHRS, St. Louis, MO.

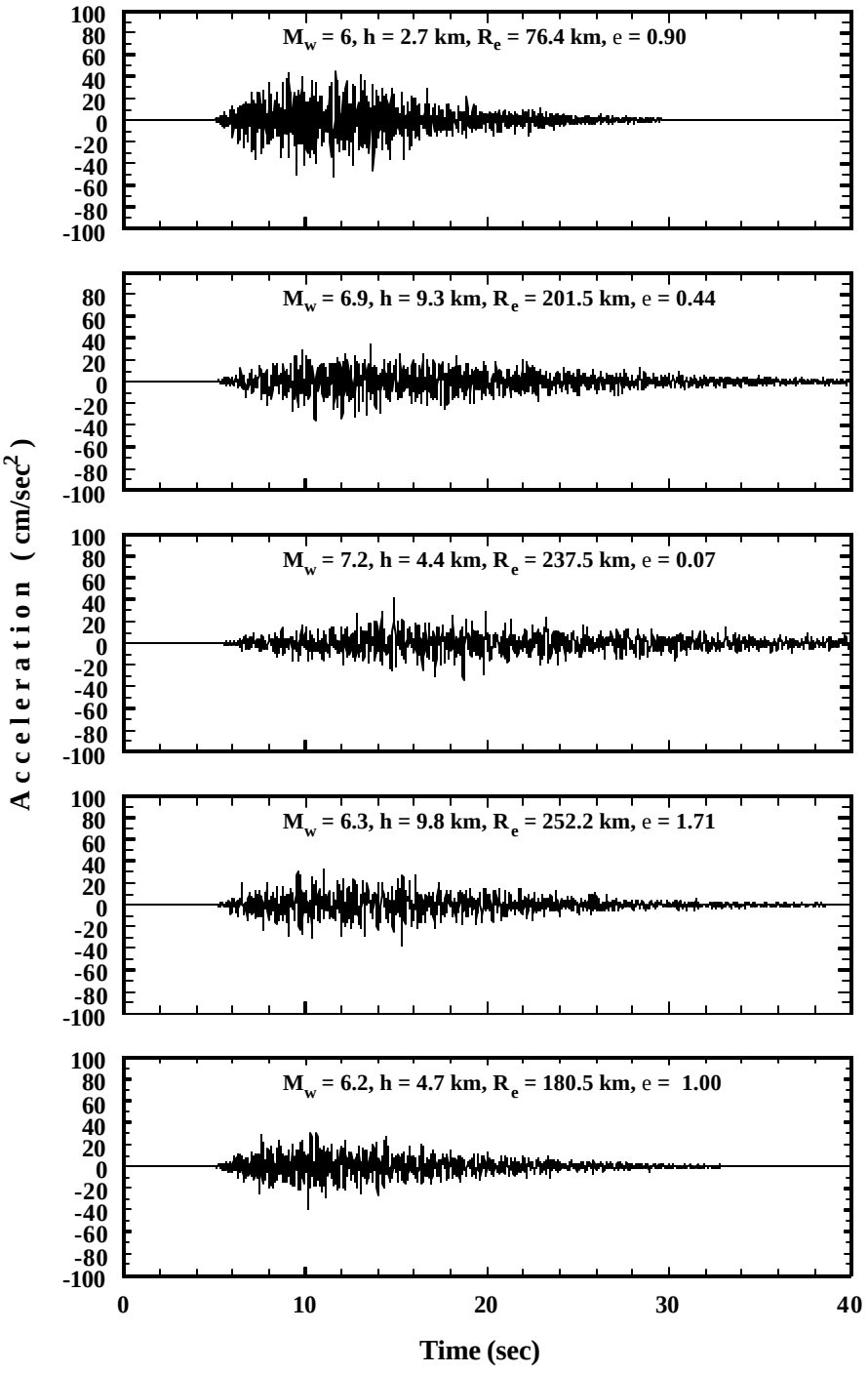

Figure 28. Suite of 10% in 50 yrs Ground Motions for Bedrock (Hard Rock), St. Louis, MO.

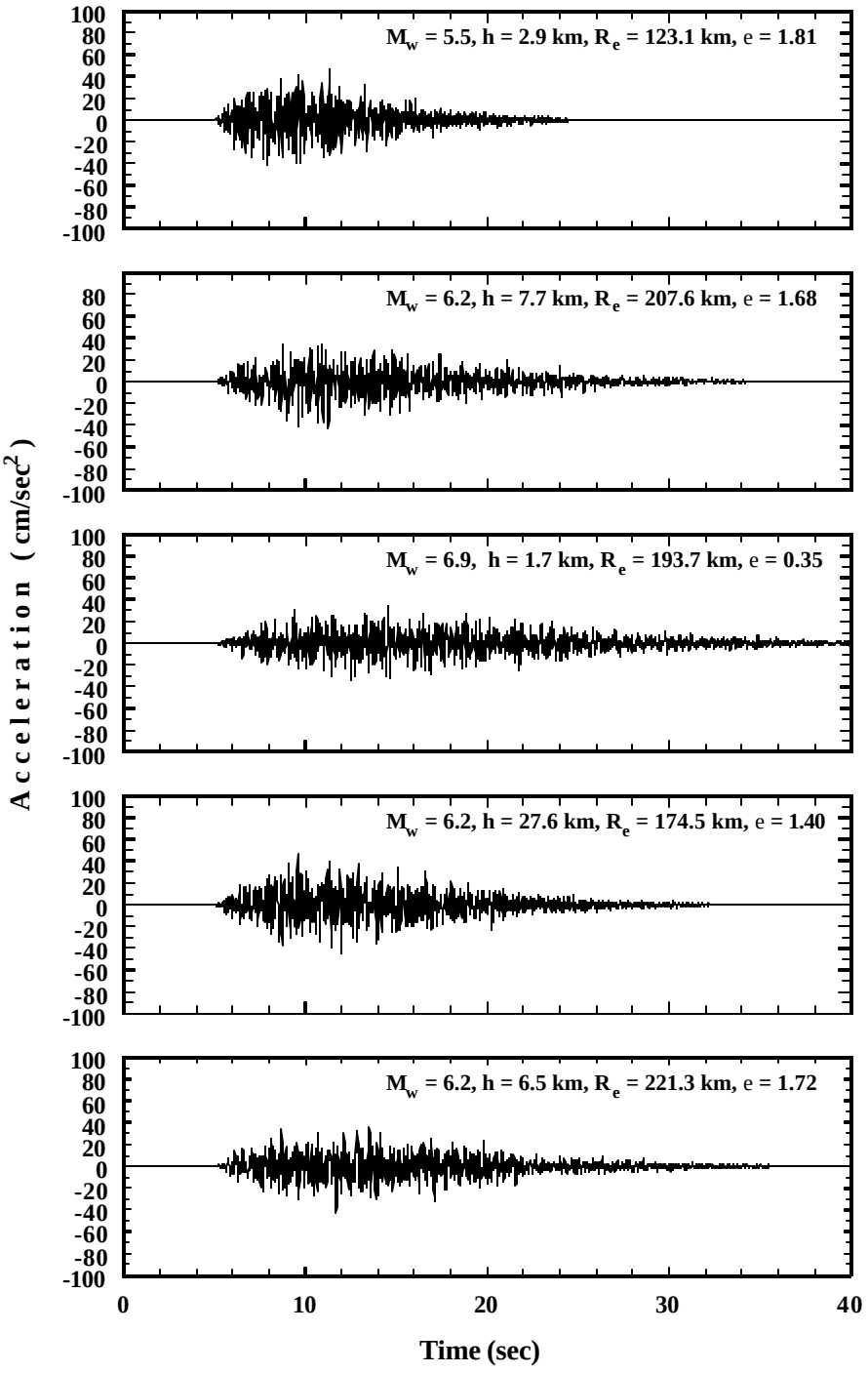

Figure 28 (continued).

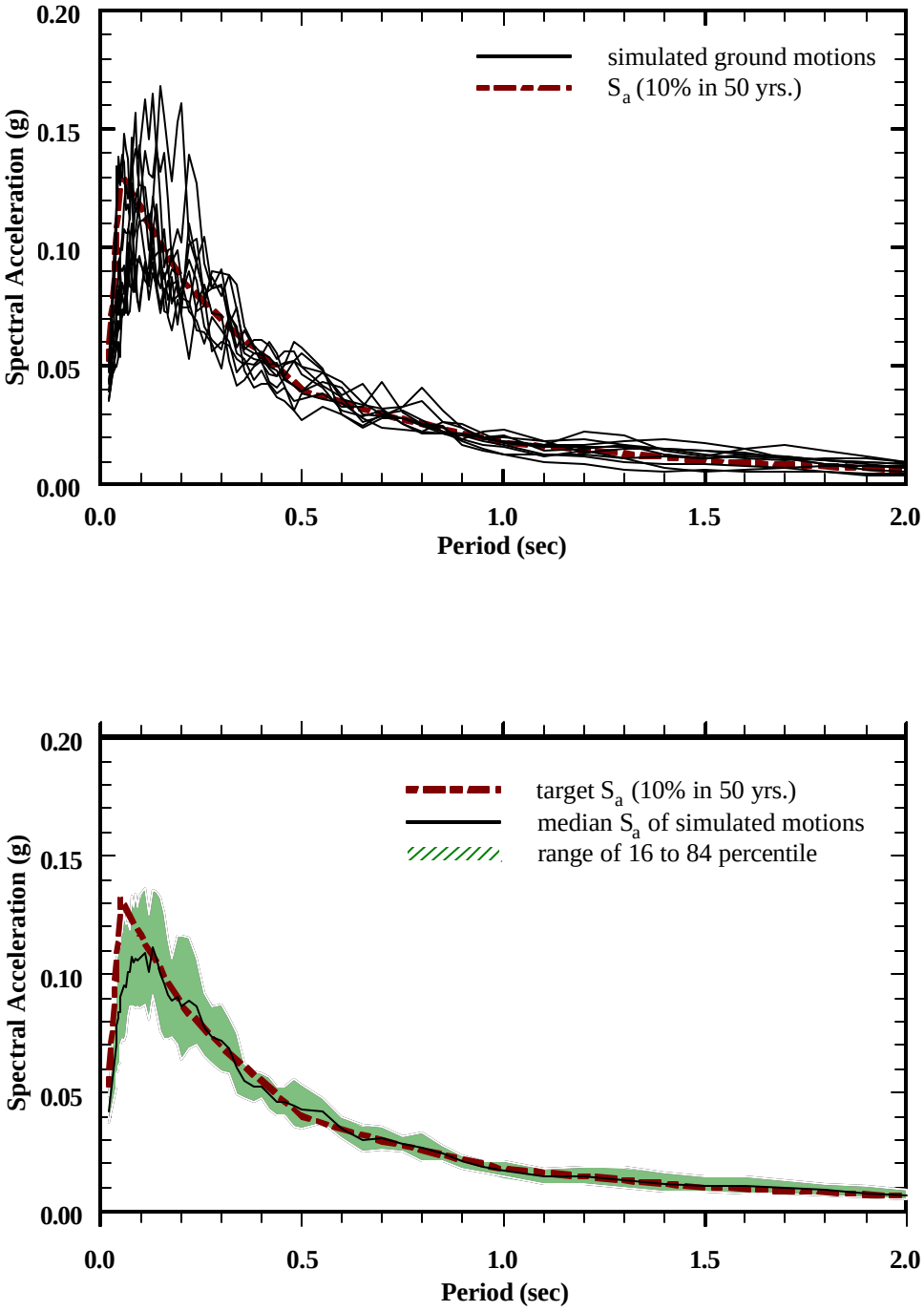

Figure 29. Response Spectra of 10% in 50 years Ground Motion Suite for Bedrock (Hard Rock) and Comparison with Target UHRS, St. Louis, MO.

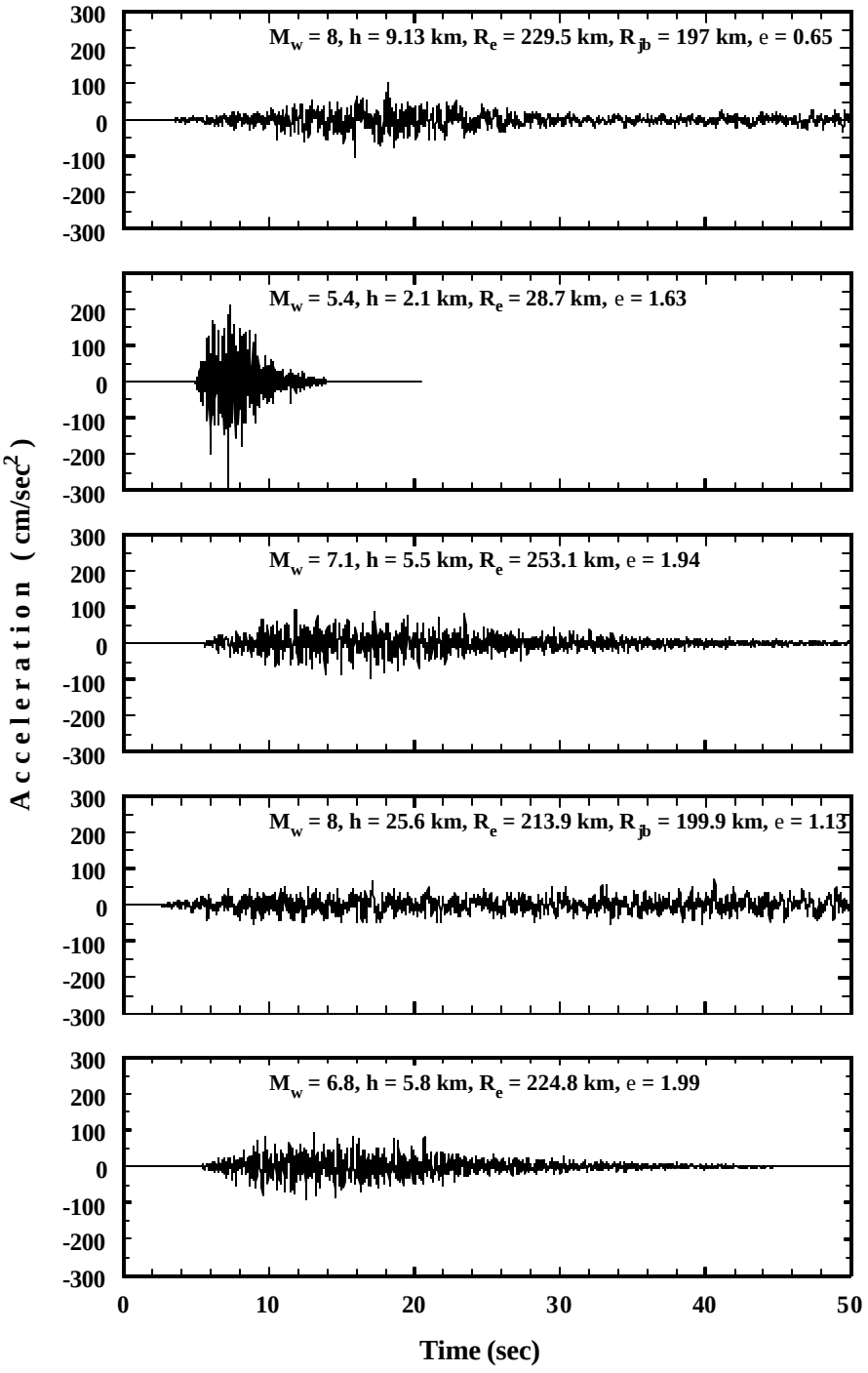

Figure 30. Suite of 2% in 50 years Ground Motions for Bedrock (Hard Rock), St. Louis, MO.

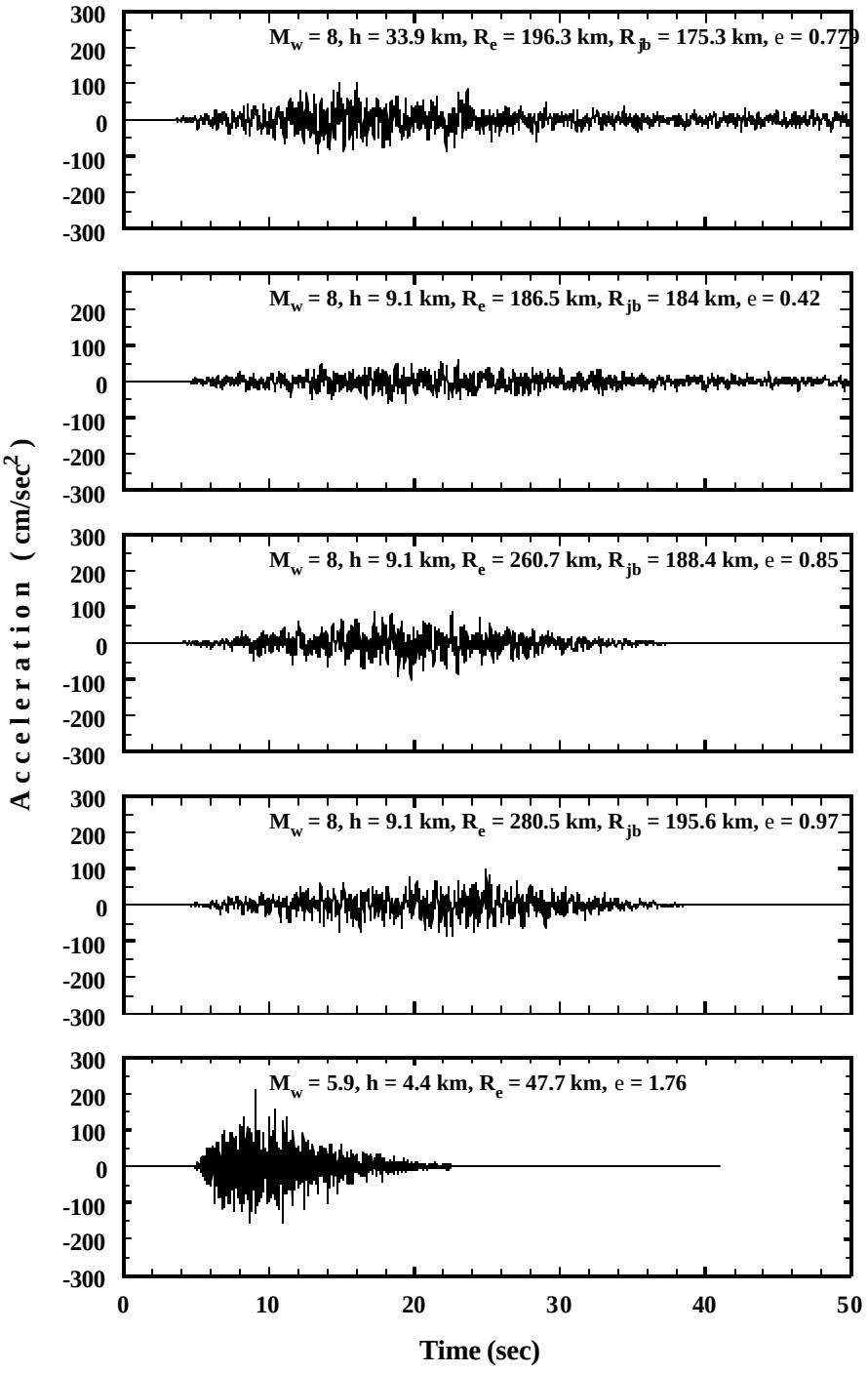

Figure 30 (continued).

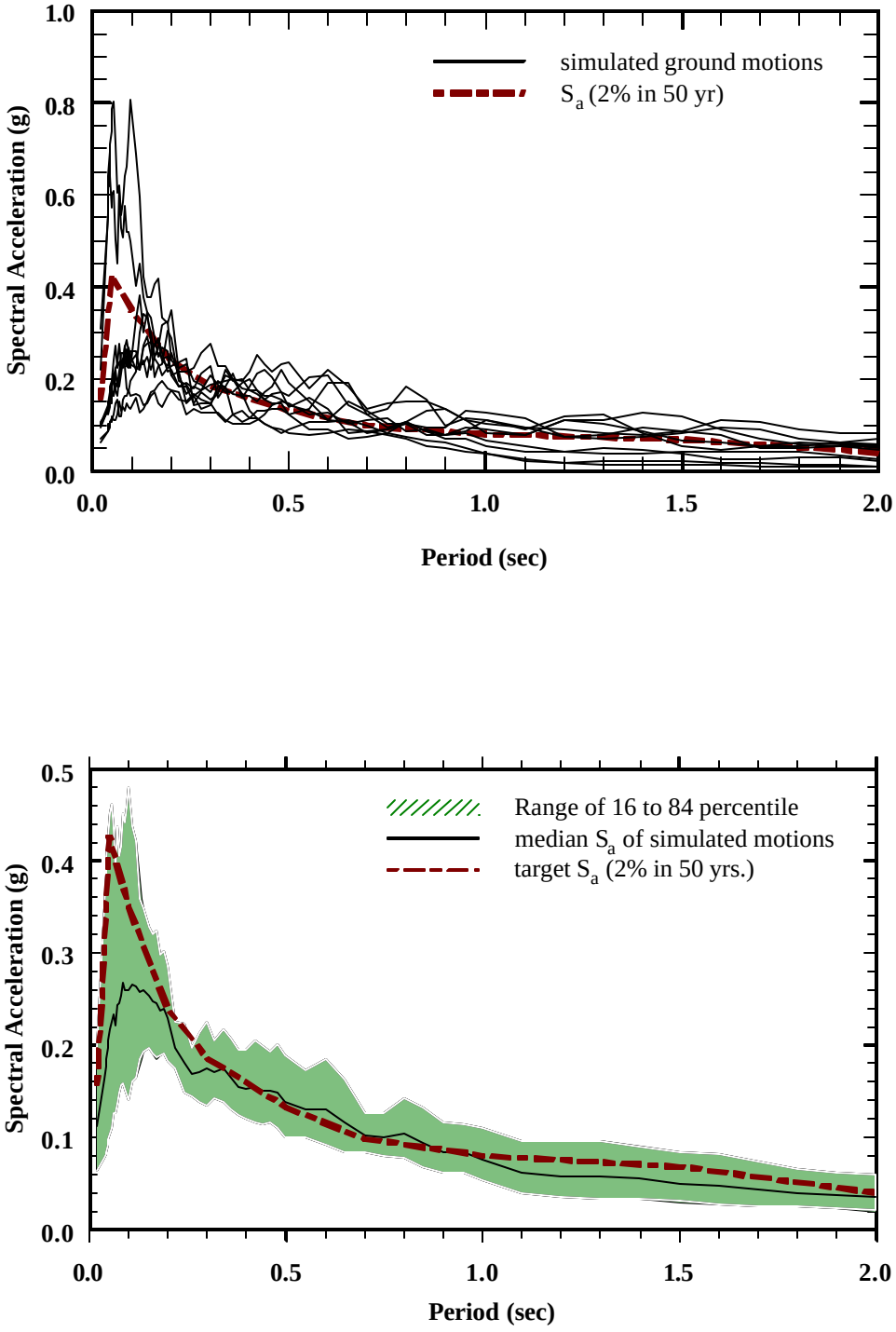

Figure 31. Response Spectra of 2% in 50 years Ground Motion Suite for Bedrock (Hard Rock) and Comparison with Target UHRS, St. Louis, MO.

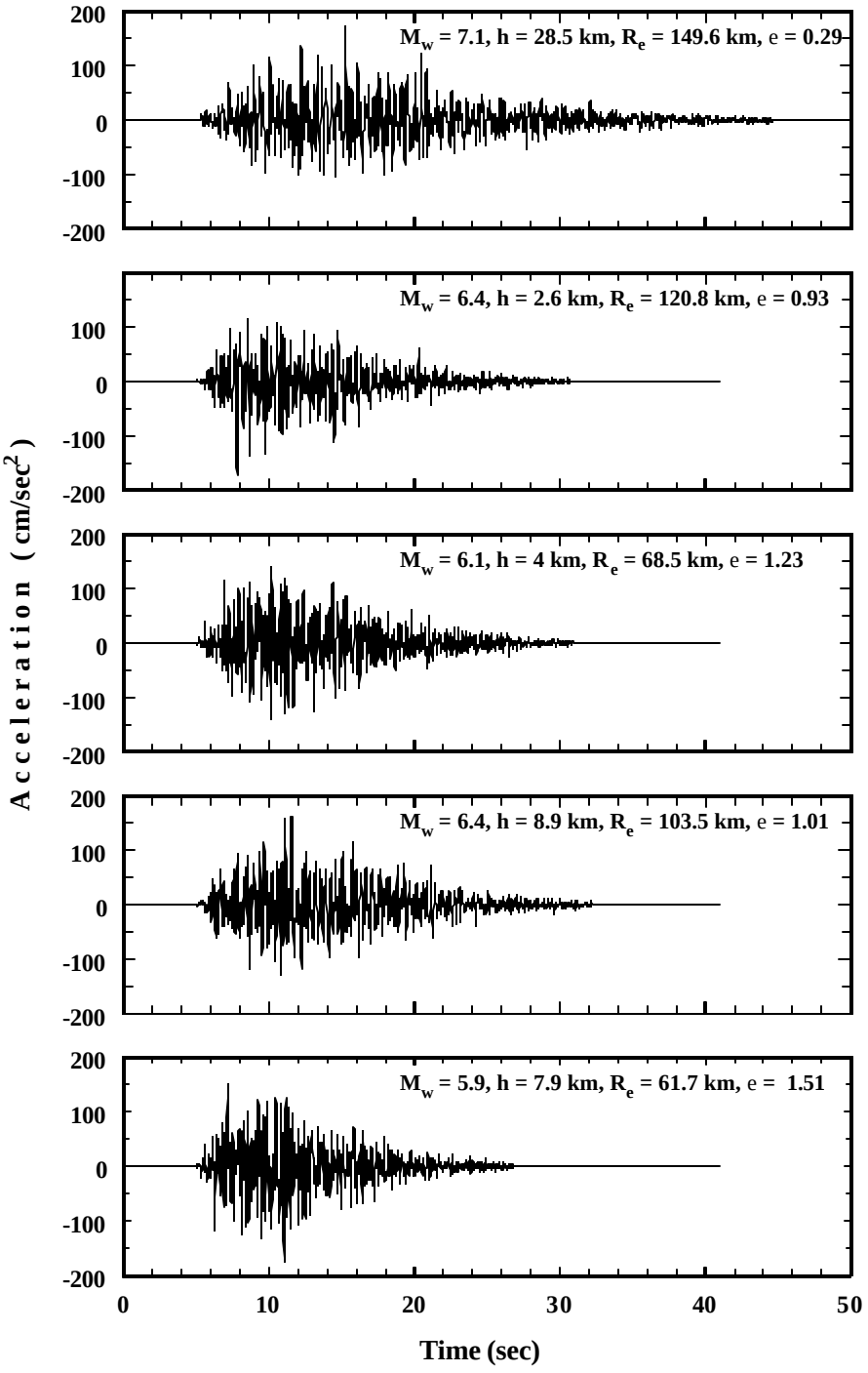

Figure 32. Suite of 10% in 50 years Ground Motions for Representative Soil Profile, Carbondale, IL.

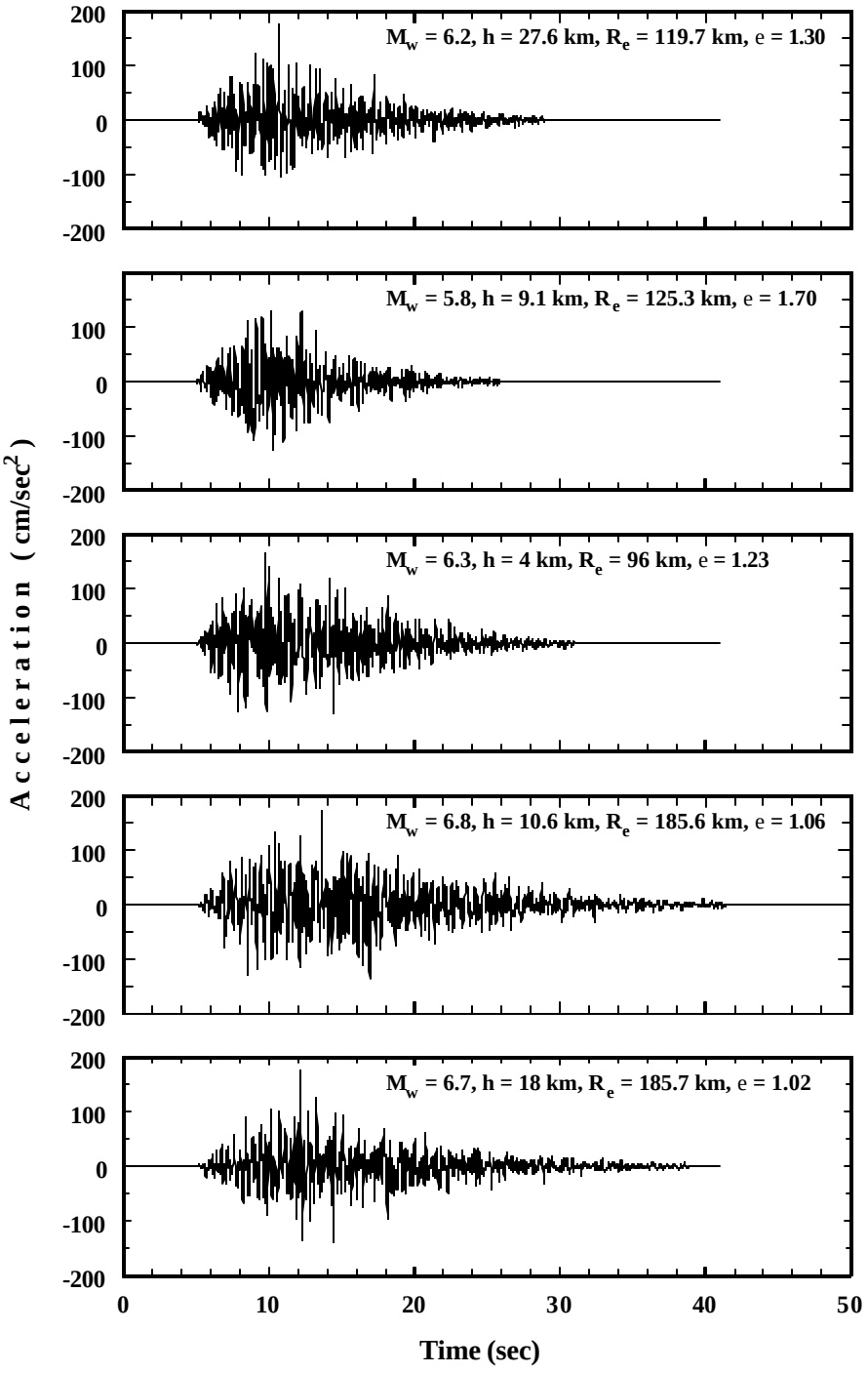

Figure 32 (continued).

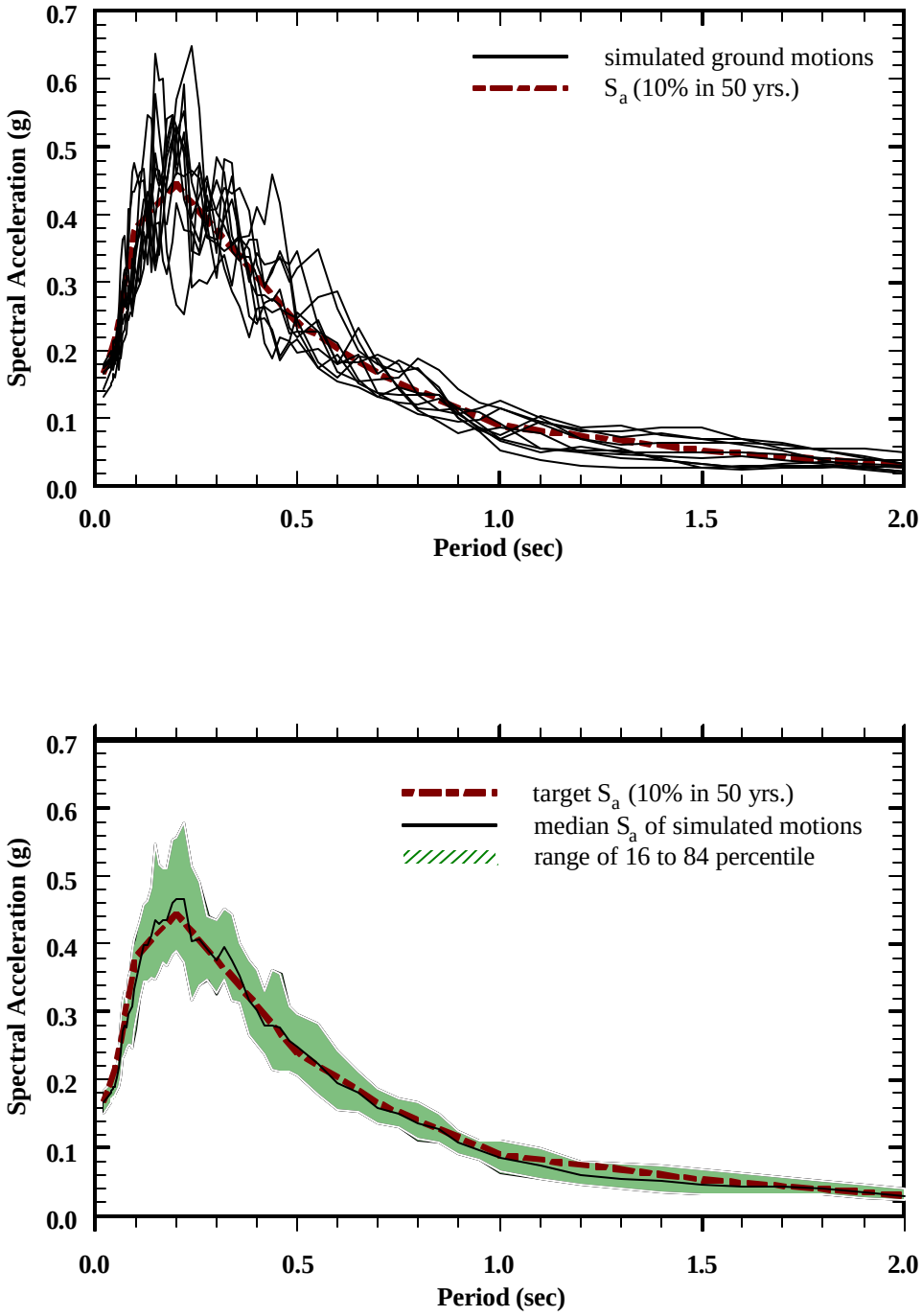

Figure 33. Response Spectra of 10% in 50 years Ground Motion Suite for Representative Soil Profile and Comparison with Target UHRS, Carbondale, IL.

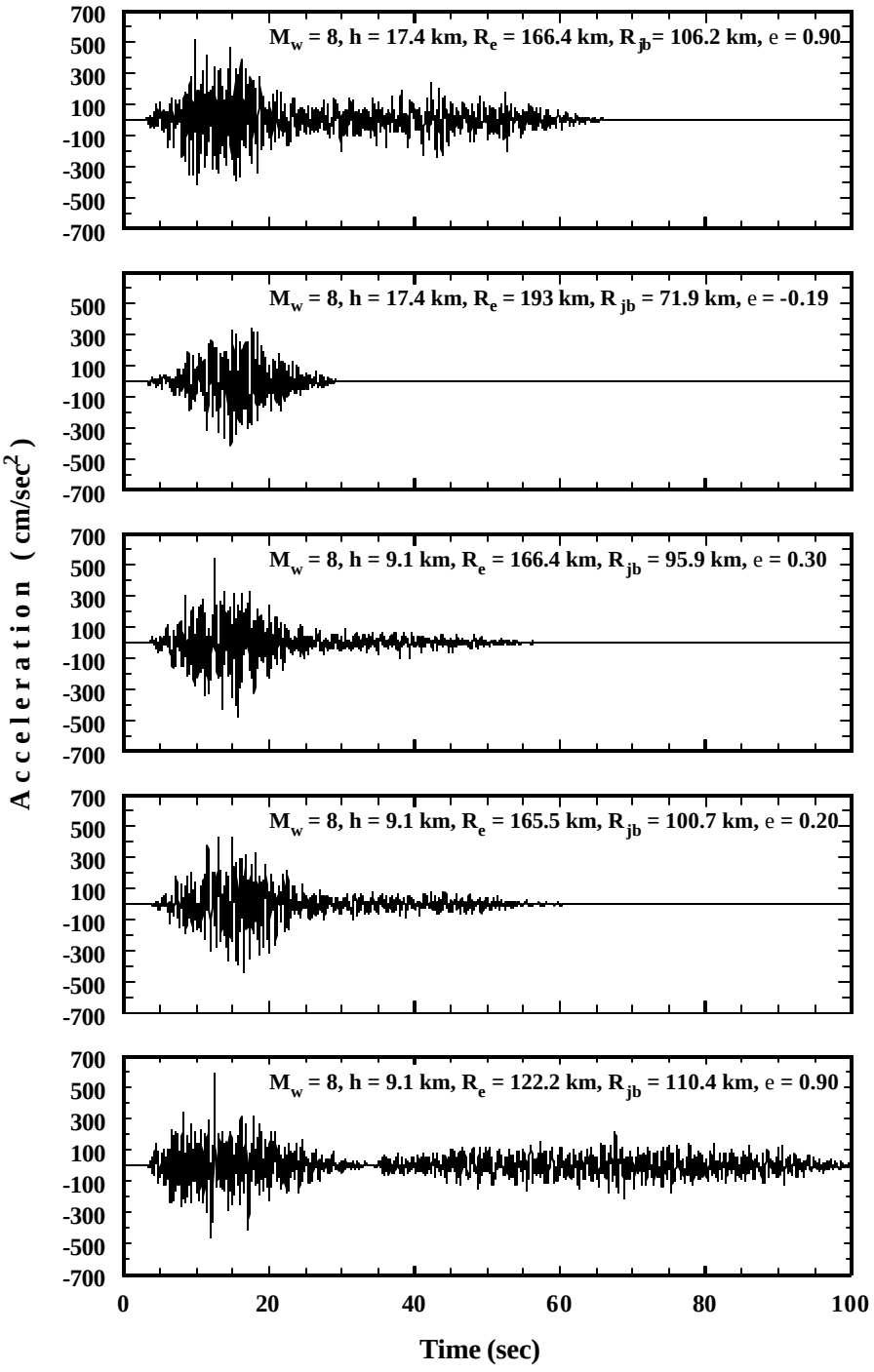

Figure 34. Suite of 2% in 50 years Ground Motions for Representative Soil Profile, Carbondale, IL.

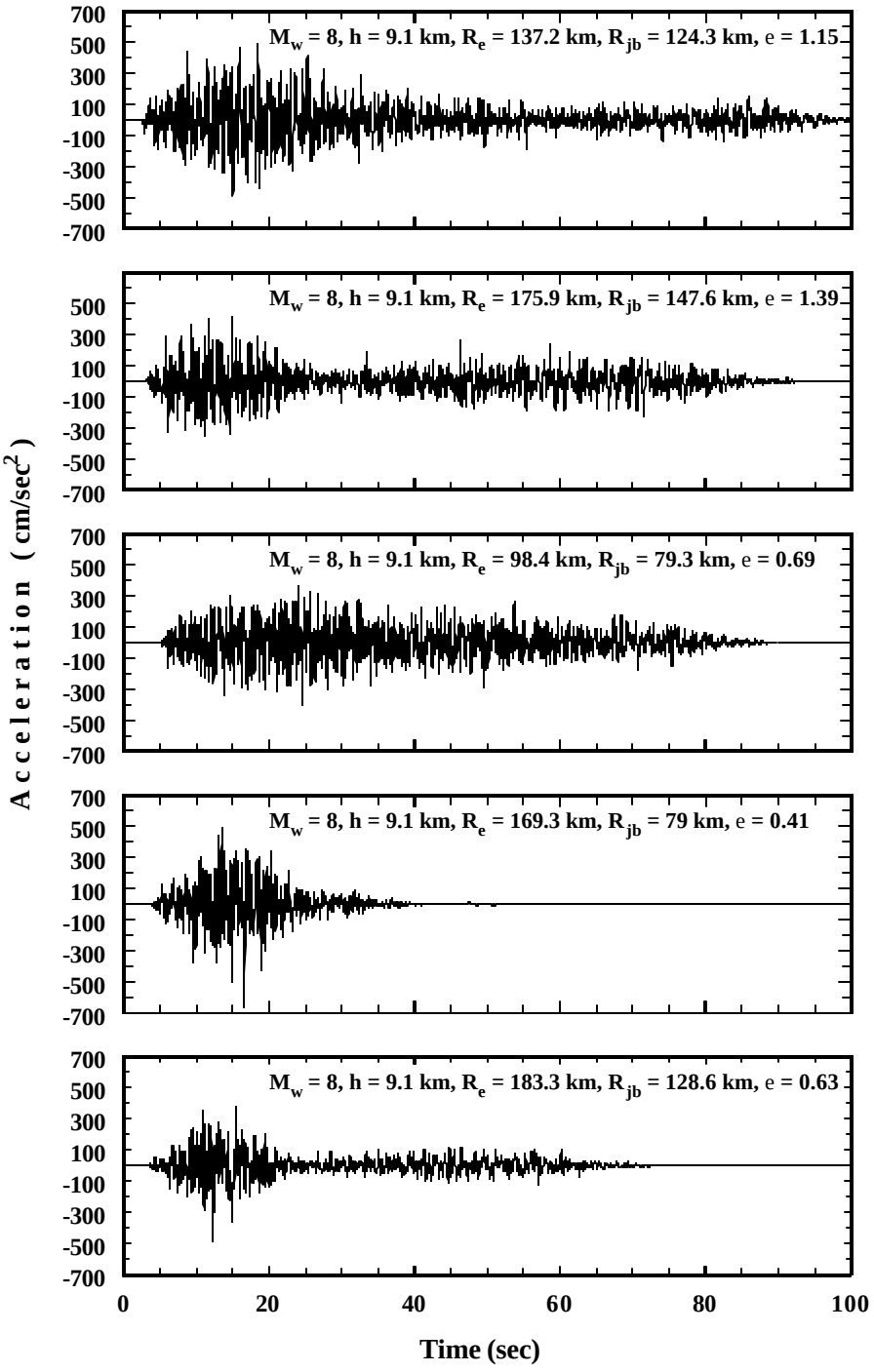

Figure 34 (continued).

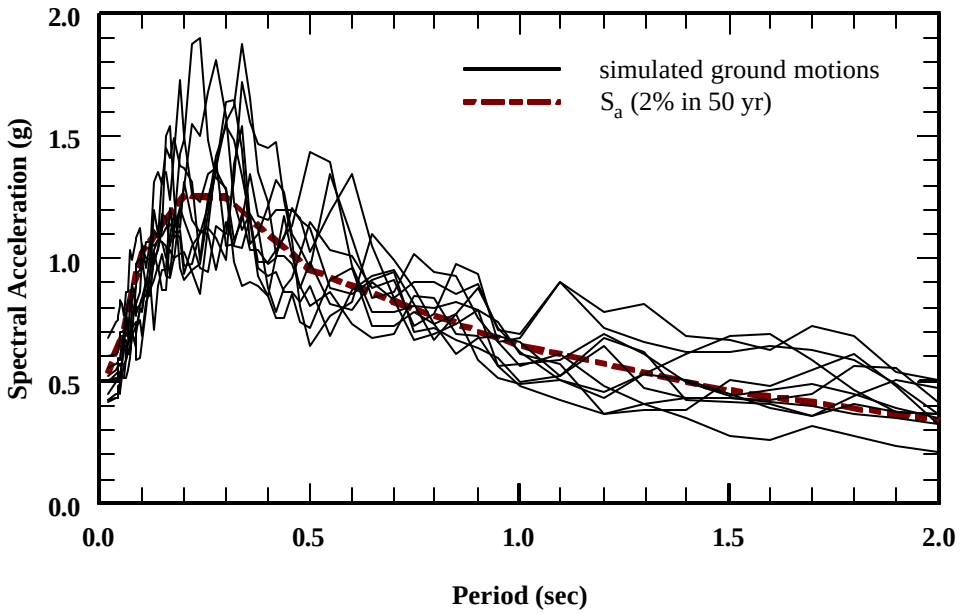

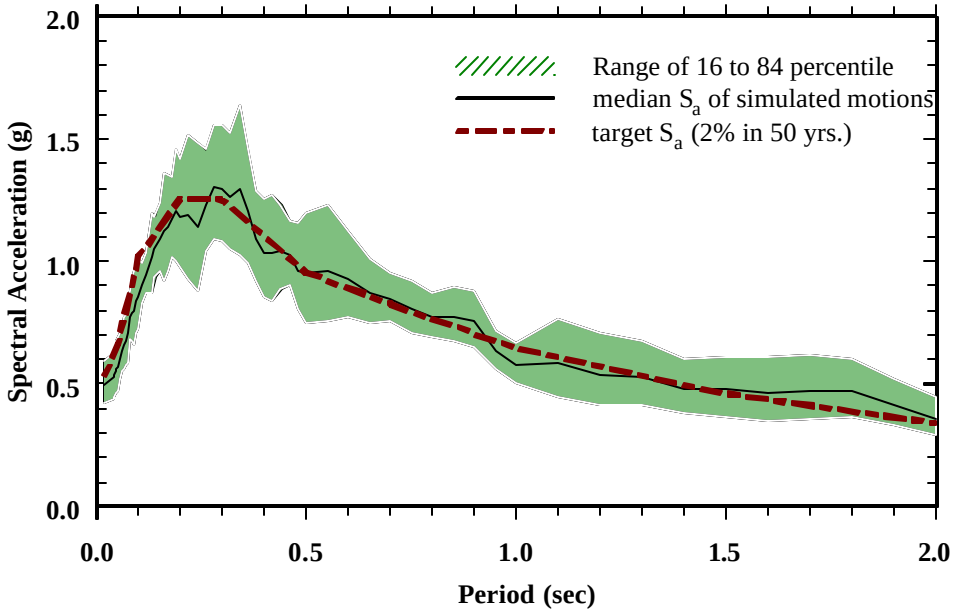

Figure 35. Response Spectra of 2% in 50 years Ground Motion Suite for Representative Soil Profile and Comparison with Target UHRS, Carbondale, IL.

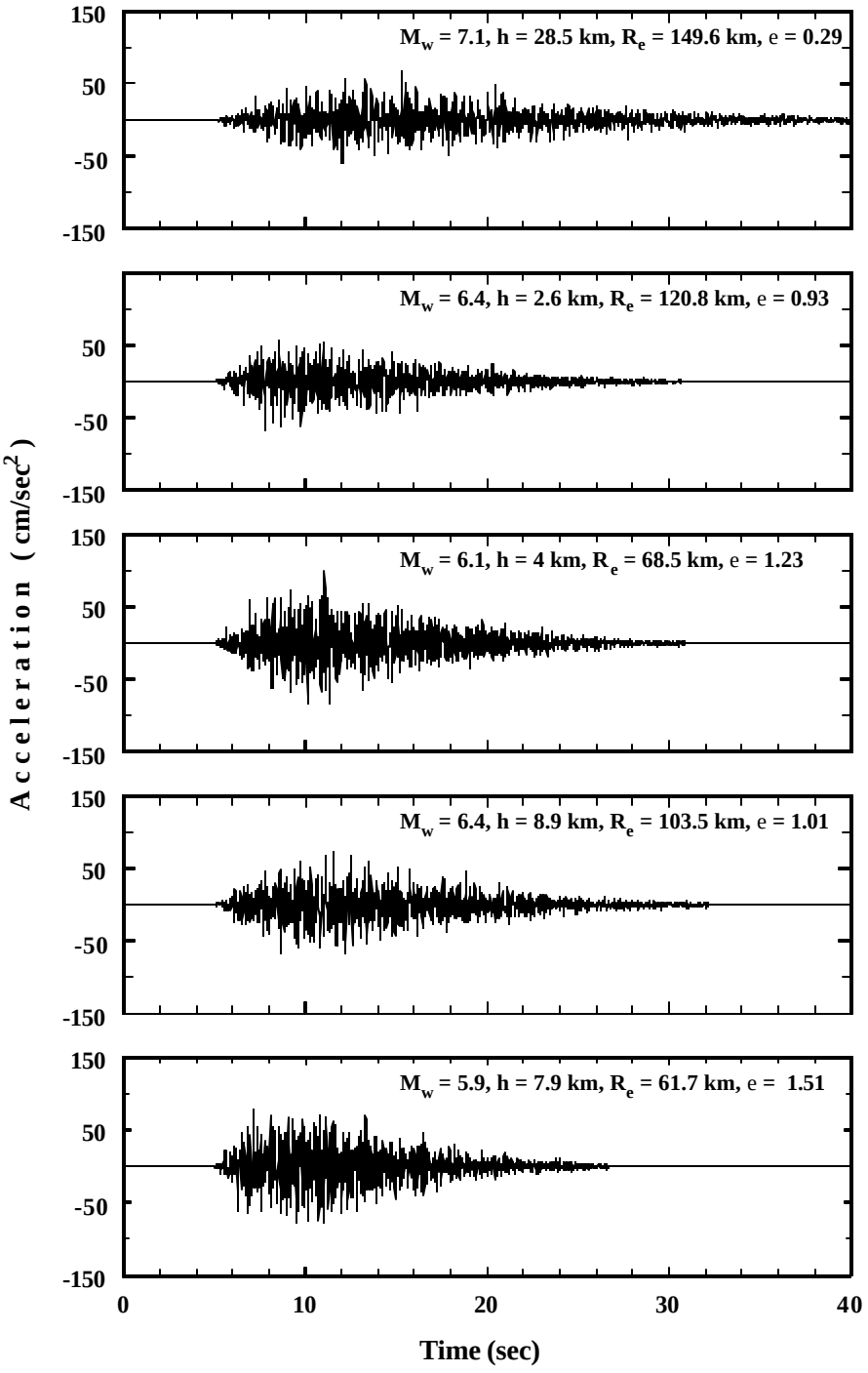

Figure 36. Suite of 10% in 50 years Ground Motions for Bedrock (Hard Rock), Carbondale, IL.

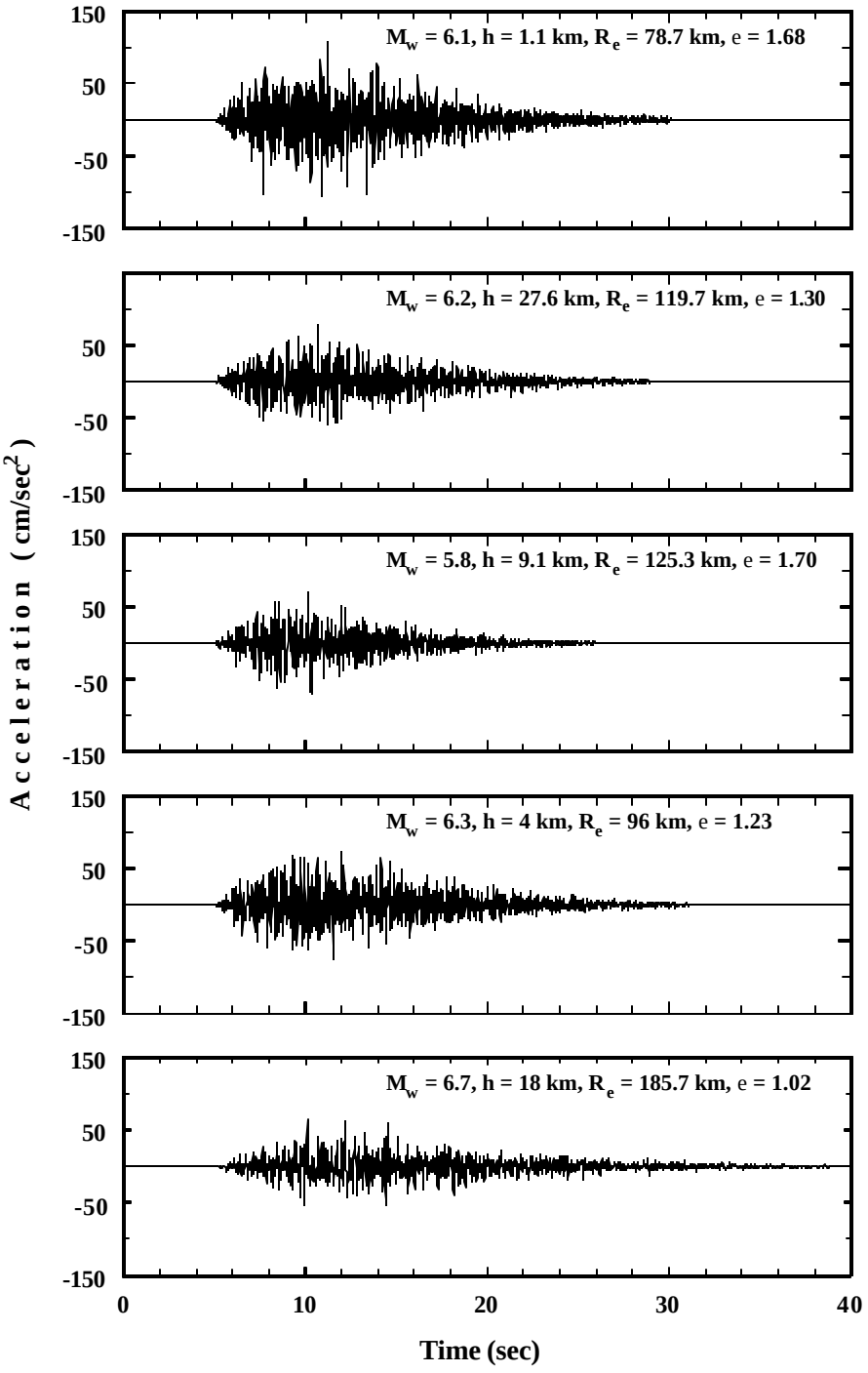

Figure 36 (continued).

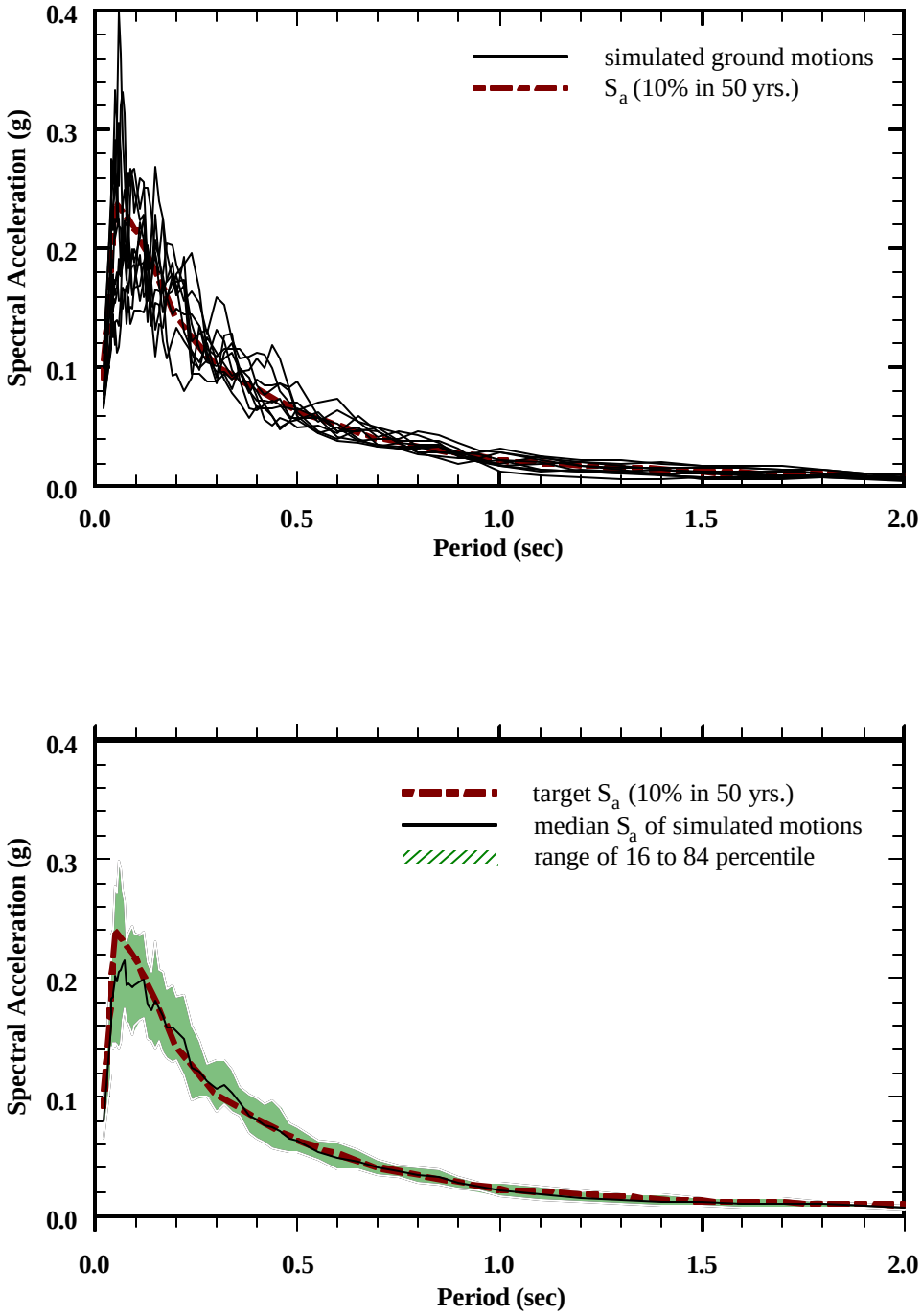

Figure 37. Response Spectra of 10% in 50 years Ground Motion Suite for Bedrock (Hard Rock) and Comparison with Target UHRS, Carbondale, IL.

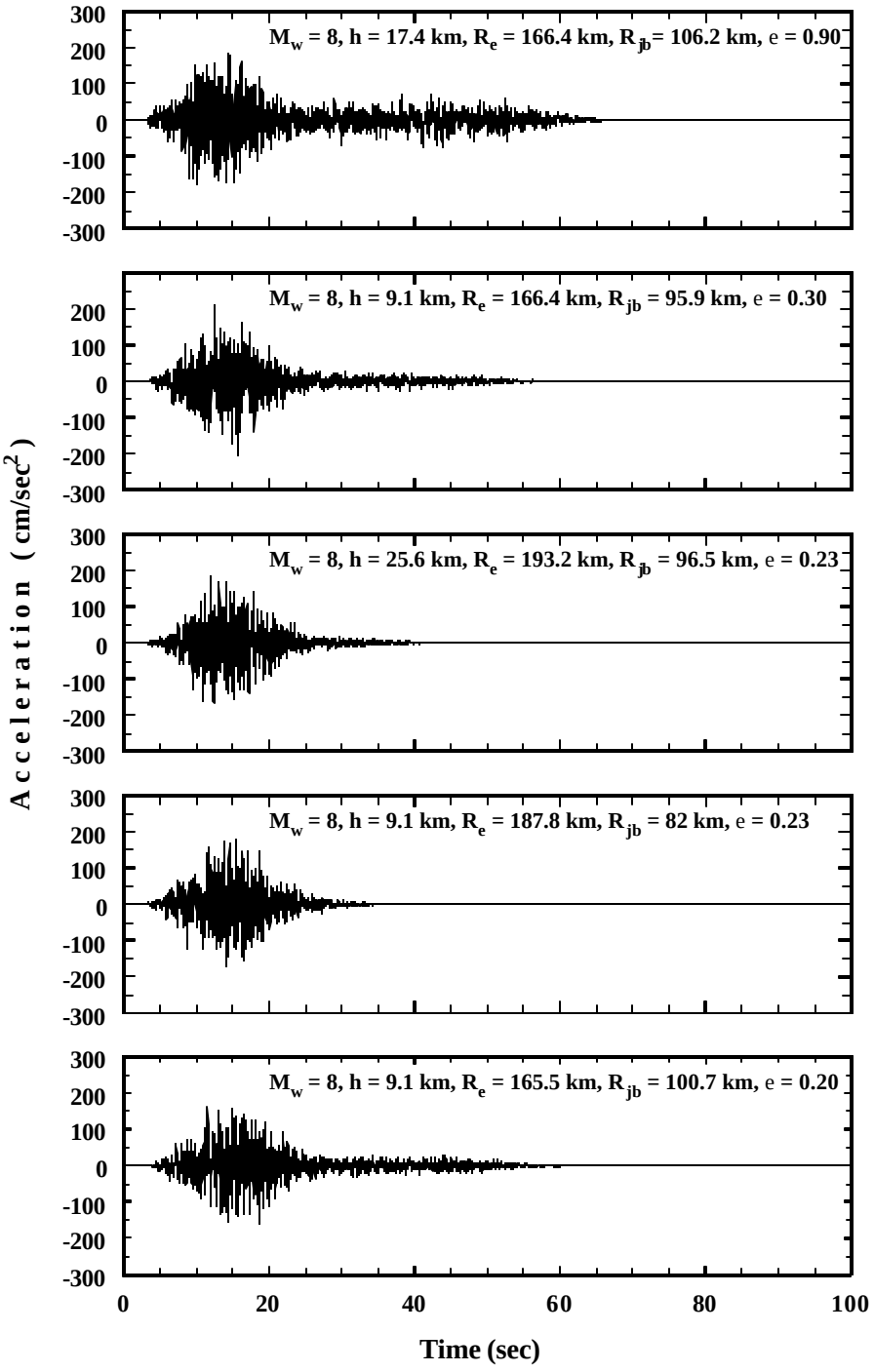

Figure 38. Suite of 2% in 50 years Ground Motions for Bedrock (Hard Rock), Carbondale, IL.

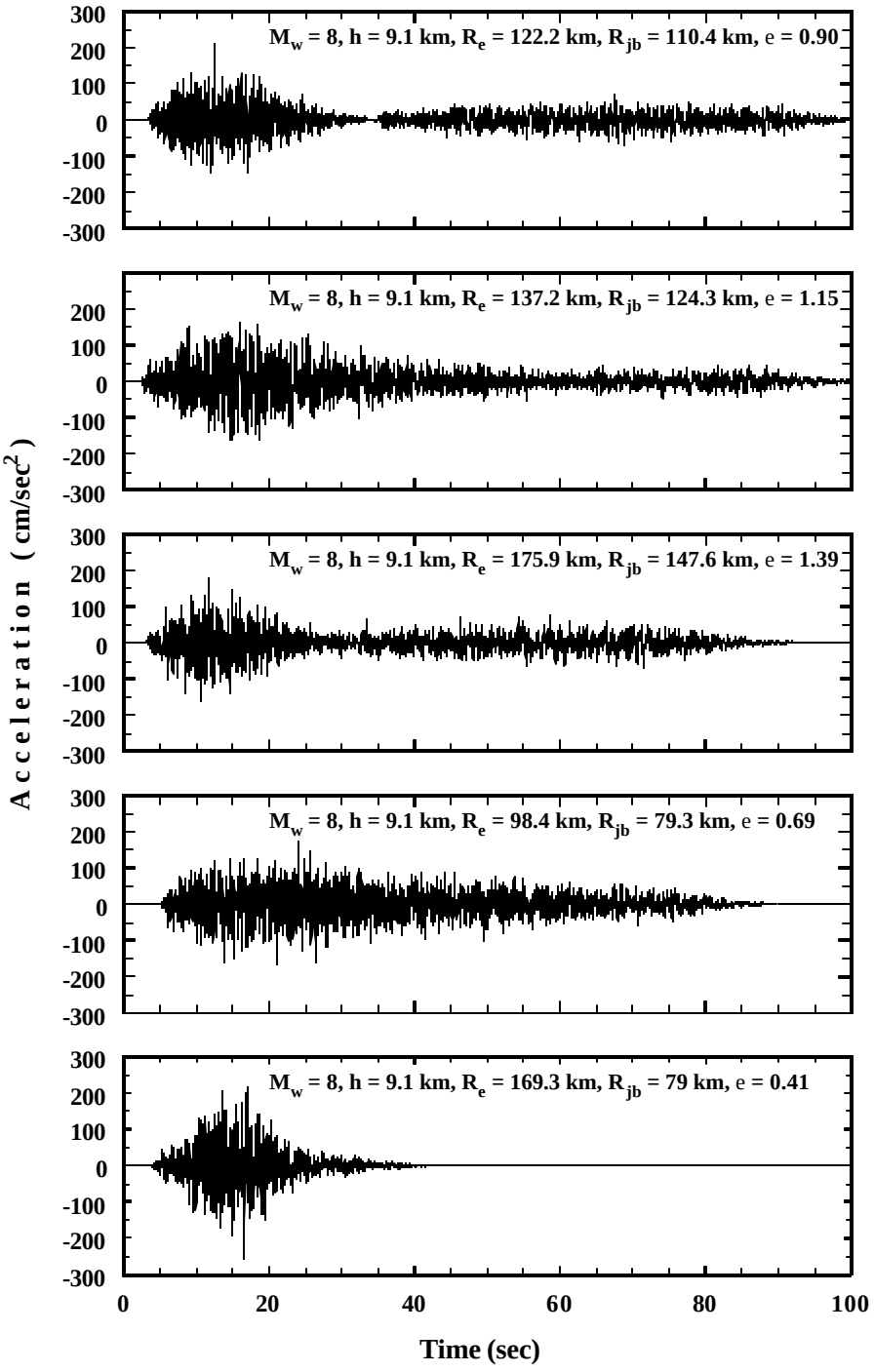

Figure 38 (continued).

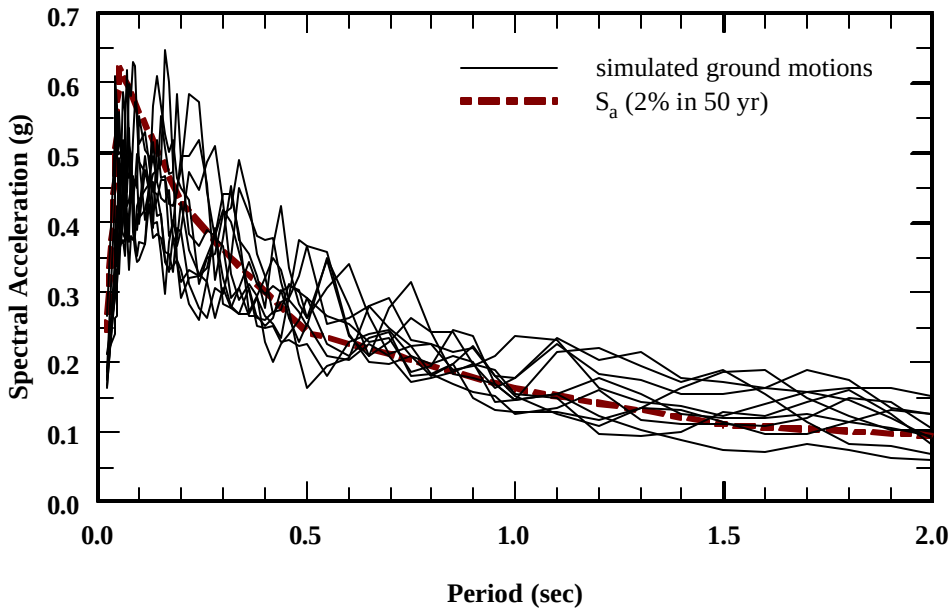

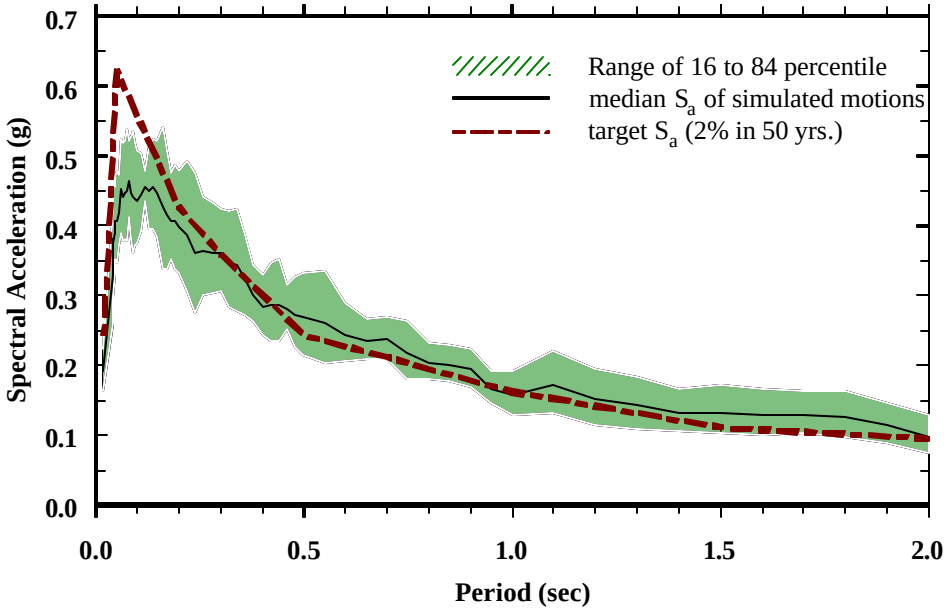

Figure 39: Response Spectra of 2% in 50 years Ground Motion Suite for Bedrock (Hard Rock) and Comparison with Target UHRS, Carbondale, IL.

Spectral Accelerations (unit: g) for 3 Mid-America Cities

Memphis, TN "Representative" Soil Profile

Period (s)	10% in 50 yrs	5% in 50 yrs.	2% in 50 yrs.
0.02	0.0792	0.1590	0.3802
0.05	0.0888	0.1800	0.4116
0.10	0.1455	0.2933	0.5775
0.20	0.2008	0.3927	0.9080
0.30	0.2015	0.4062	0.9340
0.50	0.1578	0.3351	0.8434
0.70	0.0900	0.2663	0.7187
1.00	0.0550	0.1899	0.5652
1.50	0.0310	0.1266	0.4015
2.00	0.0170	0.0899	0.2988
PGA (g)	0.0789	0.1586	0.3824

Memphis, TN Hard Rock Outcrop

Period (s)	10% in 50 yrs	5% in 50 yrs.	2% in 50 yrs.
0.02	0.0842	0.1748	0.3198
0.05	0.2324	0.4534	0.8058
0.10	0.2033	0.3987	0.7371
0.20	0.1343	0.2601	0.5950
0.30	0.1037	0.2069	0.4640
0.50	0.0653	0.1374	0.3412
0.70	0.0400	0.0960	0.2560
1.00	0.0200	0.0701	0.2104
1.50	0.0110	0.0448	0.1600
2.00	0.0070	0.0310	0.1200
PGA (g)	0.0876	0.1751	0.3212

St. Louis, MO "Representative" Soil Profile

Period (s)	10% in 50 yrs	5% in 50 yrs.	2% in 50 yrs.
0.02	0.1296	0.2129	0.3839
0.05	0.3187	0.5405	1.0430
0.10	0.3527	0.5674	1.0270
0.20	0.2162	0.3382	0.5902
0.30	0.1212	0.1918	0.3223
0.50	0.0578	0.1031	0.1893
0.70	0.0407	0.0746	0.1348
1.00	0.0238	0.0467	0.1042
1.50	0.0143	0.0350	0.0820
2.00	0.0076	0.0230	0.0500
PGA (g)	0.1300	0.2133	0.3973

St. Louis, MO Hard Rock Outcrop

Period (s)	10% in 50 yrs	5% in 50 yrs.	2% in 50 yrs.
0.02	0.0524	0.0852	0.1560
0.05	0.1319	0.2224	0.4266
0.10	0.1169	0.1938	0.3492
0.20	0.0871	0.1368	0.2394
0.30	0.0695	0.1108	0.1854
0.50	0.0401	0.0718	0.1321
0.70	0.0296	0.0538	0.0982
1.00	0.0178	0.0353	0.0800
1.50	0.0100	0.0300	0.0680
2.00	0.0064	0.0200	0.0400
PGA (g)	0.0526	0.0858	0.1570

Carbondale, IL "Representative" Soil Profile

Period (s)	10% in 50 yrs	5% in 50 yrs.	2% in 50 yrs.
0.02	0.1676	0.3011	0.5352
0.05	0.2177	0.3788	0.6607
0.10	0.3806	0.6262	1.0220
0.20	0.4451	0.7395	1.2570
0.30	0.3775	0.6878	1.2510
0.50	0.2405	0.4653	0.9551
0.70	0.1660	0.3356	0.8276
1.00	0.0900	0.2416	0.6444
1.50	0.0530	0.1587	0.4591
2.00	0.0300	0.1105	0.3392
PGA (g)	0.1620	0.2989	0.5523

Carbondale, IL Hard Rock Outcrop

Period (s)	10% in 50 yrs	5% in 50 yrs.	2% in 50 yrs.
0.02	0.0904	0.1466	0.2431
0.05	0.2398	0.3760	0.6231
0.10	0.2170	0.3441	0.5562
0.20	0.1430	0.2551	0.4271
0.30	0.1009	0.1828	0.3593
0.50	0.0631	0.1205	0.2425
0.70	0.0400	0.0871	0.2112
1.00	0.0220	0.0614	0.1619
1.50	0.0120	0.0388	0.1106
2.00	0.0090	0.0260	0.0950
PGA (g)	0.0905	0.1476	0.2444